UILU-ENG-72-2008

CIVIL ENGINEERING STUDIES

STRUCTURAL RESEARCH SERIES NO. 387

A PROBABILISTIC STUDY OF SAFETY CRITERIA FOR DESIGN

by
B. R. ELLINGWOOD
and
A. H.-S. ANG

Issued as a Technical Report
of Research Supported
by the
NATIONAL SCIENCE FOUNDATION
under Grant GK-1812X

UNIVERSITY OF ILLINOIS
URBANA, ILLINOIS
JUNE 1972

A PROBABILISTIC STUDY OF SAFETY CRITERIA FOR DESIGN

by

B. R. Ellingwood

and

A. H-S. Ang

Issued as a
Technical Report
of Research Supported by the
National Science Foundation
under
Grant GK-1812X

UNIVERSITY OF ILLINOIS
URBANA, ILLINOIS
JUNE 1972

ACKNOWLEDGMENTS

This report is based on the dissertation of Dr. B. R. Ellingwood submitted to the Graduate College, University of Illinois at Urbana-Champaign, for the degree of Ph.D. in Civil Engineering. The study was conducted under the supervision of Dr. A. H-S. Ang, Professor of Civil Engineering, as part of a research program on the probabilistic aspects of structural safety and design, supported by the National Science Foundation under research grant No. GK-1812X.

Special thanks are extended to several colleagues; to Dr. C. P. Siess, Professor of Civil Engineering, for his interest in the study and enlightening discussions on the ACI Code and reinforced concrete design, and to Dr. M. Amin and Dr. W. Tang, Associate Professor and Assistant Professor, respectively, in Civil Engineering, for their comments and discussions on various probabilistic aspects of the study.

The numerical calculations were performed on the IBM 360/75 system of the Computing Services Office of the University.

TABLE OF CONTENTS

Chapter 1

INTRODUCTION AND BACKGROUND

1.1 General Remarks

The assurance of adequate structural reliability is a principal consideration in the process of design. As calculations for engineering designs are based on mathematical models of reality, this may be a difficult task. Unavoidably, when idealizing a real situation, there are factors that may be neglected. Load models, for example, contain uncertainties resulting from lack of information or knowledge. Variabilities in structural capacity may arise from nonuniform or careless fabrication and construction procedures. The laws of structural mechanics relating loads and structural response are based on simplifications and idealizations. The design process is thereby clouded with uncertainties from a lack of complete information. Moreover, loads and resistances usually exhibit statistical dispersions. In this context, absolute safety cannot be realized.

The designer must insure that the resistance provided by his design exceeds potential load effects by a sufficient amount to insure adequate safety under adverse conditions. This is currently done within the context of working stress or ultimate strength design. These two methods, while having different philosophies, share the common feature of treating the design parameters deterministically. The allowable stresses, or load factors, are chosen so that the likelihood of failure is deemed (intuitively) to be acceptably small. Traditionally, the allowable stresses or load factors have been determined by the profession on the basis of judgment and

experience. The risks associated with a design are not and cannot be evaluated quantitatively.

Central to a rational approach to safety is the concept of an acceptable risk of failure [17, 31]. In view of the randomness of many of the design parameters, relevant criteria for safety should provide an explicit measure of the likelihood of unfavorable design response. This requires that a statistical analysis be made of those data that are random. Moreover, uncertainties associated with possible errors in modeling, estimation, and prediction also contribute to the underlying risk [8]; the assessment of the effects of these uncertainties on the reliability of a structure properly requires probabilistic analysis.

The consideration of uncertainties in prediction is invariably necessary in practice [8]. A lack of data generally makes it impossible to ascertain the exact statistical distributions of the design variables. The estimation of the modeling uncertainties underlying a mathematical solution often must be made on the basis of experience. In short, the safety criteria should be the result of a combination of statistical analysis and good judgment, in which all factors are treated in a consistent manner.

Finally, the design criteria should be simple in form. The format should preferably be similar to existing procedures; however, the allowable stresses, or load factors, should be selected more logically and systematically than is presently done.

1.2 Criteria Based on Acceptable Risk

1.2.1 Classical Reliability Analysis

Considerable research effort has been directed toward developing

the classical reliability theory [31,32]. This method assumes that loads and resistances are statistical variables, and that the necessary statistical information is available. Safety is assured by assigning a sufficiently small probability to the event that the resistance will be less than the applied load effect. In other words, the risk of failure

$$p_f = Pr(R < S) \tag{1.1}$$

is specified to be acceptably small. Denoting $\overline{R}$ and $\overline{S}$ as the mean resistance and mean load, respectively, a required load factor $\gamma = \overline{R}/\overline{S}$ may be computed, at least conceptually, from an inversion of Eq. 1.1. The load factor is thus a function of p_f and the variabilities of R and S.

In general, the required mean design resistance may be computed as

$$\overline{R} = \gamma \overline{S} \tag{1.2}$$

Alternatively,

$$\overline{R} = \overline{S} + \beta \sqrt{\sigma_R^2 + \sigma_S^2} \tag{1.3}$$

where the "safety index" β is a function of the specified risk p_f, and generally also a function of the second-order properties of R and S; β is simply the number of standard deviations of the margin of safety (R-S) above its mean for a particular risk level.

This provides the proper theoretical basis for the evaluation of the statistical quantities involved. The formulation tacitly assumes that all uncertainties in design are contained in the probability laws of R and S, which are presumed to be known. In practice, however, the probability

distributions and their parameters are seldom known precisely; moreover, there are invariably uncertainties of prediction and modeling which may not be random.

Another difficulty is that the designs are sensitive to the choice of the distribution functions at risk levels presently considered necessary to assure safety ($p_f \leq 10^{-5}$) [8,9]. Ang and Ellingwood [11] have also shown that β is distribution sensitive; furthermore, except for the normal case, β depends on the coefficients of variation (c.o.v.) of R and S as well.

In most engineering analyses involving random phenomena, only the first and second order moments, i.e., mean and variance, of the random variables are known. This information describes only the mid-range behavior of the distribution, a region in which one distribution may be indistinguishable from another, but is insufficient to describe the probability law of the variate completely. The regions of the probability distributions pertinent to the calculation of risk are the extremes of the distributions. A determination of their characteristics requires an extrapolation beyond the range of observed values, a difficulty pointed out by Freudenthal [32]. Therefore, probability models are often chosen on the basis of convenience. It is difficult to judge such a model with any degree of confidence, and the probabilities thus obtained are somewhat uncertain. In spite of these difficulties, classical reliability theory has served as the basis for some design code proposals.

1.2.2 Extension

For a design concept based on an acceptable risk, Eq. 1.1 serves

as a fundamental starting point. It has been recognized [9], however, that an extension is necessary in order to resolve the questions of sensitivity and consistency arising from an imperfect state of knowledge. Bolotin [17] notes that a risk measure is a characteristic of a random event, and is useful in a comparative rather than an absolute sense. It is necessary, then, that a viable basis for design should utilize the information that is available as consistently as possible, with the primary objective of obtaining a basis for comparison between design alternatives.

Provisions must be made for the statistical treatment of the data that are inherently random. This should allow the use of particular distributions for modeling R and S as suggested by available data. In other cases, the method should permit the use of arbitrary distributions with the knowledge that the modeling error thus introduced is acceptably small. Uncertainties in prediction and modeling must be included explicitly in the formulation of design. The delineation between the two basic types of information is convenient, and sometimes even necessary, for evaluating the uncertainty measures.

A model has been developed by Ang and others [10, 11] which accomplishes these objectives. In its basic form, a judgment factor is added to the classical reliability format to reflect the effect of imponderables on the associated risk. This is termed the "extended reliability model," and will form the basis for the safety analyses performed in this study.

1.3 Objectives and Scope of Present Study

The purpose of this investigation is to illustrate how a design

format based on an acceptable risk criterion might be developed. The extended reliability model is used as the basis. An attempt is made to give structural reliability analysis a sense of perspective.

Since present codes are formulated on an individual member basis, efforts are directed at designing individual components for a prescribed reliability. For illustrative purposes, the development will be made for simple reinforced concrete members. Strength provisions only are considered, although the theory can just as easily be applied to other requirements as well. It is then possible to make a comparison between risk-based design criteria and current design code provisions, such as the American Concrete Institute (ACI) Standard Building Code [5] which governs present reinforced concrete designs in the USA.

Chapter 2 presents a discussion of the extended reliability model. As the existing formulation is restricted to the simplest case of single resistance and load, an extension is made to account for the more realistic multiple loading case found in practice. It is shown how the basic variabilities and prediction errors may be handled in a consistent manner.

Chapter 3 contains the formulation of the flexural and shear resistance models for a concrete beam with tension reinforcement and a model for studying columns subjected to eccentric loading. An analysis of the first and second order statistics is made from existing data, and the sensitivity of the resistances in the different modes to their dependent variables is investigated.

Chapter 4 considers load models for permanent, short, and long term gravity loads, and lateral wind loads. The purpose is to obtain

representative statistics from existing load surveys from which the implied reliability of existing designs may be studied. This reliability analysis is performed in Chapter 5, where designs obtained from current ACI code requirements are evaluated from the standpoint of the underlying risk.

Chapter 6 contains some practical recommendations for the development of reliability-based design criteria.

It is hoped that this study will aid in the transition from a deterministic format to one based on acceptable risk by indicating what levels of safety (in terms of risks) are implied in current standards, and by suggesting representative statistical values appropriate for typical design situations. Progress toward implementation of a risk based code has been slow due partly to a seeming dichotomy between the complexity of a rigorous probabilistic analysis and the need for a simple form for design standards. This is unfortunate because probabilistic analysis can be the underlying basis for the formulation of design provisions, and yet the form of the design standard can remain unchanged.

1.4 Notation

The following notation is used herein:

D	random variable describing dead load (psf units).
$F_X(x)$	cumulative probability distribution function of X.
L	random variable describing live load (psf units).
N	random variable representing required judgment.
Pr(E)	probability of event E.
p_f	probability of failure.

p_o risk measure associated with basic variability defined in Sec. 2.1.2.

p_s risk measure associated with errors in prediction defined in Sec. 2.1.2.

R random variable describing member resistance.

S_i random load effect from load i.

W random variable describing wind load (psf units).

$w(\bar{\theta})$ generalized load factor defined in Sec. 2.1.3.

$\bar{X}$ predicted mean value of random variable X.

X' nominal value of random variable X, defined at some cumulative probability level.

$f_X(x)$ probability density function of X.

β the number of standard deviations above the mean of a variate, denoted the safety index.

β_o $\Phi^{-1}(1 - p_o)$

γ, γ_i central factors of safety.

Δ_X measures of prediction error in X.

Δ total prediction error in R and S.

δ_X coefficient of variation (c.o.v.) of X.

δ total basic variability in R and S.

θ ratio of mean load effects; e.g., mean live load to dead load ratio.

μ_X mean value of X.

ν factor of engineering judgment used in design.

σ_X standard deviation of X.

$\Phi(x)$ standard normal probability distribution function evaluated at x.

$\Phi^{-1}(p)$ the standard normal variable corresponding to a cumulative probability level p.

Ω_X total uncertainty in X, equal to $\sqrt{\delta_X^2 + \Delta_X^2}$.

Chapter 2

THEORETICAL FORMULATIONS

2.1 Extended Reliability Concept

2.1.1 Basic Formulation

The classical formulation of Sec. 1.2.1 can be generalized [10,11] to include the prediction errors explicitly by multiplying R and S in Eq. 1.1 by factors of engineering judgment N_R and N_S, i.e.,

$$\hat{R} = N_R R$$

$$\hat{S} = N_S S$$

The uncertainties in R and S are those associated with their inherent randomness. Their first and second order statistical properties can be determined from available data, and some probability distributions may then be assumed to model their natural variability. Because of errors in prediction, modeling, and estimation of the parameters, the assumed distributions of R and S may not be correct. The purpose of N_R and N_S is to compensate for the above errors. Presumably, then, $\hat{R}$ and $\hat{S}$ are the true resistance and load, respectively. The correct values of N_R and N_S are unknown, and hence N_R and N_S may be assumed to be random variables; the probabilities associated with these factors are necessarily judgmental [46].

Failure is then defined as $\{\hat{R} < \hat{S}\}$, and the probability of failure becomes

$$p_f = Pr(\hat{R} < \hat{S}) = Pr(N_R R < N_S S)$$

or, equivalently, with $N = N_S/N_R$,

$$p_f = Pr(R < NS) \tag{2.1}$$

where N represents the required overall "judgment factor." Assuming that R, S, and N are statistically independent,

$$p_f = \int_N Pr(R < nS)\ f_N(n)\ dn \tag{2.2}$$

From this relationship, design equations similar to Eq. 1.2 or 1.3 may be obtained.

In the implementation of this concept, it is assumed that errors in modeling and prediction are limited to errors in the predicted mean values of R and S, i.e., $\overline{R}$ and $\overline{S}$. As the true means may be either greater or less than those obtained from the data, it is assumed that the correct means of $\hat{R}$ and $\hat{S}$ can be approximated by their predicted means, $\overline{R}$ and $\overline{S}$. It then may be shown [10] that the mean judgment factor is

$$\overline{N} = E(N) = 1.0 \tag{2.3}$$

with c.o.v.

$$\Delta = \Delta_N = \sqrt{\Delta_R^2 + \Delta_S^2} \tag{2.4}$$

where Δ_R and Δ_S are prediction errors representing the uncertainties in the predicted mean values $\overline{R}$ and $\overline{S}$, respectively, and Δ_N is the combined prediction error. The distribution of N cannot be determined, and in the sequel it is assumed to be lognormal for convenience. Also note that a more elaborate treatment of the prediction errors than the above second moment approach would not be warranted.

With the introduction of the random variable N, the basic randomness and prediction errors may be treated separately. The statistics of R and S need not include prediction errors, and their probability laws may differ from that assumed for N. In the limiting case where N is unity with probability one, Eqs. 2.1 and 2.2 reduce to the classical reliability formulation. This is tantamount to assuming that there are no modeling and prediction errors present.

Designs in terms of the central factor of safety $\gamma = \overline{R}/\overline{S}$ obtained on the basis of Eq. 2.1 are shown in Fig. 2.1. As in the classical reliability analysis, these designs are not too sensitive to distributions when $p_f \geq 10^{-4}$, but when $p_f \leq 10^{-5}$, the designs are again quite distributionally sensitive. This is not surprising, for if NS is replaced by some variable S^* in Eq. 2.1, the equation has the same form as Eq. 1.1 and the difficulties associated therewith would be expected. The problem of distributional sensitivity must still be resolved if the risk model is to be useful for design.

One way to circumvent the sensitivity question is to specify that a comparative estimate of the design risk be obtained on the basis of prescribed distributions for R and S, as well as N_R and N_S. This provides a convenient basis for comparison between design alternatives; however, there will no longer be any flexibility for treating arbitrary distributions for R and S.

If R and S, as well as N_R and N_S, are prescribed to independent lognormals, $\hat{R}$ and $\hat{S}$ are also lognormals, with total uncertainties

$$\Omega_R = \sqrt{\delta_R^2 + \Delta_R^2}$$
$$\Omega_S = \sqrt{\delta_S^2 + \Delta_S^2} \qquad (2.5)$$

where δ_R and δ_S are measures of the basic variabilities in R and S, and Δ_R and Δ_S are measures of the prediction errors in $\overline{R}$ and $\overline{S}$. The risk of failure is then

$$p_f = 1 - \Phi \left[\frac{\ln \left[\overline{R}/\overline{S} \dfrac{\sqrt{1 + \Omega_S^2}}{\sqrt{1 + \Omega_R^2}} \right]}{\sqrt{\ln \left[(1 + \Omega_R^2)(1 + \Omega_S^2) \right]}} \right] \tag{2.6}$$

If Ω_R and Ω_S are not too large, say less than 0.30, Eq. 2.6 becomes

$$p_f \simeq 1 - \Phi \left[\frac{\ln(\overline{R}/\overline{S})}{\sqrt{\Omega_R^2 + \Omega_S^2}} \right] \tag{2.6a}$$

where $\Phi(x)$ is the standard normal probability distribution function. Conversely, to determine the design corresponding to a specified risk p_f, an inversion of Eq. 2.6a yields the required mean load factor as

$$\gamma = \overline{R}/\overline{S} \simeq \exp \left[\sqrt{\Omega_R^2 + \Omega_S^2}\, \Phi^{-1} (1 - p_f) \right] \tag{2.7}$$

in which $\Phi^{-1}(p)$ is the inverse of $\Phi(x)$ at probability p.

The delineation between basic randomness and errors in prediction also serves as a basis for the development of the following "alternative risk model." This is intended to permit the use of any suitable distributions (e.g., favored by available data), and to circumvent the question of distributional sensitivity.

2.1.2 Alternative Risk Measure

It may be observed from Fig. 2.1 that if designs are based on

probability measures of 10^{-4} or greater, the distribution sensitivity of designs becomes much less pronounced. In this case, the choice of distributions for R and S becomes less significant, and convenient substitutions can be made when necessary.

The measure of risk developed by Ang and Ellingwood [11] is based on this observation. It is given as

$$p_f = Pr(R < \nu S) \cdot Pr(N > h\nu) \tag{2.8}$$

in which ν is a specific value of N used in design, and h is a parameter introduced to obtain

$$Pr(R < \nu S) \cdot Pr(N > h\nu) \simeq Pr(R < NS) \tag{2.9}$$

The first part of Eq. 2.8,

$$p_o = Pr(R < \nu S) \tag{2.10}$$

may be defined as a measure of the risk associated with basic randomness, whereas the second part

$$p_s = Pr(N > h\nu) \tag{2.11}$$

is a probability associated with the prediction errors.

Assume, for convenience, that N, R, and S are lognormal; then the solution of Eq. 2.9 for h yields

$$h \simeq \exp\left[\Delta\, \Phi^{-1}(1 - p_s) + \delta\, \Phi^{-1}(1 - p_o) - \sqrt{\delta^2 + \Delta^2}\, \Phi^{-1}(1 - p_f)\right]$$

from which ν can be found from Eq. 2.11. For small c.o.v., say less than about 0.30,

$$\nu \simeq \exp\left[\sqrt{\Delta^2 + \delta^2}\,\Phi^{-1}(1 - p_f) - \delta\,\Phi^{-1}(1 - p_o)\right] \qquad (2.12)$$

where

$\delta = \sqrt{\delta_R^2 + \delta_S^2}$ is the total variability

$\Delta = \sqrt{\Delta_R^2 + \Delta_S^2}$ is the total prediction error

Although Eq. 2.12 is derived from a lognormal assumption, the resulting ν will be used for other distributions of R and S. Then, using Eq. 2.10, the required mean resistance is

$$\overline{R} = \gamma\,\overline{S} \qquad (2.13)$$

where γ is a function of ν, p_f, δ_R, and δ_S. Alternatively,

$$\overline{R} = \nu\overline{S} + \beta_o\sqrt{\sigma_R^2 + \nu^2\sigma_S^2} \qquad (2.14)$$

in which $\beta_o = \Phi^{-1}(1 - p_o)$. A comparison of Figs. 2.1 and 2.2 indicates the reduction in distribution sensitivity when the alternative risk measure is employed; this is simply due to the fact that once ν has been determined, the designs are found from Eq. 2.10, in which p_o is generally greater than 10^{-4}, although $p_f = p_o \cdot p_s$ may still be 10^{-6} or less.

It is reasonable to assume that if the basic variability δ is much larger than the prediction error Δ, the risk associated with the basic randomness should be less than that associated with modeling, and conversely. Furthermore, if δ and Δ are of the same order, the risk associated with each part should be about the same. Accordingly, it may be assumed that

$$p_o = (p_f)^{\frac{\delta}{\Delta+\delta}}$$

$$p_s = (p_f)^{\frac{\Delta}{\Delta+\delta}} \qquad (2.15)$$

For example, if $\Delta = 0$, implying no prediction error, $p_o = p_f$ and Eq. 2.12 yields $\nu = 1.0$; hence, the classical formulation is obtained.

2.1.3 The Case of Multiple Loads

The actions induced on a member are normally the result of several externally applied forces; each load may be random, with its own statistics and probability distribution. It is useful to be able to study their effects separately and in combinations. To this end, the alternative risk may be generalized as follows:

$$p_f = Pr(R < \nu(S_1 + S_2 + \ldots)) \cdot Pr(N > h\nu) \qquad (2.16)$$

in which everything else of the preceding section remains applicable. In particular, ν is calculated from Eq. 2.12, in which the determination of δ and Δ includes the uncertainties associated with all the variables in Eq. 2.16.

The question of distributional sensitivity is even more important in the multiple load case. The evaluation of Eq. 2.16 requires integration of the joint density of R, S_1, S_2. . . Generally, this integration must be performed numerically and rapidly becomes intractable as the number of variables increases. An important exception is when all variables are normal; their resulting linear combination is then normal, and probabilities

associated therewith may be easily evaluated. It will be useful to verify that the distributional insensitivity illustrated in Sec. 2.1.2 carries over to the multiple load case.

A well known result of probability theory states that if n random variables X_i, i = 1, n, are normal and mutually independent, then their sum

$$X = \sum_{i=1}^{n} X_i$$

is also normal, with mean and variance

$$\overline{X} = \sum_{i=1}^{n} \overline{X}_i$$

$$\sigma_X^2 = \sum_{i=1}^{n} \sigma_{X_i}^2$$

It follows that

$$p_o = Pr(R < \nu(S_1 + S_2 + \ldots)) = \Phi\left[- \frac{\overline{R} - \nu(\overline{S}_1 + \overline{S}_2 + \ldots)}{\sqrt{\sigma_R^2 + \nu^2(\sigma_{S_1}^2 + \sigma_{S_2}^2 + \ldots)}} \right] \quad (2.17)$$

where ν is given by Eq. 2.12. In terms of the central load factors, the required mean value of R is

$$\overline{R} = \gamma_1 \overline{S}_1 + \gamma_2 \overline{S}_2 + \ldots + \gamma_n \overline{S}_n \quad (2.18)$$

In order to generalize the solution as far as possible, define the load ratios,

$$\theta_k = \overline{S}_k / \overline{S}_1 \; ; \qquad k = 2, \ldots, n \quad (2.19a)$$

and

$$w(\overline{\theta}) = \gamma_1 + \gamma_2\theta_2 + \ldots + \gamma_n\theta_n \tag{2.19b}$$

Then substituting Eqs. 2.18 and 2.19 into Eq. 2.17 yields

$$p_o = \Phi\left[- \frac{w(\overline{\theta}) - \nu(1 + \theta_2 + \ldots + \theta_n)}{\sqrt{(w(\overline{\theta}))^2 \delta_R^2 + \nu^2(\delta_{S_1}^2 + \theta_2^2 \delta_{S_2}^2 + \ldots + \theta_n^2 \delta_{S_n}^2)}} \right] \tag{2.20}$$

in which $w(\overline{\theta})$ is the only unknown. Inverting this yields

$$w(\overline{\theta}) = \nu \frac{(1 + \theta_2 + \ldots + \theta_n)}{(1 - \beta_o^2 \delta_R^2)} + \nu \frac{\beta_o \sqrt{(1 + \theta_2 \ldots + \theta_n)^2 \delta_R^2 + (\delta_{S_1}^2 + \theta_2^2 \delta_{S_2}^2 + \ldots + \theta_n^2 \delta_{S_n}^2)(1 - \beta_o^2 \delta_R^2)}}{(1 - \beta_o^2 \delta_R^2)} \tag{2.21}$$

For a specified p_o, the corresponding value of $w(\overline{\theta})$ may be found.

When only one load is present, $\theta_k = 0$, for $k = 2, \ldots, n$, and $w(\overline{\theta})$ reduces to the load factor discussed in the preceding sections. For non-zero θ_k, the separate load factors $\gamma_1, \gamma_2, \ldots, \gamma_n$ are not uniquely determined for a given risk level. This is true for any distributions; the load factors are coupled by the requirement of a specified reliability, Eq. 2.16. Therefore, any set of $(\gamma_1, \gamma_2, \ldots \gamma_n)$ that satisfies Eq. 2.21 will yield designs with precisely the same reliability.

Current specifications increase the design loads separately, through applying load factors, to values where the likelihood of exceedance is sufficiently small. In a deterministic context, the only way to reflect the

greater uncertainty in a particular load is to increase the load factor associated with it. In a statistical sense, the true measure of safety is the risk of failure associated with the sum of all loading effects. This suggests that it is sufficient to apply one overall load factor to the sum of the load effects. If one load contains more uncertainty than others, this is reflected in its uncertainty measure, and this contributes more to the overall load factor.

However, if it is deemed desirable to retain the multiple load factor format for consistency with current deterministic criteria, suitable values of $(\gamma_1, \gamma_2, \ldots, \gamma_n)$ that satisfy Eq. 2.21 may be obtained as follows. Equation 2.20 is inverted to yield,

$$\gamma_1 + \gamma_2\theta_2 + \ldots + \gamma_n\theta_n = \nu(1 + \theta_2 + \ldots + \theta_n) + \beta_o\sqrt{(\gamma_1 + \gamma_2\theta_2 + \ldots \gamma_n\theta_n)^2\delta_R^2 + \nu^2(\delta_{S_1}^2 + \theta_2^2\delta_{S_2}^2 + \ldots + \theta_n^2\delta_{S_n}^2)}$$

Such an equation applies also to nonnormal variates, with appropriate β_o. Introducing

$$\alpha = \frac{\sqrt{(\gamma_1 + \gamma_2\theta_2 + \ldots + \gamma_n\theta_n)^2\delta_R^2 + \nu^2(\delta_{S_1}^2 + \theta_2^2\delta_{S_2}^2 + \ldots + \theta_n^2\delta_{S_n}^2)}}{(\gamma_1 + \gamma_2\theta_2 + \ldots + \gamma_n\theta_n)\delta_R + \nu(\delta_{S_1} + \theta_2\delta_{S_2} + \ldots + \theta_n\delta_{S_n})} \quad (2.22a)$$

we have,

$$(\gamma_1 + \gamma_2\theta_2 + \ldots + \gamma_n\theta_n)$$

$$= \nu(1 + \theta_2 + \ldots + \theta_n)$$

$$+ \beta_o\alpha[(\gamma_1 + \gamma_2\theta_2 + \ldots + \gamma_n\theta_n)\delta_R + \nu(\delta_{S_1} + \theta_2\delta_{S_2} + \ldots + \theta_n\delta_{S_n})]$$

or

$$\gamma_1(1 - \beta_o\alpha\delta_R) + \gamma_2(1 - \beta_o\alpha\delta_R)\theta_2 + \ldots$$

$$= \nu(1 + \beta_o\alpha\delta_{S_1}) + \nu(1 + \beta_o\alpha\delta_{S_2})\theta_2 + \ldots$$

Equating coefficients of θ_k yields

$$\gamma_k = \nu \frac{1 + \beta_o\alpha\delta_{S_k}}{1 - \beta_0\alpha\delta_R} \tag{2.22}$$

The overall load factor γ may be found directly from Eq. 2.17. In this form, the design equation is

$$\overline{R} = \gamma(\overline{S}_1 + \overline{S}_2 + \ldots + \overline{S}_n) \tag{2.23}$$

Substituting Eq. 2.23 into Eq. 2.17 and inverting gives

$$\gamma = \nu \frac{(1 + \theta_2 + \ldots + \theta_n)}{(1 + \theta_2 + \ldots + \theta_n)(1 - \beta_o^2\delta_R^2)} + \nu \frac{\beta_o\sqrt{(1 + \theta_2 + \ldots + \theta_n)^2\delta_R^2 + (\delta_{S_1}^2 + \theta_2^2\delta_{S_2}^2 + \ldots + \theta_n^2\delta_{S_n}^2)(1 - \beta_o^2\delta_R^2)}}{(1 + \theta_2 + \ldots + \theta_n)(1 - \beta_o^2\delta_R^2)} \tag{2.24}$$

There is a unique relationship between p_o and γ.

Practically, the use of the separate load factors or the overall load factor will result in exactly the same required mean resistance $\overline{R}$ for a given risk. The results contained herein are presented in terms of the multiple factors for consistency with current design formats. It should be recognized, however, that the specification of a single load factor has certain practical advantages.

The sensitivity of designs to distributions is illustrated below for two loads. The expressions used in evaluating the nonnormal cases are given in Appendix A. Since the distribution sensitivity of the alternative risk model depends on the level of p_o, it will suffice to examine the behavior of designs obtained from

$$p_o = Pr(R < S_1 + S_2)$$

at risk levels of 10^{-3} or 10^{-4}. Figures 2.3 and 2.4 illustrate the sensitivity of load factor γ_2 and the overall load factor γ to choice of distribution for $\theta_2 = 1.0$. The values are seen to be quite close, except in the case where R is Weibull and S_1 and S_2 are each Frechet. The sensitivity of γ_2 and β_o to variations in δ_R with $p_o = 10^{-3}$ is shown in Figs. 2.5 and 2.6. The results are of approximately the same sensitivity as in the fundamental case [11]. Again, β_o is a function of the statistics of R and S, except in the normal case. Figures 2.7 and 2.8 illustrate the sensitivity of γ_2 and β_o to θ_2. The designs are quite insensitive to this parameter, although there is a slight tendency for γ_2 to decrease with θ_2 for all but one set of distributions. This result indicates that the mean ratio of live to dead

loads is not a significant parameter insofar as calculating the load factors, or the underlying risk, is concerned.

Because of the distributional insensitivity exhibited, the load and resistance quantities in the alternative risk model may suitably be chosen as normal random variables. This assumption is consistent with the amount of information usually available. The normality assumption makes it possible to consider an arbitrary number of design variables without significantly increasing the complexity of the analysis.

Figures 2.9, 2.10 and 2.11 illustrate the variation of γ_L, γ_D, β_o, and ν with parameters δ_R, δ_L, Δ, and $\overline{L}/\overline{D}$, based on the assumption of normal R, S_L, and S_D, with a specified risk of $p_f = 10^{-6}$. The judgment factor ν is insensitive to δ_R, δ_L, and $\overline{L}/\overline{D}$, implying that it could be treated as a constant in a code implementation. γ_L and γ_D are nonlinear with respect to δ_R, but nearly linear with respect to δ_L. Furthermore, γ_D varies only slightly with δ_L, indicating that the load factor coupling is not significant. Note that β_o varies with δ_R, δ_L, and Δ, illustrating that β_o is a function of the risk and the uncertainties, as seen from Eq. 2.15. Figure 2.11 reveals that these design factors are all insensitive to the mean load ratio, indicating that separate provisions for treating $\overline{L}/\overline{D}$ need not be considered in a reliability based code. Changes in γ_L, γ_D, and ν are affected most by changes in δ_R, especially when $\delta_R \geq 0.10$; control of this parameter is, therefore, most important. In all cases, β_o implies that p_o is of the order at which the question of distributional sensitivity does not arise.

2.1.4 Risk Analysis of Existing Designs

It has been demonstrated in Secs. 2.1.2 and 2.1.3 that reliability theory provides a logical basis for the determination of designs. It also furnishes a basis for analyzing the underlying probability of failure of existing designs.

For prescribed lognormal distributions, the analysis phase is relatively simple and straightforward. In a structure with a mean resistance $\overline{R}$ subjected to a total mean load effect $\overline{S}$, the associated risk is given by Eq. 2.6 after the uncertainties Ω_R and Ω_S are determined.

In the case of the alternative risk model, the analysis phase is more involved. Suppose first that the variables are normal. Since ν and p_o are functions of p_f which is unknown, p_o cannot be computed from Eq. 2.20 directly; likewise, β_o in Eq. 2.21 is unknown. It is therefore necessary to solve Eq. 2.20 or its inverse numerically for p_f. The inverse is easier to work with, and is

$$\frac{w(\overline{\theta}) - \nu(1 + \theta_2 + \ldots + \theta_n)}{\sqrt{w^2\delta_R^2 + (\delta_{S_1}^2 + \theta_2^2\delta_{S_2}^2 + \ldots + \theta_n^2\delta_{S_n}^2}} - \beta_o = 0 \qquad (2.25)$$

where ν and β_o are functions of p_f, and $w(\overline{\theta})$ can be determined if the design is specified.

This equation, while admitting only one root for p_f, is highly nonlinear with respect to this variable. The root can be obtained using the Newton-Raphson method of iteration. With

$$f(p_f) = 0,$$

$$p_{f_{i+1}} = p_{f_i} - \frac{f(p_{f_i})}{f'(p_{f_i})} \tag{2.26}$$

In order to avoid calculations with very small numbers, it is preferable to determine the solution in terms of the variable $\log_{10} p_f$; that is, with $x = \log_{10} p_f$, and $f(p_f)$ defined in Eq. 2.25,

$$f(x) = f[p_f(x)] \left|\frac{dp_f}{dx}\right|$$

$$x_{k+1} = x_k - \frac{f(x)}{f'(x)} \tag{2.27}$$

$f'(x)$ must be found numerically, and was computed using Lagrangian interpolation polynomials. Convergence is quite rapid, requiring only a few cycles of iteration; p_f is then obtained by taking the antilogarithm of x.

If the variables are nonnormal, Eqs. 2.25 and 2.26 may still be written for any arbitrary distributions. The determination of p_o and β_o becomes more complex, however. p_o must be evaluated by numerical integration, as in Appendix A, and its inverse β_o must be found by some interpolative scheme; $\partial\beta_o/\partial p_f$ required in Eq. 2.26 must also be found numerically. This numerical integration-interpolation process must be performed for each cycle in the Newton-Raphson iteration, as p_o is not available in standard form except when all variables involved are normally distributed.

2.2 Analysis of Uncertainties

2.2.1 First Order Approximations

In order to use the reliability equations of the previous section, the statistics (i.e., mean and c.o.v.'s) of R, S_1, S_2, ..., as well as the c.o.v.'s of N_R, N_{S_1}, N_{S_2}, ..., must be known. Frequently, these variables are functions of other variables. For example, the flexural capacity of a concrete beam with tension reinforcement is a function of the area and strength of the steel, compressive strength of concrete, and the geometry of the section. Each is a random variable with its own probability distribution and related statistics.

In practice, only the first and second moments may be available; the precise distributions are generally not known. Consequently, the risk must be determined on the basis of convenient distributions or of distributions favored by available data. The main problem, therefore, in the evaluation of risk requires the assessment and analysis of the uncertainties. Although the exact statistical analysis of uncertainties is involved, an approximate analysis is sufficient for practical purposes. This is based on the Taylor series expansion of a function about the mean values of its dependent variables [24,10].

If Y is a function of n random variables X_1, X_2, ..., X_n; i.e.,

$$Y = g(X_1, X_2, \ldots, X_n) \tag{2.28}$$

the Taylor series about the mean value $(\overline{X}_1, \overline{X}_2, \ldots, \overline{X}_n)$ is

$$Y = g(\bar{X}_1, \ldots, \bar{X}_n) + \sum_{j=1}^{n} \left(\frac{\partial g}{\partial X_j}\right)_o (X_j - \bar{X}_j)$$

$$+ \frac{1}{2} \sum_{j=1}^{n} \sum_{k=1}^{n} \left(\frac{\partial^2 g}{\partial X_j \partial X_k}\right)_o (X_j - \bar{X}_j)(X_k - \bar{X}_k) + \ldots \quad (2.29)$$

where the partial derivatives are evaluated at $(\bar{X}_1, \ldots, \bar{X}_n)$. Truncating terms of order two and higher is tantamount to linearizing Y. By assuming that $X_1, \ldots, X_n$ are mutually uncorrelated and taking expectations of both sides, the mean and variance of Y are found as

$$\bar{Y} \simeq g(\bar{X}_1, \ldots, \bar{X}_n) \quad (2.30)$$

$$\sigma_Y^2 \simeq \sum_{j=1}^{n} \left(\frac{\partial g}{\partial X_j}\right)_o^2 \sigma_{X_j}^2 \quad (2.31)$$

If the second order term in Eq. 2.29 is retained, the mean and variance of Y are

$$\bar{Y} \simeq g(\bar{X}_1, \ldots, \bar{X}_n) + \frac{1}{2} \sum_{j=1}^{n} \left(\frac{\partial^2 g}{\partial X_j^2}\right)_o \sigma_{X_j}^2 \quad (2.32)$$

$$\sigma_Y^2 \simeq \sum_{j=1}^{n} \left(\frac{\partial g}{\partial X_j}\right)_o^2 \sigma_{X_j}^2 + \sum_{j=1}^{n} \left(\frac{\partial g}{\partial X_j}\right)_o \left(\frac{\partial^2 g}{\partial X_j^2}\right)_o E[(X_j - \bar{X}_j)^3]$$

$$+ \frac{1}{4} \left\{ \sum_{j=1}^{n} \left(\frac{\partial^2 g}{\partial X_j^2}\right)_o^2 E[(X_j - \bar{X}_j)^4] + 4 \sum_{j=1}^{n-1} \sum_{k=j+1}^{n} \left(\frac{\partial^2 g}{\partial X_j^2}\right)_o \left(\frac{\partial^2 g}{\partial X_k^2}\right)_o \sigma_{X_j}^2 \sigma_{X_k}^2 \right.$$

$$\left. - \sum_{j=1}^{n} \left(\frac{\partial^2 g}{\partial X_j^2}\right)_o^2 \sigma_{X_j}^4 \right\} \quad (2.33)$$

In this case, it is necessary to have the third and fourth moments of X_j to

evaluate σ_Y; however, these are usually unavailable in practice. If all X_j are normal,

$$E[(X_j - \overline{X}_j)^3] = 0$$

$$E[(X_j - \overline{X}_j)^4] = 3\sigma_{X_j}^4$$

and the variance of Y then becomes

$$\sigma_Y^2 \simeq \sum_{j=1}^{n} \left(\frac{\partial g}{\partial X_j}\right)_o^2 \sigma_{X_j}^2 + \sum_{j=1}^{n-1} \sum_{k=j+1}^{n} \left(\frac{\partial^2 g}{\partial X_j^2}\right)_o \left(\frac{\partial^2 g}{\partial X_k^2}\right)_o \sigma_{X_j}^2 \sigma_{X_k}^2$$

$$+ \frac{1}{2} \sum_{j=1}^{n} \left(\frac{\partial^2 g}{\partial X_j^2}\right)_o^2 \sigma_{X_j}^4 \qquad (2.34)$$

If the c.o.v. of X_j are not large, and Eq. 2.28 is not highly nonlinear, Eqs. 2.30 and 2.31 are sufficient for estimating the mean and variance (or c.o.v.) of Y. As an example, consider the flexural equation of a reinforced concrete beam. The derivatives and c.o.v. are given in Chapter 3; the purpose here is to indicate the error typically associated with neglecting higher order terms. Using Eqs. 2.30 and 2.31,

$$\overline{M}_T = 0.879\, \overline{A}_s\, \overline{f}_y\, \overline{d}$$

$$\sigma_{M_T}^2 = 0.010020\, (\overline{A}_s\, \overline{f}_y\, \overline{d})^2$$

Using Eqs. 2.32 and 2.34,

$$\overline{M}_T = 0.876\, \overline{A}_s\, \overline{f}_y\, \overline{d}$$

$$\sigma^2_{M_T} = 0.010032\ (\overline{A}_s\ \overline{f}_y\ \overline{d})^2$$

The differences are clearly not significant. Equations 2.30 and 2.31 are used in the sequel to estimate the means, and uncertainty measures necessary for evaluating Eq. 2.16.

The predicted mean value of the resistance or load may be found from Eq. 2.30, and its basic variability (c.o.v.) by rewriting Eq. 2.31 as

$$\delta_Y^2 \simeq \sum_{j=1}^{n} c_j^2\ \delta_{X_j}^2 \tag{2.35}$$

in which

$$c_j = \frac{1}{\overline{Y}}\ \left(\frac{\partial g}{\partial X_j}\right)_o\ \overline{X}_j \tag{2.36}$$

The prediction errors may be attributed entirely to the errors in the mean prediction; that is, the estimator of the true mean μ_{X_j} is considered a random variable. Effectively, this means [10]

$$N_j \tilde{=} \mu_{X_j}/\overline{X}_j$$

with mean 1 and variance Δ_j^2. The true mean of Y may be written approximately as

$$\mu_Y \simeq g(N_1\overline{X}_1,\ N_2\overline{X}_2,\ \ldots,\ N_n\overline{X}_n) \tag{2.37}$$

The prediction error in μ_Y is found by expanding Eq. 2.39 about $(\overline{N}_1,\ \overline{N}_2,\ \ldots,\ \overline{N}_n)$. The result is

$$E[\mu_Y] \simeq \overline{Y} \tag{2.38}$$

$$\Delta_{\mu_Y}^2 = \frac{1}{\bar{Y}^2} \sum_{j=1}^{n} \left(\frac{\partial g}{\partial N_j}\right)_o^2 \Delta_j^2 \tag{2.39}$$

Now, since

$$\left(\frac{\partial g}{\partial N_j}\right)_o = \bar{X}_j \left(\frac{\partial g}{\partial X_j}\right)_o$$

and $\Delta_{\mu_Y} = \Delta_Y$, the prediction error in Y is

$$\Delta_Y^2 = \sum_{j=1}^{n} c_j^2 \Delta_j^2 \tag{2.40}$$

where c_j are the same constants defined in Eq. 2.36.

2.2.2 Estimation of Uncertainties

For purposes of analysis and design, the mean and variance of a variable are estimated from whatever data is available. Since the true mean is unknown, a prediction error, Δ, is assigned to the predicted mean, to account for inaccuracies in its estimation. If information is available to evaluate the accuracy of the estimated mean, a rough estimate of Δ may be obtained from this information.

For example, suppose an engineer specifies that a certain parameter X, which has random characteristics, should have the value $\bar{x}$ in the design of a certain product, and a number of these products are fabricated on this basis. When a sample of the products is evaluated after their fabrication, it is found that the values of X actually obtained take on a number

of values, $x_1, x_2, \ldots, x_n$, in which $x_j \neq \bar{x}$ in general, and also in which their mean $\hat{\mu}_X \neq \bar{x}$. The variability of $(x_1, \ldots, x_n)$ about $\hat{\mu}_X$ is a measure of the basic randomness of X. The difference between $\hat{\mu}_X$ and $\bar{x}$ is a measure of the error in mean value prediction. When a number of samples are taken, sample means of each may be computed, in which $\hat{\mu}_{X_j} \neq \bar{x}$ in general. The means $\hat{\mu}_{X_j}$ define a histogram for the true mean μ_X, of which the second order statistic yields the prediction error Δ_X.

Suppose the predicted mean value of a random variable X is denoted $\bar{x}$. The total variance is $E[(X - \bar{x})^2]$, the second moment of X with respect to its predicted mean. The variance about the correct mean, μ_X, is always a minimum mean square value.[27] Hence

$$E[(X - \bar{x})^2] \geq E[(X - \mu_X)^2] \tag{2.41}$$

The difference between these two quantities is a measure of the prediction error associated with the mean value. $E[(X - \bar{x})^2]$ may be written as

$$E[(X - \bar{x})^2] = E[(X - \mu_X + \mu_X - \bar{x})^2]$$

and assuming $E[(X - \mu_X)(\mu_X - \bar{x})] = 0$,

$$E[(\mu_X - \bar{x})^2] = E[(X - \bar{x})^2] - E[(X - \mu_X)^2] \tag{2.42}$$

An estimate of $E[(\mu_X - \bar{x})^2]$ is desired.

Suppose m sets of data are available on X, with n_m independent samples in each set, i.e., $(x_{11}, x_{12}, \ldots, x_{1n_1}), \ldots, (x_{m1}, \ldots, x_{mn_m})$. Then

$$\hat{E}[(\mu_X - \bar{x})^2] \simeq \frac{1}{m} \sum_{i=1}^{m} \frac{1}{n_i} \sum_{j=1}^{n_i} (x_{ij} - \bar{x})^2$$

$$- \frac{1}{m} \sum_{i=1}^{m} \frac{1}{n_i} \sum_{j=1}^{n_i} (x_{ij} - \bar{x}_i)^2 \qquad (2.43)$$

where

$$\bar{x}_i = \frac{1}{n_i} \sum_{j=1}^{n_i} x_{ij}$$

A similar equation arises in the theory of the analysis of variance [27] when it is desired to test hypotheses regarding mean values obtained from different sets of data describing a random phenomenon.

In the most frequent case where only one set of data is available, $m = 1$. Then

$$\hat{E}[(\mu_X - \bar{x})^2] \simeq \frac{1}{n} \sum_{i=1}^{n} (x_i - \bar{x})^2 - \frac{1}{n} \sum_{i=1}^{n} (x_i - \bar{x}_1)^2 \qquad (2.44)$$

The variability is given as

$$\delta_X^2 \simeq \hat{E}[(X - \mu_X)^2]/\bar{x}_1^2 \qquad (2.45)$$

and the prediction error as

$$\Delta_X^2 \simeq \hat{E}[(\mu_X - \bar{x})^2]/\bar{x}_1^2 \qquad (2.46)$$

This provides a rough estimate of the prediction error as a systematic comparison is made between measured and predicted mean values. Intuitively, if the predicted and true values are widely separated, Δ_X will be large, as indicated by Eq. 2.46. This method is useful when $\bar{x}$ in Eq. 2.42 is well

defined, e.g., when test data corresponding to specified design values are available. The prediction error may then be estimated by systematically comparing the test data, representing values actually obtained, with the corresponding values originally specified for the design. An example of this will be seen in Sec. 3.2.2, where field measurements for the effective depth of longitudinal reinforcement are compared to the depth specified on the working drawings.

In many situations, the available information may be more limited. In such cases, probabilistic assumptions may be invoked to assess the errors in the predicted mean values. For example, if only the range of the mean is known, an estimate of Δ may be obtained by assuming some appropriate distribution for the mean over this range [12], say uniform, and Δ may be found from its second moment.

If no data is available, Δ must be chosen on the basis of intuition and professional judgment. In this case, the choice of Δ would reflect the degree of confidence placed by the engineer in the accuracy of his prediction, and his past experience in similar situations.

Chapter 3

RESISTANCE MODELS

3.1 Objectives and Scope

The purpose of this chapter is to formulate resistance models for flexure, shear, and combined bending and axial thrust for use in the extended reliability formulation. The development is made for reinforced concrete members.

For purposes of this study, member strength is considered to be the governing design criterion. The primary objective is to statistically analyze existing strength equations upon which current ACI provisions are based. Conclusions can then be drawn from which future reliability based codes can be developed. Questions regarding serviceability and stability are not considered, although they can be resolved with the same approach used for strength.

The members are prismatic, and resistances at arbitrary points along a member are assumed to be perfectly correlated. It has been pointed out [14] that within-member variability is insignificant compared to that among separate members. Correlation of strength within a member is usually quite high. The implication is that failure will occur at the point of maximum load effect. Moreover, it is assumed that yield strengths and reinforcing bar areas are also perfectly correlated within a member.

It is assumed that existing expressions for strength upon which present ACI provisions are based are sufficient to determine the random

function describing the resistance. Some of these expressions are entirely empirical in nature. It may be argued, however, that the expressions represent the best current estimate of the strength as a function of the variables known to affect it, and hence should be used to predict its mean value.

The reinforcement is assumed to have an elastic-perfectly plastic stress-strain curve, and strain hardening effects are neglected. The modulus of elasticity E_s is assumed constant. The reinforcement stress-strain curve is hence statistically defined by the yield strength variable f_y. Data for steel strength is usually available only in terms of its yield stress [38]. Moreover, the variation in E_s is small [1].

3.2 Flexure

3.2.1 Equations of Flexural Capacity

The beam is assumed to be reinforced in tension only. The equation for the flexural capacity may be derived from conditions of equilibrium, together with assumptions discussed elsewhere [16,58]. It is

$$M = A_s f_s d \left(1 - \eta \frac{A_s}{bd} \frac{f_s}{f_c}\right) \qquad (3.1)$$

in which $\eta = k_2/k_1k_3$, a factor describing the concrete stress block properties. If the reinforcement yields before the concrete reaches its limiting strain, a tension failure occurs and $f_s = f_y$. If the concrete reaches its limiting strain before the steel yields, a compression failure occurs; the reinforcement stress is found by solving a strain compatibility equation simultaneously with the steel stress-strain curve. The solution is

$$f_s = \sqrt{\left(\frac{E_s \varepsilon_{cu}}{2}\right)^2 + k_1 k_3 f_c E_s \varepsilon_{cu} \frac{bd}{A_s}} - \frac{1}{2} E_s \varepsilon_{cu} \qquad (3.2)$$

The moment capacity is given by substituting this f_s into Eq. 3.1. In practice, this kind of failure is to be avoided.

The reinforcement ratio is defined as

$$p = \frac{A_s}{bd} \qquad (3.3)$$

The value of p at which the steel reaches yield and the concrete reaches its ultimate strain simultaneously is denoted the balanced reinforcement ratio, p_b, and is

$$p_b = k_1 k_3 \frac{f_c}{f_y} \frac{E_s \varepsilon_{cu}}{E_s \varepsilon_{cu} + f_y} \qquad (3.4)$$

In the ACI provisions, a tension failure is assured by requiring that $p \leq 0.75 p_b'$, computed deterministically. However, p and p_b are random variables, and hence there is a risk of a compression failure even when the beam is designed to fail in tension. This has actually been observed [26]. It occurs because variations in steel and concrete strength are sufficient to produce sections where the actual balanced reinforcement ratio is less than the one specified for design.

For a reliability based design, the value of p_b must be less than p with an acceptably small probability α_b, i.e.,

$$Pr(\hat{p}_b < \hat{p}) \leq \alpha_b \qquad (3.5)$$

Assuming lognormal $\hat{p}_b$ and $\hat{p}$,

$$\alpha_b \simeq \Phi\left[\frac{\ln\ (\overline{p}/\overline{p}_b)}{\sqrt{\Omega_p^2 + \Omega_{p_b}^2}}\right] \tag{3.5a}$$

This equation serves as a basis for selecting a reinforcement ratio for design. The required mean value $\overline{p}$ satisfying the above is

$$\overline{p} \simeq \overline{p}_b \exp\ [\ \sqrt{\Omega_p^2 + \Omega_{p_b}^2}\ \ \Phi^{-1}\ (\alpha_b)\ ] \tag{3.6}$$

where the statistics of p and p_b are found from methods of Sec. 2.2.1 as

$$\overline{p} = \frac{\overline{A}_s}{\overline{b}\ \overline{d}} \tag{3.7}$$

$$\Omega_p^2 = \Omega_{A_s}^2 + \Omega_b^2 + \Omega_d^2 \tag{3.8}$$

$$\overline{p}_b = \overline{k_1 k_3}\ \frac{\overline{f}_c}{\overline{f}_y}\ \ \frac{E_s\ \overline{\varepsilon}_{cu}}{E_s \overline{\varepsilon}_{cu} + \overline{f}_y} \tag{3.9}$$

$$\Omega_{p_b}^2 = \left(\frac{E_s \overline{\varepsilon}_{cu} + 2\overline{f}_y}{E_s \overline{\varepsilon}_{cu} + \overline{f}_y}\right)^2 \Omega_{f_y}^2 + \Omega_{f_c}^2 + \Omega_{k_1 k_3}^2 + \left(\frac{\overline{f}_y}{E_s \overline{\varepsilon}_{cu} + \overline{f}_y}\right)^2 \Omega_{\varepsilon_{cu}}^2 \tag{3.10}$$

The failure of a reinforced concrete beam may be described as

$$\{\text{Failure}\} = \{\text{Failure in Tension} \bigcup \text{Failure in Compression}\}$$

These events are assumed to be mutually exclusive and collectively exhaustive.

Hence by the theorem of total probability,

$$\Pr(\text{Failure}) = \Pr(\text{Failure}|\hat{p} \leq \hat{p}_b) \cdot \Pr(\hat{p} \leq \hat{p}_b) + \Pr(\text{Failure}|\hat{p} > \hat{p}_b) \cdot \Pr(\hat{p} > \hat{p}_b) \quad (3.11)$$

where the probabilities of failure are computed by Eq. 2.8 or Eq. 2.16, i.e.,

$$\Pr(\text{Failure}|\hat{p} \leq \hat{p}_b) = \Pr(M_T \leq \nu_T(S_1 + \ldots)) \Pr(N_T \geq h\nu_T) \quad (3.12)$$

$$\Pr(\text{Failure}|\hat{p} > \hat{p}_b) = \Pr(M_C \leq \nu_C(S_1 + \ldots)) \Pr(N_C \geq h\nu_C) \quad (3.13)$$

It will subsequently be demonstrated that if α_b in Eq. 3.5 is chosen sufficiently small,

$$\Pr(\text{Failure}|\hat{p}_b < \hat{p}) \cdot \Pr(\hat{p}_b < \hat{p}) << \Pr(\text{Failure}|\hat{p} \leq \hat{p}_b) \cdot \Pr(\hat{p} \leq \hat{p}_b) \quad (3.14)$$

and reliability based designs may be found from consideration of tension failures only.

3.2.2 Analysis of Uncertainties

Influence of Uncertainties of Individual Variables

The first and second order statistics of the flexural capacity M are found by applying the methods of Sec. 2.2.1. For a beam failing in a tension mode,

$$M_T = A_s f_y d \left(1 - \eta \frac{A_s}{bd} \frac{f_y}{f_c}\right) \quad (3.15)$$

where A_s, f_y, f_c, b, d, and η are all random variables. The predicted mean value of M_T is

$$\overline{M}_T = \overline{A}_s \overline{f}_y \overline{d} \left(1 - \overline{\eta} \frac{\overline{A}_s}{\overline{b}\,\overline{d}} \frac{\overline{f}_y}{\overline{f}_c}\right) \tag{3.16}$$

Its corresponding variability is,

$$\delta^2_{M_T} = \left(\frac{1 - 2\overline{\eta}q}{1 - \overline{\eta}q}\right)^2 (\delta^2_{f_y} + \delta^2_{A_s}) + \left(\frac{\overline{\eta}\,q}{1 - \overline{\eta}\,q}\right)^2 (\delta^2_{f_c} + \delta^2_b + \delta^2_\eta) + \left(\frac{1}{1 - \overline{\eta}\,q}\right)^2 \delta^2_d \tag{3.17}$$

where

$$q = \overline{p} \frac{\overline{f}_y}{\overline{f}_c} \tag{3.18}$$

Δ_{M_T} may be found by replacing the δ's of each variable in Eq. 3.17 with the corresponding Δ's.

The mean and variability of the capacity of a beam failing in compression are estimated by first finding the statistics for f_s from Eq. 3.2:

$$\overline{f}_s = \sqrt{\left(\frac{E_s \overline{\varepsilon}_{cu}}{2}\right)^2 + \overline{k_1 k_3}\ \overline{f}_c E_s \overline{\varepsilon}_{cu} \frac{\overline{b}\,\overline{d}}{\overline{A}_s}} - \frac{1}{2} E_s \overline{\varepsilon}_{cu} \tag{3.19}$$

$$\delta^2_{f_s} = g_1^2 (\delta^2_{f_c} + \delta^2_{A_s} + \delta^2_b + \delta^2_d + \delta^2_{k_1 k_3}) + g_2^2 \delta^2_{\varepsilon_{cu}} \tag{3.20}$$

where

$$g_1 = \frac{E_s \overline{\varepsilon}_{cu} \overline{k_1 k_3}\ \overline{f}_c}{2\,\overline{p}\,\overline{f}_s\, g_3}$$

$$g_2 = g_1 + \frac{1}{\bar{f}_s}\left[\frac{1}{g_3}\left(\frac{E_s\bar{\varepsilon}_{cu}}{2}\right)^2 - \frac{1}{2}E_s\bar{\varepsilon}_{cu}\right]$$

$$g_3 = \sqrt{\left(\frac{E_s\bar{\varepsilon}_{cu}}{2}\right)^2 + E_s\bar{\varepsilon}_{cu}\,\overline{k_1k_3}\,\frac{\bar{f}_c}{\bar{p}}}$$

Then replace $\bar{f}_y$ with $\bar{f}_s$ in Eq. 3.18 and δ_{f_y} (Δ_{f_y}) with δ_{f_s} (Δ_{f_s}) in Eq. 3.17 to find δ_{M_C} (Δ_{M_C}) from Eq. 3.17.

The uncertainties in the different variables above contribute to the uncertainty in M_T or M_C; however, their contributions are not uniform. The sensitivity of $\bar{M}_T$, δ_{M_T} and Δ_{M_T} (or statistics of M_C) to their component variables may be analyzed by studying the behavior of the coefficients in Eq. 3.17. These coefficients indicate the local variation of M_T with respect to a parameter at their respective mean values, e.g.,

$$\frac{dM_T}{\bar{M}_T}\Big/\frac{df_y}{\bar{f}_y} = \frac{1 - 2\bar{\eta}\,q}{1 - \bar{\eta}\,q} \qquad (3.21)$$

Their behavior is illustrated as a function of q in Fig. 3.1. A small value of q implies a lightly reinforced section, low steel yield strength, or high concrete compressive strength.

For lightly reinforced sections, the mean flexural capacity $\bar{M}_T$ is affected most by the accuracy of the estimated values of $\bar{f}_y$, $\bar{A}_s$, and $\bar{d}$; errors in $\bar{f}_c$, $\bar{b}$, and $\bar{\eta}$ will have less effect. As the amount of reinforcement is increased, these parameters and $\bar{d}$ become more significant. For a given ratio $\bar{f}_y/\bar{f}_c$, this implies that $\bar{p}$ is approaching $\bar{p}_b$, and the likelihood of a compression failure is increased.

Uncertainties in M_T, i.e., δ_{M_T} and Δ_{M_T}, depend primarily on the respective uncertainties in f_y, A_s, and d. The coefficients for all parameters except d are less than unity; the effect of such a coefficient is to reduce the contribution of the associated variability or prediction error. For small values of $\bar{p}$, it is conceivable that δ_{M_T} will be less than δ_{f_y} or δ_{f_c}. When q is small, δ_{M_T} is relatively insensitive to δ_{f_c}. This implies that poor concrete quality control has a relatively small effect on the variability in flexural capacity. It is clear that poor workmanship, reflected by large variabilities in d, will have a significant effect in increasing the dispersion, especially when $\bar{p}$ is large.

A similar analysis to determine the sensitivity of $\bar{p}_b$ and Ω_{p_b} to their component variables may be performed by studying the coefficients in Eq. 3.10; this is shown in Fig. 3.2. Estimates of $\bar{f}_y$ and Ω_{f_y} are most important in determining $\bar{p}_b$ and Ω_{p_b}; contributions from $\bar{\varepsilon}_{cu}$ and $\Omega_{\varepsilon_{cu}}$ are not significant. The concrete quality, reflected by Ω_{f_c}, may be important to the uncertainties in p_b. This indicates that good concrete quality is significant to flexural design from the standpoint of reducing the probability of failure occurring in the compression mode.

Evaluation of Individual Uncertainty Measures

The purpose of this section is to illustrate how the uncertainties underlying each design parameter may be evaluated from available data.

Information on the steel yield strength f_y is generally available from mill tests. Julian [38] reported data from 171 tests on No. 3 to No. 10 bars with a nominal strength of 40 ksi. Values ranged from 38.95 ksi to 64.9 ksi with a mean of 47.7 ksi and a c.o.v. of 0.12. The c.o.v. is high due to lumping the test results of different bar sizes. Baker's data [14]

for nominal 40 ksi reinforcement indicates a decrease in mean value from 50.4 ksi for No. 3 bars to 44.1 ksi for No. 8 bars. The associated c.o.v. do not vary consistently with size, and range from about 0.07 to 0.11. When all bars are obtained from the same manufacturer, a c.o.v. as low as 0.05 is possible. For high strength reinforcement with a nominal yield of 60 ksi, the mean values decrease from 71.8 ksi for No. 3 bars to 62.2 ksi for No. 9 bars, and the c.o.v. varies between 0.06 and 0.12, but again not according to size. Tests by Chow and Gardner [22] of 20 No. 5 bars of intermediate grade steel show a mean of 49.9 ksi and c.o.v. of 0.073.

The sample mean value is clearly affected by the size of the bar. A designer may not know what size will be used, as several different combinations may yield the same $\overline{A}_s$. To obtain a design from Eq. 3.16, a best estimate of $\overline{f}_y$ is made and a prediction error may be applied to account for this size effect. On the basis of available data, it is assumed that $\overline{f}_y = 47.7$ ksi for intermediate grade reinforcement and $\overline{f}_y = 64$ ksi for high strength reinforcement. The uncertainty in the estimated mean strength due to size effects is about 0.04.

Commercial mill testing procedures may give strengths somewhat higher than would be found under actual service conditions [38]. ASTM test methods determine the unstable upper yield point rather than the stable lower yield point; Julian estimates the error induced as 0.05-0.10. The high time rate of strain used in commercial testing causes an apparent increase in the yield strength, with an overestimation of approximately 0.10 [38]. Mean yield strengths may vary from mill to mill for nominally identical material. Censoring test data for material failing to meet specifications [14] also tends to raise the reported test data.

On the basis of available data, representative values of the basic variabilities are $\delta_{f_y} = 0.09$ for intermediate grade reinforcement, and $\delta_{f_y} = 0.07$ for high strength reinforcement. The prediction error would include the uncertainty due to bar sizes, errors in mill test reporting, and strain rate effect; this is estimated to be $\Delta_{f_y} = 0.12$, which is the result of

$$\sqrt{(0.04)^2 + (0.05)^2 + (0.10)^2}$$

representing the effects of the above three sources of uncertainty.

Data on the compressive strength f_c of concrete is available from tests on standard cylinders. The distribution of f_c often exhibits approximately normal behavior [1,3]. The nominal compressive strength f'_c is implied by the ACI code to be the 10 percentile value of f_c for ultimate strength design.

The report of ACI Committee 214 [3] contains results of 92 tests of concrete cylinders with $f'_c = 3000$ psi. The mean was 3456 psi, with a c.o.v. of about 0.12. Further data is included of 164 field tests on nominal 3000 psi concrete supplied by a ready-mix company over a one year period. The dispersion of observed sample mean concrete strength can be obtained from data defining the mean $\overline{f}_c$ delivered during each monthly period. Analysis of this data yields a prediction error for the measured $\overline{f}_c$ of 0.07.

The data based prediction error must be augmented by other factors. Strain rates and duration of load are important to strength [50]. A difference in strength of about 15 percent has been observed between high and low strain rates, with higher strengths corresponding to higher strain rates. The sustained load strength averages about 80 percent of the short time

strength. These factors are partially offset by the increase in actual concrete strength with time over the 28 day strength used to determine $\overline{f}_c$. Confinement of the concrete raises its strain capacity and its compressive strength [23]. Uncertainties in $\overline{f}_c$ arise from the direction of casting, which is particularly important in vertically cast members. Workmanship, degree of compaction, and curing conditions will also affect in-situ mean strength and its dispersion. A comparison of the strength of in-place concrete with strength derived from standard tests reveals that field-cured cylinders indicate a strength 10 to 21 percent higher than the actual strength determined from drilled cores [15]. These must be used to augment the uncertainties in the sample mean estimated above. Assuming that these latter factors contribute a combined uncertainty of 0.16, we obtain

$$\Delta_{f_c} = \sqrt{(0.07)^2 + (0.16)^2} = 0.18$$

When reasonable care is taken in the mixing, placement, and curing of the concrete, representative values of the uncertainties for f_c, therefore, are $\delta_{f_c} = 0.12$ and $\Delta_{f_c} = 0.18$.

The statistics of the limiting concrete strain are needed to determine the statistics of the balanced reinforcement ratio p_b, and the associated probabilities of tension or compression failure. Test results in the form of plots of $\overline{\varepsilon}_{cu}$ vs. $\overline{f}_c$ [42,33,58] indicate that $\overline{\varepsilon}_{cu}$ is about 0.004. There is a slight tendency for $\overline{\varepsilon}_{cu}$ to decrease with $\overline{f}_c$. The variability is estimated from these plots to be between 0.10 to 0.15; Allen [1] suggested 0.12. Confinement of the concrete tends to increase its ultimate strain

capacity [23]. The manner in which the strain is measured affects its magnitude; as strains tend to concentrate above the cracks [58], the strain will depend on the gage length used to measure it. The quality of the information available to evaluate the statistics of ε_{cu} is poor. It seems reasonable, however, to set $\overline{\varepsilon}_{cu}$ constant at 0.004. The value of 0.003 specified by the ACI code represents a conservative value of strain [35]. The prediction error in the assumed mean is estimated as $\Delta_{\varepsilon_{cu}} = 0.10$.

There is limited data to evaluate the statistical variability in member dimensions b and t and effective depth to reinforcement d [36,37]. Indications are that these variables are approximately normal (within constraints furnished by member size). Uncertainties in d may be attributed to faulty construction of the reinforcement cage, deflection of the bars under their own weight, initial crookedness of the bars, and careless construction practices on the site. Uncertainties in b and t arise from erection of the concrete formwork. As in the case of f_c, these variables are dependent on the quality of workmanship employed.

Nondestructive tests have been used to obtain data on d for slabs constructed in Stockholm, Sweden [36]. The specified depth on the working drawings was 144 mm. This corresponds to the engineer's best prediction of the mean, $\overline{d}$. The values measured in the field range from 121.0 mm to 144.9 mm. The variability and prediction error may be found from this data by the method described in Sec. 2.2.2. With $\overline{d}$ = 144 mm, and μ_d = 140.2 mm, Eq. 2.42 becomes

$$\hat{E}[(\mu_d - \overline{d})^2] \simeq \hat{E}[(d - 144)^2] - \hat{E}[(d - 140.2)^2]$$
$$= 62.26 - 48.03 = 14.23$$

from which $\delta_d = 0.049$ and $\Delta_d = 0.027$. Values obtained in an earlier set of tests [37] give $\delta_d = 0.079$ and $\Delta_d = 0.053$.

For the total member thickness t, data obtained by Johansson and Warris indicates $\delta_t = 0.042$ and $\Delta_t = 0.01$. Variabilities in d and t can be significantly reduced by using prefabricated units. Johnson's data gives $\delta_t = 0.044$ and $\Delta_t = 0.01$. No information is available for b, but it is reasonable to assume that $\delta_b \simeq \delta_t$ and $\Delta_b \simeq \Delta_t$, as the uncertainties arise from the same source. It is obvious that d represents the most unpredictable dimension; unfortunately it is also an important parameter in determining the statistics of M_T.

A report of the Building Research Advisory Board [21] recommends allowable tolerances of -1/4 in. to 1/2 in. on overall member dimensions and ± 1/4 in. on effective depth d. The ACI code specifies tolerances of ± 1/4 in. when d is less than 24 in. Under the assumption of normality and a probability of 95 percent that these tolerances will be met, the implied variability in b (or t) is about $0.15\sqrt{b}$ and for d, $0.13\sqrt{d}$. This represents what is currently considered acceptable. The greater allowable dispersion in b is reasonable in that this variable is not as significant as d in assuring design adequacy.

In further analysis, it is assumed that the c.o.v.'s and prediction errors in b and t are 0.04 and 0.02 respectively, and for d, $\delta_d = 0\ 07$ and $\Delta_d = 0.05$; these may be slightly conservative.

Variabilities in the steel area* A_s may be found from the variability of the individual bar areas a_{s_i} or bar dimmeters. If it is assumed that

---

* It is recognized that with the new ASTM specification, $A_s f_y$ should be taken as a single variable; accordingly, test data would be used to evaluate the lumped variability in $A_s f_y$.

the individual areas are perfectly correlated within a member, then $\delta_{A_s} = \delta_{a_s}$. The assumption of perfect correlation is conservative and not unreasonable if all bars come from the same manufacturer.

Baker's results [14] indicate the c.o.v. of bar diameter is about 0.015 for small bars, with a tendency to decrease for large bars; thus, $\delta_{a_s} \simeq 0.03$. Analysis of certain data provided through the courtesy of Professor C. P. Siess [53] indicates that for No. 5 bars, $\delta_{a_s} = 0.015$ and $\Delta_{a_s} = 0.021$; for No. 8 bars, $\delta_{a_s} = 0.012$ and $\Delta_{a_s} = 0.025$; and that for No. 14 bars, $\delta_{a_s} = 0.014$ and $\Delta_{a_s} = 0.01$. Prediction uncertainties arise from fabrication errors. There is a tendency for the bar sizes to increase as the rolls wear [14]. Carelessness in placement at the site may cause error. In addition, the mean areas of smaller diameter bars are less predictable.

The ASTM acceptance criteria on bar sizes [6] are based on maximum allowable departures from specified nominal weights; for a single bar, the maximum is 6 percent under and by lot, 3 1/2 percent under. If it is assumed that 95 percent of the bars meet required specifications, and the bar weights are approximately normally distributed, the implied variability in weight with respect to the specified nominal value is about 0.021, and since area is proportional to unit weight, $\delta_{a_s} \simeq 0.021$ also. These are of the same order as those obtained from the above data, and represent what is currently acceptable. Representative values of the uncertainties in A_s are therefore taken as $\delta_{A_s} = 0.02$ and $\Delta_{A_s} = 0.03$. These estimates may be on the conservative side.

The variables η and $k_1 k_3$ are related to the concrete stress distribution in the compression zone at failure. They are modeling variables

and are necessary because the distribution of the concrete stress at ultimate and the location of the resultant compression force are not known exactly. Hognestad, et. al. [35] suggested a value $\overline{\eta} \simeq 0.59$ as adequate, as M_T is insensitive to $\overline{\eta}$. Figure 8 in their paper indicates that $\delta_\eta \simeq 0.05$. A statistical analysis by R. C. Elstner [42] of beams failing in tension led to $\overline{\eta} \simeq 0.593$. Some of the uncertainty in η may be attributed to uncertainty in the steel stress at failure. The equivalent stress factor k_1k_3 decreases with f_c [42,33]; analysis of data provided in these references indicates that $\delta_{k_1k_3} \simeq 0.12$. The ACI code specifies that $k_1k_3 = 0.72$ when $f'_c \leq 4000$ psi. In subsequent analysis, it is assumed that $\Delta_{k_1k_3} \simeq 0.05$ and that Δ_η is negligible.

The results of the above analyses are summarized in Table 3.1. These uncertainty measures will be used in later reliability analyses.

TABLE 3.1

Uncertainties in Design Parameters

Parameter	Predicted Mean	Basic Variability	Prediction Error
f_y (Nominal 40 ksi)	47.7 ksi	0.09	0.12
f_y (Nominal 60 ksi)	64.0 ksi	0.07	0.12
f_c (Nominal 3 ksi)	3.5 ksi	0.12	0.18
f_c (Nominal 4 ksi)	4.7 ksi	0.12	0.18
A_s		0.02	0.03
b		0.04	0.02
d		0.07	0.05
t		0.04	0.02
k_1k_3	0.72	0.12	0.05
η	0.59	0.05	0.0
ε_{cu}	0.004	0.12	0.10

3.2.3 Uncertainties of Flexural Capacity

The statistics of M_T, M_C and p_b can be found using the uncertainties defined in Table 3.1. The probability of occurrence of a tensile or compressive failure is estimated from Eq. 3.5a.

Table 3.2 shows the variation of δ_{p_b}, Ω_{p_b} and the probability of a compression failure, α_b', when $\overline{p} = 0.75p_b'$, with δ_{f_c}, the quality of the

TABLE 3.2

Statistics of p_b and Probability that Failure Will be Compressive

	$\overline{f}_y = 47.7$, $\overline{f}_c = 3.5$, $\overline{p}_b = .0376$, $0.75\ p_b' = 0.0278$				
δ_{f_c}	0.10	0.12	0.15	0.20	0.25
δ_{p_b}	0.198	0.209	0.227	0.263	0.303
Ω_{p_b}	0.315	0.321	0.334	0.359	0.389
α_b'	0.211	0.218	0.230	0.249	0.275
	$\overline{f}_y = 64$, $\overline{f}_c = 4.7$, $\overline{p}_b = .0342$, $0.75p_b' = 0.0213$				
δ_{f_c}	0.10	0.12	0.15	0.20	0.25
δ_{p_b}	0.184	0.196	0.216	0.253	0.294
Ω_{p_b}	0.311	0.318	0.330	0.356	0.386
α_b'	0.09	0.096	0.106	0.122	0.145

concrete. p_b' is the ACI balanced reinforcement ratio computed with nominal values of f_y', f_c', and $\varepsilon_{cu} = 0.003$. The probabilities α_b as a function of $\overline{p}$ computed from Eq. 3.5a are shown in Figs. 3.3 and 3.4. Poor concrete quality control causes the uncertainties in p_b and the probability of a compression failure to increase, but the increases in α_b is not significant

except when $\bar{p}$ is small. Risks α_b' associated with the value $0.75p_b'$, as required in the ACI code, range from 0.21 when $\delta_{f_c} = 0.10$ to 0.27 when $\delta_{f_c} = 0.25$, for $\bar{f}_y = 47.7$ ksi and $\bar{f}_c = 3.5$ ksi. Similar values have been found by other investigators [1,26]. Probabilities of compression failures are reduced when high strength reinforcement is used, as indicated in Fig. 3.4; this is attributable in part to a smaller δ_{f_y}.

In the context of risk based design, the likelihood that a section designed to fail in tension will actually fail in compression is controlled by specifying that the probability of this unfavorable event is acceptably small. Design values of $\bar{p}$ at risk levels of 0.05, 0.01 and 0.001 are given in Table 3.3 (for various δ_{f_c}) for intermediate grade and high strength reinforcement. All are less than the ACI values, and decrease as δ_{f_c} increases.

TABLE 3.3

Required $\bar{p}$ for Specified α_b

	$\bar{f}_y = 47.7$ ksi $\quad \bar{f}_c = 3500$ psi				
α_b \ δ_{f_c}	0.10	0.12	0.15	0.20	0.25
0.05	0.0213	0.0209	0.0204	0.0196	0.0185
0.01	0.0170	0.0167	0.0162	0.0153	0.0143
0.001	0.0134	0.0130	0.0126	0.0117	0.0106
	$\bar{f}_y = 64$ ksi $\quad \bar{f}_c = 4700$ psi				
α_b \ δ_{f_c}	0.10	0.12	0.15	0.20	0.25
0.05	0.0194	0.0191	0.0187	0.0180	0.0170
0.01	0.0156	0.0153	0.0149	0.0140	0.0131
0.001	0.0123	0.0120	0.0116	0.0107	0.0098

When the concrete quality is poor, the beam dimensions are forced to increase, resulting in a loss in design economy.

Figure 3.5 shows the behavior of δ_{M_T} and Δ_{M_T} as functions of $\bar{p}$, resulting from the uncertainties of the individual variates of Table 3.1. From these results, we see that δ_{M_T} and Δ_{M_T} are virtually constant for the values of $\bar{p}$ of interest, and can be considered invariant with $\bar{p}$. Furthermore, δ_{M_T} is not significantly affected by the quality control of concrete, particularly when $\bar{p}$ is small. This can be inferred also from the coefficients of Eq. 3.17.

The magnitude of δ_{M_T} estimated herein is somewhat larger than values obtained from beam test data. The latter typically range from 0.03 to 0.05 [22,42,58]; these results, however, are for laboratory specimens presumably fabricated under carefully controlled conditions, whereas the above δ_{M_T} and Δ_{M_T} refer to uncertainties in a member fabricated under field conditions, and thus would be expected to be higher.

Equation 3.17, Fig. 3.1 and the c.o.v. listed in Table 3.1 suggest that f_y, d, and f_c are the only significant variables contributing to δ_{M_T} and Δ_{M_T}; moveover, when q is small, the uncertainties in f_c may also be neglected. For example, if $\bar{p} = 0.015$, $\bar{f}_y = 47.7$ and $\bar{f}_c = 3.5$, $q = 0.204$, and

$$\delta_{M_T} = \sqrt{.745\delta_{f_y}^2 + .0189\delta_{f_c}^2 + 1.292\delta_d^2}$$

whence

$$\delta_{M_T} = \sqrt{.00604 + .000272 + .00632} = 0.112$$

compared to $\delta_{M_T} = 0.114$ when all variables are included. If δ_{f_c} is neglected

in the above, $\delta_{M_T} = 0.111$; if only δ_{f_y} is considered, we have $\delta_{M_T} = 0.078$. When a member is fabricated under carefully controlled conditions, the variability in M_T is primarily due to δ_{f_y}.

The basic variability and prediction error in M_C are also shown in Fig. 3.5. Insensitivity to $\bar{p}$ is again apparent, but in this case, δ_{f_c} is significant in determining δ_{M_C}, and thus concrete quality is important. The uncertainties in flexural capacity are higher for compressive failures than for tension failures. This has also been found from laboratory tests [42] where $\delta_{M_C} \simeq 0.083$ was reported.

3.3 Shear

3.3.1 Equations of Shear Capacity

Current design philosophy attempts to provide beams for which the ultimate strength is governed by flexure rather than shear. This is done to insure ductility and provide adequate warning of impending failure. This philosophy can be retained in a reliability based design, by insuring that the probability of failure of a member in shear is less than that in flexure.

The shear-diagonal tension failure mechanism is a combined stress problem in which both shear and flexural stresses have a part [2,19,40]. The distribution of shear stresses across the section is indeterminate. Web reinforcement is provided to transfer stresses across the diagonal cracks so that full flexural capacity can be developed. The contributions of the concrete compression zone and web steel to shear capacity are also interrelated. An interactive relationship between flexure and shear is not available, and in accordance with present practice, flexure and shear are treated

independently for design purposes.

The shear capacity of a section is determined from a modification of the "truss analogy" model, written as [16]

$$V = V_c + V_{ws} \tag{3.22}$$

in which V_c is the shear at inclined cracking in a member without web reinforcement, and V_{ws} is the shear carried by the web reinforcement when it is at incipient yield. In the absence of other statistical models for analyzing shear capacity, Eq. 3.22 will serve as the basis for the reliability analysis.

The shear at inclined cracking in a member without web reinforcement can be written as

$$V_c = v_{cu} bd \tag{3.23}$$

in which v_{cu} is the nominal shear stress at inclined cracking; it is an average uniform stress over the area bd. It will be assumed that the web reinforcement consists of vertical stirrups, and that the stirrups are of the same size. If the ultimate load in shear is obtained when the web steel stress is at the yield level, the shear carried by the web reinforcement at ultimate load is $V_{ws} = n_c A_v f_y$, where A_v is the area of the stirrup, and n_c is the number of stirrups crossing the diagonal crack. Assuming the diagonal crack to have a horizontal projected length of d [16], and with a stirrup spacing of s_{st},

$$V_{ws} = \frac{d}{s_{st}} A_v f_y \tag{3.24}$$

The shear capacity then is

$$V = v_{cu} bd + \frac{d}{s_{st}} A_v f_y \tag{3.25}$$

To insure that every potential diagonal crack is crossed by at least one stirrup, a maximum stirrup spacing is set at [5]

$$s_{st} \leq d/2 \tag{3.26}$$

3.3.2 Evaluation of Uncertainties in Shear

A number of variables are common to the shear and flexural capacities. To evaluate the statistics of shear capacity, then, it is necessary to define the uncertainties associated with A_v and s_{st}, and to determine the mean and variance of v_{cu}.

Stirrups are often formed from smaller sized standard reinforcing bars. In this case $A_v = 2a_s$, and therefore $\delta_{A_v} = \delta_{a_s}$, and $\Delta_{A_v} = \Delta_{a_s}$, where uncertainties in a_s have already been evaluated for flexure. There is no data available to evaluate the uncertainties in s_{st}, but as these pertain to the fabrication of the reinforcing cage, it is reasonable to assume that the uncertainties in s_{st} are about the same as those of d.

According to the ACI [5] the shear strength is calculated nominally as,

$$v'_{cu} = 1.9 \sqrt{f'_c} + 2500 pd \frac{V}{M} \leq 3.5 \sqrt{f'_c} \tag{3.27}$$

in which $\sqrt{f'_c}$ is presumably a measure of the strength of concrete in tension. Test results [2] indicate that v'_{cu} of Eq. 3.27 underestimates the observed

nominal shear stress at a section when V/M is small; this equation was deliberately chosen to be somewhat conservative for the reason that shear failures tend to be quite sudden. For reliability analysis, therefore, the conservative bias in Eq. 3.27 should be removed. This can be accomplished by assuming that the equivalent shear stress on a section is

$$v_{cu} = \phi_1 v'_{cu} + \varepsilon_1 \leq 3.5 \sqrt{f_c} \tag{3.28}$$

where ϕ_1 is a quantity reflecting the bias, v'_{cu} is given in Eq. 3.27 and ε_1 is a zero mean error. A suitable value of $\overline{\phi}_1$ is 1.18, the overall mean ratio of test values to calculated values reported in Table 5.20 of reference 2. The mean equivalent shear stress is then

$$\overline{v}_{cu} = \overline{\phi}_1 \overline{v}'_{cu} \leq 3.5 \sqrt{\overline{f}_c} \tag{3.29}$$

and its variance is

$$\sigma^2_{v_{cu}} = \overline{\phi}_1^2 \sigma^2_{v'_{cu}} + \sigma^2_{\varepsilon_1} \tag{3.30}$$

where $\sigma^2_{v'_{cu}}$ is obtained through Eq. 3.27 as

$$\sigma^2_{v'_{cu}} = \left(\frac{1.9}{2\sqrt{\overline{f}_c}} \right)^2 \sigma^2_{f_c} + \left(2500 \frac{1}{\overline{b}} \frac{\overline{V}}{\overline{M}} \right)^2 \sigma^2_{A_s}$$

$$+ \left(-2500 \frac{\overline{A}_s}{\overline{b}^2} \frac{\overline{V}}{\overline{M}} \right)^2 \sigma^2_b$$

Using the ACI requirement that $\overline{V}/\overline{M} \leq 1/\overline{d}$, a conservative and simplified estimate of $\sigma^2_{v'_{cu}}$ is

$$\sigma^2_{v'_{cu}} \simeq \bar{f}_c \, \delta^2_{f_c} + (2500\bar{p})^2 \, (\delta^2_{A_s} + \delta^2_b) \tag{3.31}$$

$\sigma^2_{\varepsilon_1}$ can be evaluated from test data [2] available in the form of calculated versus test values of $(v_{cu}/\sqrt{f_c})$, giving a relationship

$$\frac{v_{cu}}{\sqrt{f_c}} = \phi_1 \left(\frac{v'_{cu}}{\sqrt{f_c}} \right) + \frac{\varepsilon_1}{\sqrt{f_c}} = \phi_1 \frac{v'_{cu}}{\sqrt{f_c}} + \varepsilon$$

From the data reported by Moody, et. al. [2], we obtain an average variance of $\sigma^2_\varepsilon = 0.095$. Now since $\varepsilon_1 = \sqrt{f_c}\,\varepsilon$, and $\bar{\varepsilon} = 0$, $\sigma^2_{\varepsilon_1} \simeq (\sqrt{\bar{f}_c})^2 \, \sigma^2_\varepsilon = 0.095 \, \bar{f}_c$. Hence

$$\sigma^2_{v_{cu}} \simeq \bar{\phi}^2_1 \, [\, \bar{f}_c \delta^2_{f_c} + (2500\bar{p}\,)^2 (\delta^2_{A_s} + \delta^2_b)\,] + 0.095 \, \bar{f}_c \tag{3.32}$$

For example, suppose that $\bar{f}_c = 3500$ psi and $\bar{p} = 0.02$. Then $\sigma^2_{v_{cu}} = 409$, and if $\bar{v}'_{cu} = 2\sqrt{\bar{f}_c}$, then $\bar{v}_{cu} = 140$ psi and $\delta_{v_{cu}} \simeq 0.15$.

The prediction error in v_{cu} arises from errors in using $\bar{\phi}_1 = 1.18$ and in the mean values of the quantities in Eq. 3.29, as well as the imperfections of Eq. 3.29, and can be given as

$$\Delta^2_{v_{cu}} = \Delta^2_{\phi_1} + \Delta^2_{v'_{cu}} \tag{3.33}$$

Reference 2 gives mean values of ϕ_1 for different sets of data; on this basis, we obtain $\Delta_{\phi_1} = 0.09$, whereas $\Delta^2_{v'_{cu}}$ is obtained as

$$\Delta^2_{v'_{cu}} \simeq [\, \bar{f}_c \, \Delta^2_{f_c} + (2500\bar{p}\,)^2 (\Delta^2_{A_s} + \Delta^2_b)\,] / (\, \bar{v}'_{cu})^2 \tag{3.34}$$

For example, if $\overline{p} = 0.02$, $\overline{f}_c = 3500$ psi, $\overline{v}'_{cu} = 2\sqrt{\overline{f}_c}$, and using uncertainties previously determined, $\Delta^2_{v'_{cu}} = 0.0083$, and thus $\Delta_{v_{cu}} \simeq \sqrt{.0081 + .0083} = 0.13$.

An inspection of data provided in Ref. 2 indicates that the shear capacity defined in Eq. 3.25 also consistently underestimates the observed capacity. Part of this bias is due to the bias in v'_{cu}; however, when this effect is removed, Eq. 3.25 is still conservative with respect to observed data. This suggests that the statistics of shear capacity used in assessing the reliability should be treated similarly to those of v_{cu}. The total shear capacity is therefore assumed to be

$$V_T = \phi_2 V + \varepsilon_2 \tag{3.35}$$

where ϕ_2 is the bias arising from the truss analogy equation, V is defined in Eq. 3.25, and ε_2 is a mean zero error as before. A suitable value of $\overline{\phi}_2$ is 1.15, obtained from comparing calculated to test values of V/bd in Table 6.1 of Ref. 2, once the bias in v_{cu} has been removed. The mean is

$$\overline{V}_T = \overline{\phi}_2 \overline{V} \tag{3.36}$$

where, using the methods of Sec. 2.2.1,

$$\overline{V} = \overline{v}_{cu} \overline{b}\, \overline{d} \left(1 + \frac{1}{r_s}\right) \tag{3.37}$$

in which

$$r_s = \frac{\overline{V}_c}{\overline{V}_{ws}} = \frac{\overline{v}_{cu} \overline{b}\, \overline{d}}{\frac{\overline{d}}{\overline{s}_{st}} \overline{A}_v \overline{f}_y} \tag{3.38}$$

When a value of r_s is found such that the probability of failure in shear

is less than that in flexure, sets of $(\bar{A}_v, \bar{s}_{st})$ can be found from Eq. 3.38 that determine the web reinforcement needed; thus r_s is a shear design parameter. The variability of V_T is

$$\delta^2_{V_T} = \delta^2_V + \frac{\sigma^2_{\varepsilon_2}}{(\bar{\phi}_2\ \bar{V})^2} \tag{3.39}$$

where δ^2_V is

$$\delta^2_V = \left(\frac{r_s}{1 + r_s}\right)^2(\delta^2_{v_{cu}} + \delta^2_b) + \left(\frac{1}{1 + r_s}\right)^2(\delta^2_{f_y} + \delta^2_{A_V} + \delta^2_{s_{st}}) + \delta^2_d \tag{3.40}$$

$\sigma^2_{\varepsilon_2}$ can be obtained from test data available [2] in the form of calculated versus test values of (V/bd), giving the relationship

$$\left(\frac{V_T}{bd}\right) = \phi_2\left(\frac{V}{bd}\right) + \frac{\varepsilon_2}{bd} = \phi_2\left(\frac{V}{bd}\right) + \varepsilon$$

From these data, $\sigma^2_\varepsilon = 2097$. Now since $\varepsilon_2 = (bd)\varepsilon$, and $\bar{\varepsilon} = 0$, $\sigma^2_{\varepsilon_2} = (\bar{b}\ \bar{d})^2\sigma^2_\varepsilon = 2097\ (\bar{b}\ \bar{d})^2$. Hence

$$\delta^2_{V_T} = \delta^2_V + \frac{2097}{\bar{\phi}^2_2[\bar{v}_{cu}(1 + \frac{1}{r_s})]^2} \tag{3.41}$$

If $r_s = 1$, $\bar{p} = 0.02$, and $\bar{f}_c = 3500$ psi, then $\delta_{V_T} \simeq 0.15$.

The prediction error in V_T is

$$\Delta^2_{V_T} = \Delta^2_{\phi_2} + \Delta^2_V \tag{3.42}$$

where Δ_V is found from Eq. 3.40 by replacing the c.o.v. with the prediction errors, and Δ_{ϕ_2} is estimated to be about 0.06. If $r_s = 1$, $\Delta_V = 0.107$, and

$$\Delta_{V_T} = \sqrt{\overline{0.107}^2 + \overline{0.06}^2} \simeq 0.12$$

The coefficients in Eq. 3.40 define the significance of the uncertainties in the respective variables to the uncertainties in the shear capacity V. This is illustrated in Fig. 3.6 as a function of r_s. When a large amount of web reinforcement is provided (small r_s), $\overline{V}$ and Δ_V are highly dependent on the statistics of A_v, f_y, and s_{st}, but this dependency rapidly decreases as r_s increases and v_{cu} and b become more significant. For large r_s, corresponding to very light web reinforcement,

$$\delta_V^2 \simeq \delta_{v_{cu}}^2 + \delta_b^2 + \delta_d^2$$

thus, approaching a beam without web reinforcement.

Figure 3.7 illustrates the behavior of δ_V, Δ_V, δ_{V_T} and Δ_{V_T} calculated from Eq. 3.40 and 3.41, as functions of r_s, using the uncertainties in Table 3.1. For illustrative purposes, it has been assumed, that $\overline{p} = 0.02$, and $\overline{f}_c = 3500$ psi. The uncertainties in shear capacity increase as the relative amount of web reinforcement is decreased. On the basis of this analysis, concrete quality control does not appear to be especially significant due to the dominance of the second term in Eq. 3.41, and that f_c enters the expression for v_{cu} in terms of its square root. It would be useful to have some test data to verify whether this is indeed the case. It may be observed that the variabilities are higher for the shear capacity than for the flexural capacity.

3.4 Axial Thrust and Bending

3.4.1 Introductory Remarks

The strength of a column subjected to an eccentric axial force may be visualized with an interaction diagram for the section, a locus of pairs of thrust and moment values which, according to ultimate strength theory, will cause failure. The interaction diagram for reinforced concrete sections has two distinct regions. For small load eccentricities, failure is governed by the concrete reaching its maximum useful strain while the reinforcement stress is still elastic; this is termed a compression failure. For large eccentricities, the reinforcement yields first, followed by a secondary compression failure in the concrete; this is termed a tension failure. The point on the interaction diagram at which the concrete would crush at the same time the steel yields is termed the balanced point.

The interaction diagram is found from considerations of equilibrium and strain compatibility [45]. For a symmetrically reinforced rectangular section,

$$P = k_1 k_3 f_c bc + A_s(f_{s_c} - f_{s_t} - k_3 f_c) \tag{3.43}$$

$$M = Pe = k_1 k_3 f_c bc\left(\frac{t}{2} - k_2 c\right) + A_s\left(d - \frac{t}{2}\right)(f_{s_c} + f_{s_t} - k_3 f_c) \tag{3.44}$$

where c is the depth to the neutral axis, and e is measured from the plastic centroid of the section. Proceeding from strain compatibility, f_{s_c} and f_{s_t} are obtained from the stress-strain diagram for the reinforcement, and P and M are found from Eqs. 3.43 and 3.44 [45]. The curve is thus defined

implicitly, as there is no closed form function describing jointly the behavior of P and M, which is needed to evaluate the respective statistics. Moveover, uncertainties in f_{s_c} and f_{s_t} are not defined.

Alternatively [42], if it is assumed that the compression and tension reinforcement have yielded, solving Eqs. 3.43 and 3.44 simultaneously for c and substituting back into Eq. 3.43 yields

$$P_T = \frac{f_c bt}{2\eta}\left\{\sqrt{\left(\frac{e}{t}-\frac{1}{2}\right)^2 + 4\eta\,\frac{1}{f_c}\,\frac{A_s}{bt}\left[k_3 f_c + (2f_y - k_3 f_c)\left(\frac{d}{t}-\frac{1}{2}\right)\right]}\right.$$
$$\left. - \left(\frac{e}{t}-\frac{1}{2}\right)\right\} - k_3 f_c A_s \qquad (3.45)$$

for tension failures. For the compression case, an attempt to determine the steel stresses in a manner similar to that used for compression failures in beams leads to a complicated cubic equation to be solved for the stresses. In lieu of this, the strength in the compression zone may be taken as a line decreasing linearly from the concentrically loaded axial capacity P_o to the balanced point axial capacity P_b. Thus,

$$P_C = \frac{P_o}{1 + \left(\frac{P_o}{P_b} - 1\right)\frac{e}{e_b}} \qquad (3.46)$$

Equations 3.45 and 3.46 explicitly define the axial capacity in terms of material strengths, section parameters, and load eccentricity, and are given in Section 19 of ACI 318-63. As it is necessary to have this explicit relationship to evaluate the statistics of resistance, they will be used in the subsequent reliability analysis, in spite of their approximations.

3.4.2 Analysis of Failure Events Under Combined Loads

Little work has been done on the statistical theory of reinforced concrete members subjected to combined thrust and bending. Shah [52] performed a regression analysis of existing column test data which indicates the statistical adequacy of the ACI strength formulas. Tichy and Vorlicek [55] presented a discussion of interaction curves in general; Rosenblueth and Esteva [49] indicated conceptually how probabilities associated therewith might be determined. The statistical analysis is complicated by the resistance being a function of the relative load effects. Resistance and load are therefore no longer statistically independent, and simplifications must be sought before the reliability can be assessed by Eqs. 2.8 and 2.16.

An interaction curve for a reinforced concrete section is shown in Fig. 3.8. The regions defining tensile and compressive failures are denoted as G_T and G_C, respectively. The load vector S is the resultant of applied thrust S_P and moment S_M. Since S and the balanced point are random, it is not known which part will govern the design, particularly when the load eccentricity is close to the balanced eccentricity e_b.

Since the regions of tension and compression failures are mutually exclusive and collectively exhaustive,

$$\{\text{Failure}\} = \{\text{Failure in Compression} \bigcup \text{Failure in Tension}\}$$

where

$$\{\text{Failure in Compression}\} = (\hat{G}_C < \hat{S} \bigcap \hat{e} \leq \hat{e}_b)$$

$$\{\text{Failure in Tension}\} = (\hat{G}_T < \hat{S} \bigcap \hat{e} > \hat{e}_b)$$

The probability of failure is then given as

$$\Pr(\text{Failure}) = \Pr(\hat{G}_C < \hat{S} | \hat{e} \leq \hat{e}_b) \cdot \Pr(\hat{e} \leq \hat{e}_b) + \Pr(\hat{G}_T < \hat{S} | \hat{e} > \hat{e}_b) \cdot \Pr(\hat{e} > \hat{e}_b) \quad (3.47)$$

The density functions of G_C and G_T depend on the relative load effects; consequently, further simplifications are required.

If the eccentricity e of the applied thrust is assumed to be known, then S_P and S_M are perfectly correlated; moreover, the capacity is statistically independent of the applied load. This is tantamount to assuming that the vector S is random in magnitude but not in point of application and direction. If the axial and moment capacities are perfectly correlated, the event $(\hat{G}_C < \hat{S})$ implies $(\hat{P}_C < \hat{S}_P)$, (or $(\hat{G}_T < \hat{S})$ implies $(\hat{P}_T < \hat{S}_P)$), i.e., axial capacity is less than applied axial load. Then

$$P_f = \Pr(\hat{P}_C \leq \hat{S}_P | \hat{e} \leq \hat{e}_b) \cdot \Pr(\hat{e} \leq \hat{e}_b) + \Pr(\hat{P}_T < \hat{S}_P | \hat{e} > \hat{e}_b) \cdot \Pr(\hat{e} > \hat{e}_b) \quad (3.48)$$

If e_b is also known, the failure probabilities are simply

$$P_f = \Pr(\hat{P}_C \leq \hat{S}_P), \qquad e \leq e_b$$
$$P_f = \Pr(\hat{P}_T \leq \hat{S}_P), \qquad e > e_b \quad (3.49)$$

The statistics of P_C and P_T may be found from a systematic evaluation of Eqs. 3.45 and 3.46.

When the variance of e_b is small, $\Pr(e \leq e_b)$ is close to zero or

unity except in the neighborhood of the balanced point. In such cases, the safety criteria furnished by Eqs. 3.49 are a good approximation to that obtained from Eq. 3.48. Furthermore, if the underlying risk is evaluated on the basis of

$$p_f' = \max[(Pr(\hat{P}_C < \hat{S}_P) \cdot Pr(\hat{P}_T < \hat{S}_P)] \tag{3.50}$$

then $p_f < p_f'$. For example, if $p_e = Pr(\hat{e} < \hat{e}_b)$,

$$p_f = P_C \cdot P_e + P_T \cdot (1 - p_e)$$

$$= (p_C - p_T) \cdot p_e + p_T$$

Suppose that $p_T > p_C$; then $(p_C - p_T) < 0$, and $p_f < p_T = p_f'$. A similar result is obtained when $p_C > p_T$. Conversely, if a design for a specified risk level p_f' is obtained on the basis of

$$D_c = \max [D_c(\text{compression}), D_c(\text{tension})] \tag{3.51}$$

then $p_f(D_c) \leq p_f'$. This has been verified numerically.

For simplicity, the design phase of the study (i.e., determining a design for a specified risk) will be based on Eq. 3.51. There are conceptual as well as numerical difficulties in using Eq. 3.48 for this purpose, because for a given risk p_f, $Pr(\hat{P}_C < \hat{S}_P)$ and $Pr(\hat{P}_T < \hat{S}_P)$ are not uniquely determined. For a given design, however, the total probability of failure can be computed without difficulty using Eq. 3.48.

3.4.3 Uncertainties in Thrust and Bending

The balanced eccentricity e_b is a function of the steel and

concrete strength and the member dimensions. For balanced conditions in a symmetrically reinforced rectangular section, in which the area of the concrete displaced by the compression steel is neglected,

$$e_b = \frac{M_b}{P_b} = \frac{k_1 k_3 f_c bc(\frac{t}{2} - k_2 c) + 2A_s f_y (d - \frac{t}{2})}{k_1 k_3 f_c bc}$$

where c is determined as

$$c = \frac{E_s \varepsilon_{cu}}{E_s \varepsilon_{cu} + f_y} d$$

It is convenient to nondimensionalize the eccentricity and proceed in terms of the eccentricity ratio e_b/t instead; whence

$$\frac{e_b}{t} = \frac{1}{2} - k_2 \frac{E_s \varepsilon_{cu}}{E_s \varepsilon_{cu} + f_y} (\frac{d}{t}) + 2p \frac{f_y}{k_1 k_3 f_c} (\frac{d}{t} - \frac{1}{2}) \frac{E_s \varepsilon_{cu} + f_y}{E_s \varepsilon_{cu}} \qquad (3.52)$$

where $p = A_s/bd$ (as in flexure). The mean of e_b/t is found by evaluating Eq. 3.52 at the mean values of its variables; its basic variability is

$$\delta^2_{e_b/t} = c_1^2 \delta^2_{f_y} + c_2^2 (\delta^2_{f_c} + \delta^2_{A_s} + \delta^2_b + \delta^2_{k_1 k_3}) + c_3^2 \delta^2_d + c_4^2 \delta^2_t + c_5^2 \delta^2_{\varepsilon_{cu}} \qquad (3.53)$$

and similarly for the prediction error $\Delta^2_{e_b/t}$, where c_1, c_2, c_3, c_4, and c_5 are defined in Appendix B. The behavior of these coefficients as functions of $\bar{p}$ is illustrated in Fig. 3.9. All of these coefficients increase as the amount of reinforcement increases except c_5, which remains approximately constant. Small variations in $\bar{\varepsilon}_{cu}$ therefore have little effect on $\overline{e_b/t}$, and the contribution of uncertainties in ε_{cu} to those of e_b/t are practically

independent of $\overline{p}$. The uncertainty in e_b/t will increase as $\overline{p}$ increases.

The probability of a compression or tension failure, i.e., $Pr(\hat{e/t} \leq \hat{e_b/t})$ or $Pr(\hat{e/t} > \hat{e_b/t})$, can be computed assuming lognormal $\hat{e_b/t}$ and $\hat{e/t}$. Thus,

$$Pr(\hat{e/t} > \hat{e_b/t}) = \Phi\left[\frac{\ln\left[\frac{\overline{e/t}}{\overline{e_b/t}}\,\frac{\sqrt{1+\Omega^2_{e_b/t}}}{\sqrt{1+\Omega^2_{e/t}}}\right]}{\sqrt{\ln\left[(1+\Omega^2_{e_b/t})(1+\Omega^2_{e/t})\right]}}\right] \tag{3.54}$$

The behavior of $Pr(\hat{e/t} \geq \hat{e_b/t})$ as a function of $\overline{e/t}$ is illustrated in Fig. 3.10. Table 3.4 shows the behavior of $\Omega_{e_b/t}$ as a function of δ_{f_c} and $\overline{p}$.

TABLE 3.4

Total Uncertainty in e_b/t ($\Omega_{e_b/t}$)

$\overline{f_y} = 47.7$, $\overline{f_c} = 3.5$, $\overline{\varepsilon_{cu}} = 0.004$, $\overline{p} = \overline{A_s}/\overline{bd}$

		δ_{f_c}				
$\overline{p}$	$\overline{e_b/t}$	0.10	0.12	0.15	0.20	0.25
0.01	0.436	0.171	0.173	0.178	0.188	0.200
0.02	0.636	0.224	0.228	0.234	0.249	0.266
0.03	0.835	0.254	0.258	0.266	0.283	0.302
0.04	1.035	0.273	0.278	0.286	0.304	0.325
0.05	1.235	0.286	0.291	0.300	0.318	0.341

Poor concrete quality increases the uncertainty in e_b/t, especially when the section is heavily reinforced. For a given load eccentricity ratio, poor quality control raises the probability of a compression type failure, but this increase is not significant. The addition of more reinforcement will also increase the probability of a compression failure for a given $\overline{e/t}$, as would be expected.

The axial capacity in the compression and tension modes of failure is defined from Eqs. 3.45 and 3.46. The means are found by evaluating P_C or P_T at the mean values of their dependent variables and the variabilities and prediction errors are evaluated as

$$\begin{Bmatrix} \delta_P^2 \\ \Delta_P^2 \end{Bmatrix} = \sum c_k^2 \begin{Bmatrix} \delta_k^2 \\ \Delta_k^2 \end{Bmatrix} \tag{3.55}$$

where c_k are given in Appendix C. The probabilities of failure in combined bending and thrust may then be investigated as functions of the material properties, geometry, and dimensionless eccentricity ratio $\overline{e/t}$.

Figures 3.11 and 3.12 illustrate the variation of the constants c_k in Eq. 3.55 with $\overline{e/t}$; since the balanced point is random, the curves for tension and compression failure are shown for the entire range of $\overline{e/t}$; note, however, that P_T determined from Eq. 3.45 is not valid when the stress in the tensile reinforcement is less than f_y. For compression failures, estimates in concrete strength and the section geometry are most significant in predicting the mean capacity. The uncertainty in the capacity depends primarily on those of f_c, k_1k_3, d, and f_y; the contributions of the uncertainties in A_s, t, and ε_{cu} are insignificant. When the failure is tensile, estimates of

$\overline{A_s}$, $\overline{f_y}$, $\overline{d}$, and $\overline{t}$ are most important in predicting the mean capacity, and $\overline{f_c}$ and $\overline{b}$ become less significant as $\overline{e/t}$ increases. Variations in $\overline{e}$ are important in both cases, except when $\overline{e/t}$ is very small. A state of pure flexure is approached as $\overline{e/t}$ becomes large; here, $c_{f_y} \to c_{A_s}$ and $c_{f_c} \to c_b$, consistent with the flexural formulation. In this latter case, the uncertainty in the capacity is dominated by δ_{f_y}, δ_{A_s}, δ_d and δ_t. The coefficient c_t becomes zero in the vicinity of the balanced point, since at this point, the capacity is independent of t.

It may be observed that $c_{k_1 k_3}$ and c_e in Fig. 3.11 tends to zero as $\overline{e/t} \to 0$; this is a consequence of using Eq. 3.46 to evaluate the necessary derivatives. However, it is not reasonable that the uncertainties in k_3 and e would have no effect on the uncertainties in P_c when $\overline{e/t} = 0$; this must be pointed out as a shortcoming in the use of Eq. 3.46 to evaluate δ_{P_c} and Δ_{P_c}.

Figures 3.13 and 3.14 show the variations of δ_P and Δ_P as functions of $\overline{e/t}$, using the uncertainties from Table 3.1. The effect of poor concrete quality on the tension capacity is insignificant except for small $\overline{e/t}$, which is not a region of practical interest. When failure is compressive, concrete quality is more important, as δ_P depends significantly on δ_{f_c} in this case.

Available test data [22,42] indicate that the basic variability in capacity ranges from 0.059 to 0.085. These values are less than those computed from a systematic analysis of the uncertainties associated with each variable. The reason is the same as indicated previously in the flexural formulation, reflecting the difference between laboratory specimens and those constructed in the field. In particular, d may be carefully controlled in the laboratory, but may not be on the site, and, as shown in Figs. 3.11

and 3.12, contributes significantly to the overall variability in capacity.

The problem of assuring adequate strength of a beam column in shear has not been considered. The presence of compressive axial load tends to increase the shear capacity of a member. Conceptually, the problem can be resolved by replacing V_c in Eq. 3.22 and 3.23 by an expression reflecting this increase in strength [16]. The probability of failure in shear of a member designed for bending and thrust can then be computed and its adequacy in shear determined in a manner similar to the approach used for beams.

Chapter 4

LOAD MODELS

4.1 Introductory Remarks

A structure may be subjected to many types of loads. These may consist of permanent loads from the weight of the system and permanent fixtures, live loads from occupancy, temporary equipment, and movable partitions, lateral loads associated with wind and earthquake, temperature stresses, residual stresses induced during fabrication, and stresses induced by differential settlement [48]. Such load effects occur in many combinations.

Normally, two cases are considered in design:

1. Total Load = Dead Load + Live Load
2. Total Load = Dead Load + Live Load + Lateral Load

Traditionally, the total design load is computed as the sum of the respective nominal maximum values.

The loads are frequently variable in time, as well as random. The complete description of such a load history must be given as a stochastic process. The statistics necessary to define the process are unavailable, since they require continuous load monitoring throughout the lifetime of the system. Instead, the time dependent effects may be included by determining the statistics of the distribution of maximum load with extreme value statistics [39, 43]. Since the distribution of live loads is time-variant, the time scale involved is important in combining various loads [10].

In design against dead and live loads only, for example, the extreme value of the live load over the lifetime of the structure is of interest, since the time scale is long and the live load magnitude changes slowly with time. When wind loads are combined with dead and live loads, however, short-term live loads should be considered, as the duration of strong winds is from 10 minutes to one hour [29].

In the following, dead, live and wind loads are considered. It is assumed in the reliability analysis that the load types are independent, and are mutually independent of the resistance. In this study, only simplified load models are used, although sophisticated stochastic process live load models may be available [34,44]. Existing load survey data [43] are used to obtain the required live load statistics.

4.2 Dead Load

Dead load is defined as resulting from the weight of the elements comprising the structure, permanent equipment, and installations.

The weight of a structure is quite predictable when the geometry is specified, and depends on the unit weights of the elements and their dimensions. The weight per unit length of a reinforced concrete member is

$$W_o = w_c A_c + w_{st} A_{st} \tag{4.1}$$

where w_c and w_{st} are unit weights of concrete and steel, and A_c and A_{st} are the respective areas. The variability in W_o is derived from the variabilities of the unit weights and dimensions; thus,

$$\delta_{W_o}^2 \simeq c_1^2 (\delta_{w_c}^2 + \delta_b^2 + \delta_t^2) + c_2^2 (\delta_{w_{st}}^2 + \delta_{A_{st}}^2) \qquad (4.2)$$

where

$$c_1 = \frac{\bar{w}_c}{\bar{w}_c + \frac{\bar{A}_{st}}{\bar{A}_c} \bar{w}_{st}}$$

$$c_2 = \frac{\frac{\bar{A}_{st}}{\bar{A}_c} \bar{w}_{st}}{\bar{w}_c + \frac{\bar{A}_{st}}{\bar{A}_c} \bar{w}_{st}}$$

and where δ_b, δ_t, and δ_{A_s} are given in Table 3.1. Indications are [18] that δ_{w_c} is about 0.03; $\delta_{w_{st}}$ ranges from about 0.02 for large bars to about 0.05 for small bars. From Eq. 4.2, with $\bar{A}_{st}/\bar{A}_c$ typically between 0.01 and 0.08, depending on the type of member, the variability in member weight is approximately equal to the first term in Eq. 4.2; hence $\delta_{W_o} \simeq 0.06$. If the weight along a member is highly correlated, the uncertainty in the dead load δ_D for the member is approximately equal to δ_{W_o}.

The prediction error in W_o is estimated as

$$\Delta_{W_o}^2 \simeq c_1^2 (\Delta_{w_c}^2 + \Delta_b^2 + \Delta_t^2) \qquad (4.3)$$

where Δ_b and Δ_t are taken from Table 3.1, and δ_{w_c} is assumed to be negligible. Equations 4.2 and 4.3 then represent the uncertainties in the dead weights of the structural members.

The contribution of permanent equipment to the overall load can be estimated accurately, as their specifications may be obtained from the

manufacturer. This source of uncertainty is expected to be insignificant. Additional uncertainty in the permanent load arises from the weight of nonstructural elements, such as partitions [18] Such uncertainty can only be estimated subjectively, and may be combined with Δ_{W_o}. The total prediction error in the dead load is then assumed to be $\Delta_D \simeq 0.10$.

The load-induced action resulting from the dead load is

$$S_D = c_D D \tag{4.4}$$

where D is the dead load acting on the member, and c_D is an influence coefficient translating the applied load to a load effect acting on the member. Clearly, c_D depends on the failure mode considered. As uncertainties in c_D arise from errors pertaining to the structural analysis, they are assumed to be of the prediction type.

The mean dead load effect is

$$\overline{S}_D = \overline{c}_D \overline{D} \tag{4.5}$$

and its variability is

$$\delta_{S_D} = \delta_D \tag{4.6}$$

The prediction error is

$$\Delta^2_{S_D} = \Delta^2_{c_D} + \Delta^2_D \tag{4.7}$$

in which Δ_{c_D} reflects the degree of confidence attributed to the analysis procedure. Uncertainties in analysis are assumed to be on the order of 0.05 - 0.10 (include assumptions in analysis, such as spatial distribution of loads, degree of continuity, etc.).

4.3 Live Loads on Buildings

4.3.1 Methodology

Live loads are those arising from movable equipment and fixtures, occupants, and other nonpermanent effects. There may be a wide variety of loadings possible which may not be foreseen by the designer. Also important is the time-dependency of the loads and their spatial correlation.

An early study [13] assumes that the floor load on an area is the result of a large number of independent load intensities. Then assuming the intensity w is normally distributed,

$$w = \overline{w} + \beta \sigma_w / \sqrt{A} \qquad (4.8)$$

where $\overline{w}$ and σ_w are the mean and standard deviation of the intensity. The important result here is that the c. o. v. of the intensity is a function of the tributary area A; this has been borne out by existing load surveys [20, 43]. Hasofer's stochastic model [34] indicates a dependence of the c. o. v. of load intensity on the tributary area and the type of occupancy. Peir's [44] stochastic analysis considers load correlation and time dependency, and design loads are presented as a function of the number of stories and the tributary area. Neither model postulates a suitable equation for the design live load.

Surveys conducted by Dunham [30] indicate that as the loaded tributary area increases, the maximum load intensity decreases; furthermore, the equivalent column load intensity decreases significantly as the

number of floors above it increases. This is because it is unlikely that all floors or floor areas will be loaded to maximum values simultaneously. The design rule adopted by the American Standard Building Code [7], allowing a reduced live load of

$$L_{nom} = L_{spec} (1 - 0.0008 (A_{trib} - 150)) \qquad (4.9)$$

for tributary area greater than 150 ft^2, with a reduction limited to 60 percent, represents the current acceptable basis for live load evaluation.

Within the present state of knowledge, a study of live loads based on the first-order approximate analysis should be more than adequate. However, a model suitable for common design usage that relates the factors known to affect the live load has yet to be developed, and more data is necessary before such a relationship can be found [20].

Existing load surveys do not reflect the time-dependency of the load, as the measurements are instantaneous values in the overall context of the loading history. To reflect time variability, Kármán [39] assumes that the occupancy changes a certain number of times during the lifetime of a structure, and that the load intensities in successive occupancy periods are identically distributed as the instantaneous intensity, and are statistically independent. The distribution of maximum load intensity during the lifetime then may be obtained using extreme value statistics, i.e.,

$$F_{Q_{max}}(x) = [F_Q(x)]^N$$

where N is the number of occupancies and F_Q is the distribution function of the instantaneous load intensity. For a 50 year lifetime, the number of occupancy changes may be expected to be between 5 and 20.

Statistics reported by Mitchell and Woodgate [43] from an extensive load survey of office buildings are used to define the live load in this study. The statistics for instantaneous live load intensity on floors other than basement and ground levels are shown in Fig. 4.1, along with the extreme value statistics for maximum load found from Kármán's formulation, with 12 occupancy changes. The dependence of the statistics on the loaded area is clear. The data-based histograms show a definite positive skewness for small areas, a result also obtained by others [20]. For larger areas, the histograms exhibit approximately normal behavior.

Determination of Column Loads

To determine the column load reduction for a general case, the correlation between loads on different floors must be known or assumed. There are reasons why these loads may be interdependent. Certain areas are consistently loaded on all floors. In office and apartment buildings, different users may use successive floors for similar functions, and floor loading patterns tend to be replicated.

Suppose a column supports M floors. The load intensity L_i on the i^{th} floor is distributed over an area A tributary to the column, assumed to be the same on each floor. In an approximate sense, the column load Y is

$$Y = A \sum_{i=1}^{M} L_i \qquad (4.10)$$

Its mean and variance are then

$$\bar{Y} = A \sum_{i=1}^{M} \bar{L}_i$$

$$\mathrm{Var}(Y) = A^2 \sum_{i=1}^{M} \sum_{j=1}^{M} \rho_{ij}\, \sigma_{L_i}\, \sigma_{L_j} \tag{4.11}$$

where ρ_{ij} is the correlation coefficient between the loads on floors i and j. Now if the load intensities on each floor are assumed to be identically distributed; i.e., $\bar{L}_i = \bar{L}$, $\sigma_{L_i} = \sigma_L$, and $\delta_{L_i} = \delta_L$, and with $\rho_{ij} = \rho_{ji}$, $\rho_{ii} = 1$,

$$\bar{Y} = M A \bar{L}$$

$$\mathrm{Var}(Y) = M A^2 \sigma_L^2 + 2 A^2 \sigma_L^2 \sum_{i=1}^{M-1} \sum_{j=i+1}^{M} \rho_{ij}$$

and

$$\delta_Y = c_R\, \delta_L \tag{4.12}$$

where

$$c_R = \frac{1}{M} \left(M + 2 \sum_{i=1}^{M-1} \sum_{j=i+1}^{M} \rho_{ij} \right)^{1/2} \tag{4.13}$$

The "reduction coefficient" c_R is a function of the number of floors supported and the load correlation between them. If perfect correlation exists, $\delta_Y = \delta_L$, and if the loads are statistically independent, $\delta_Y = \delta_L/\sqrt{M}$; in reality, δ_Y will fall somewhere in between.

c_R has the effect of reducing the nominal live load intensity per floor in determining the total load on a column; the mean column load intensity per floor does not change, however. The nominal design load per floor at a cumulative probability q, S_q, will decrease as the number of floors increases because the variance of the load decreases. It should be pointed out that c_R is different from the conventional load-reduction factor, although it serves the same purpose.

An estimate of the correlation is made by calculating the load reductions at the 99 percent level corresponding to several assumed correlation functions and comparing these to data-based computed reductions [43]. Intuitively, ρ_{ij} should depend inversely on the separation between floors i and j. Simple linear, quadratic, and exponential functions were assumed. On this basis, results show that significant correlation exists between floors that are less than four or five stories apart, but that the correlations are negligible for floors that are more widely separated.

A linearly decreasing correlation function of the form

$$\rho_{ij} = 1 - (j - i)/4 \qquad (4.14)$$

gives a reasonable and slightly conservative bound to the test results of Mitchell and Woodgate, and is used in the subsequent analysis.

Figure 4.2 shows the variation of the reduction coefficient c_R with the number of stories supported by the column. The rate of reduction decreases as the number of floors increases, suggesting some value beyond which further reductions can be ignored. The rate is greatest when less than ten stories are involved. Figure 4.3 shows the variation of the

reduced c. o. v. of column load intensity with tributary area. The rate of reduction decreases as the area increases. In a practical sense, values of M and A can be set beyond which no further reduction is allowed. From Figs. 4.2 and 4.3, suitable cutoff points may be M = 15 - 20 stories, and A ≃ 500 ft.^{2}.

The load effect on a structural element is obtained by integrating the product of the load intensity and the influence function over the tributary area. The effects of load concentrations can thereby be assessed. The equivalent uniformly distributed load (EUDL) that produces the same load effect may then be determined, which is actually the load of interest in design. Mitchell and Woodgate have computed the EUDL required to cause the same internal effect (beam shear, moment, etc.) as that resulting from actual loads measured in their survey. Load concentration factors (LCF) are computed which, when multiplied by the 99 percentile intensity, yield the 99 percentile EUDL.

It is assumed in the sequel that the load intensities are normally distributed. In the present study, the evaluation is in terms of mean values, but the LCF computed above are for 99 percentile values; it is assumed that the mean EUDL is obtained by multiplying the mean intensity by the LCF, and that the c.o.v. of this EUDL is δ_L obtained from Fig. 4.1. The uncertainty in spacewise variability is reflected in the choice of the prediction error Δ_L. It is also assumed that the column load reduction factor c_R is applicable to both the permanent and short-term live loads.

It appears that additional study is required to obtain a more exact description of load correlation over different tributary areas and floor levels.

4.3.2 Analysis of Uncertainties

The load-induced action resulting from live load is

$$S_L = c_L L \tag{4.15}$$

where L is the EUDL intensity, and c_L is an influence coefficient translating the applied load intensity to the required load effect. Uncertainties in c_L arise from errors pertaining to the structural analysis, and are assumed to be entirely of the prediction type.

The mean live load effect is

$$\overline{S_L} = \overline{c_L}\ \overline{L} \tag{4.16}$$

For the design of a beam, the basic variability in the load effect is

$$\delta_{S_L} = \delta_L \tag{4.17}$$

and for column design,

$$\delta_{S_L} = c_R\ \delta_L \tag{4.18}$$

where δ_L is the c.o.v. of load intensity, which depends on the tributary area. If dead and live load only are considered, the long-term load statistics should be used; however, if wind effects are included, the instantaneous live loads would be appropriate. c_R is selected from Fig. 4.2, depending on the number of floors supported.

The prediction error in S_L, reflecting the imponderables in the load models and the errors in the structural analysis, is

$$\Delta^2_{S_L} = \Delta^2_{c_L} + \Delta^2_L \tag{4.19}$$

where Δ_{c_L} is a measure of the degree of confidence attributed to the analysis, and Δ_L arises from the assumptions used to model the live loads, i.e., those regarding load concentration effects, load reduction and correlation, and time dependency.

Rosenblueth and Esteva [49] estimated that the uncertainty due to spacewise variability and load concentration is approximately $(1.2)^2 V_L^2/A$; using Mitchell and Woodgate's survey, they found $V_L \simeq 1.4$. Uncertainties in time-dependent effects arise from approximating the extreme of the continuous load process using instantaneous load measurements; the uncertainty associated with this is assumed to be $\Delta_T \simeq 0.10$. The load reduction is assigned a prediction error of $\Delta_{LR} \simeq 0.15$ for a beam, and $\Delta_{LR} \simeq 0.20$ for a column supporting more than one floor. Then

$$\Delta_L^2 \simeq \frac{(1.68)^2}{A} + \Delta_T^2 + \Delta_{LR}^2 \qquad (4.20)$$

The 99 percentile design loads computed with the method outlined above compare quite well with those obtained by Peir [44] from a more sophisticated analysis. For the design of a beam with a tributary area of 500 ft^2 in which the support moment governs the design, the 99 percent EUDL is computed to be

$$S_{.99} = (LCF)\,\bar{L}\,(1 + 2.33\,\delta_L)$$

$$= (1.25)\,(27.4)\,(1 + 2.33 \times .27) \simeq 56 \text{ psf}$$

Corresponding values determined by Peir range from about 43 psf to 52 psf, depending on the load combinations considered. A slightly conservative result is similarly obtained for columns.

4.4 Wind Loads

4.4.1 Introductory Remarks

Wind effects are often important in the design of tall buildings. An accurate analysis of wind-induced loads should consider the turbulent, random nature of wind and the dynamic response of the system to it. A reasonable way to do this is to introduce a gust factor reflecting the wind statistics and dynamic characteristics of the structure by which the static forces can be multiplied [29, 57]. The resulting wind pressure can then be used in a static analysis.

Comprehensive analyses of wind-induced pressures and related structural responses are available [29, 57]. A brief discussion of the method of approach and its significance to design is given here.

4.4.2 The Gust Factor

Wind velocity is characterized by a steady-state mean velocity U_s, obtained as the average over duration t_d, and a fluctuating component $u(y,z,t)$, usually assumed to be a stationary Gaussian process. The total wind velocity is then

$$U = U_s + u(y,z,t) \tag{4.21}$$

The steady-state velocity increases with height approximately in accordance with the power law profile

$$\frac{U_s}{U_G} = \left(\frac{z}{z_G}\right)^{\alpha} \tag{4.22}$$

where z_G and U_G are the gradient height and velocity, and α depends on the location; in cities, $\alpha \simeq 0.4$.

The pressure acting on a point is related to the velocity by

$$p = \frac{1}{2} \rho c_p U^2$$

where ρ is the mass density of air ($\rho \simeq 0.0025$ slugs/ft^3), and c_p is a pressure coefficient. Denoting the reference velocity at 30 ft as $U_o = U_s(30)$, the mean steady-state pressure at a height h on a building is

$$\overline{p} = \frac{1}{2} \rho c_p U_o^2 \left(\frac{h}{30}\right)^{2\alpha} \tag{4.23}$$

and the mean wind pressure profile is

$$\overline{p}(z) = \overline{p} \left(\frac{z}{h}\right)^{2\alpha} \tag{4.24}$$

The total static plus dynamic response of the structure is

$$Y(z/h,t) = \overline{Y}\, \phi(z/h)\, (1 + y(t)) \tag{4.25}$$

where $\overline{Y}$ is a generalized coordinate, $y(t)$ is a dimensionless dynamic response function, and $\phi(z/h)$ is the mode shape associated with the fundamental natural frequency f_o. It is assumed that the first mode dominates the response, and that the mode shape is $\sqrt{3}\ z/h$. When the pressure is integrated over the area on which it acts, the statistics of $y(t)$ may be found in terms of those of $u(y,z,t)$ from the theory of random vibration [41]. Using approximations suggested by Davenport [29],

$$E\,[y(t)] = 0$$

$$\sigma_y^2 = \frac{16}{3} k \left(\frac{30}{h}\right)^{2\alpha} \left[\frac{\pi}{\beta} g_1 g_2 g_3 + g_4\right] \tag{4.26}$$

where k is a surface roughness factor taken as 0.05 in cities, β is the total mechanical and aerodynamic damping, and

$$g_1 = \frac{1}{1 + \frac{c_y}{2} \left(\frac{30}{h}\right)^{\alpha} \frac{f_o b}{U_o}}$$

$$g_2 = \frac{1}{1 + \frac{c_z}{3} \left(\frac{30}{h}\right)^{\alpha} \frac{f_o h}{U_o}}$$

$$g_3 = \frac{\left(4000 \frac{f_o}{U_o} \left(\frac{30}{h}\right)^{\alpha}\right)^2}{\left[1 + \left(4000 \frac{f_o}{U_o} \left(\frac{30}{h}\right)^{\alpha}\right)^2\right]^{4/3}} \tag{4.27}$$

$$g_4 = 6\left[1 - \frac{1}{\left[1 + \left(\frac{1500}{h}\right)^2\right]^{1/3}}\right]$$

in which $c_y \simeq 20$ and $c_z \simeq 8$. Terms g_1 and g_2 represent the effects of spatial correlation of u(y,z,t), and g_3 is an empirical expression [29] for the spectral density of u. Collectively, they represent the contribution

to σ_y^2 from frequencies where $f \simeq f_o$. The contribution from other frequencies is given approximately by g_4.

The gust factor is defined from Eq. 4.25 to be

$$G = \max_{0 \leq t < t_d} [1 + y(t)] \tag{4.28}$$

Since G is a random variable, a suitable design value may be chosen such that the probability of exceedance is sufficiently small. Let

$$M = \max_{0 \leq t \leq t_d} y(t)$$

be a random variable of unknown distribution. If y(t) is Gaussian, it may be shown [28] that the distribution function for M is approximately

$$F_M(x) \simeq \exp[-f_o t_d \exp(-x^2/2\sigma_y^2)]$$

If x_q is specified such that $q = 1 - F_M(x_q)$, the gust factor associated with exceedance level q is $G_q = 1 + x_q$. If the exceedance level is associated with the characteristic extreme x_c, then $F_M(x_c) = 1/e$, and

$$x_c = \sqrt{2 \ln(f_o t_d)}\, \sigma_y$$

The design gust factor is then [29]

$$G_D = 1 + \sqrt{2 \ln(f_o t_d)}\, \sigma_y \tag{4.29}$$

The design wind pressure profile is found by combining Eqs. 4.29 and 4.24, i.e.,

$$W(z) = G_D \bar{p} (z/h)^{2\alpha} \tag{4.30}$$

4.4.3 Wind Load Statistics and Uncertainties

The mean gust factor is

$$\overline{G}_D = G_D\left(\overline{k}, \overline{\alpha}, \overline{\beta}, \overline{f}_o, \overline{U}_o, \overline{c}_y, \overline{c}_z\right) \tag{4.31}$$

and its variability and prediction error are

$$\begin{Bmatrix} \delta^2_{G_D} \\ \Delta^2_{G_D} \end{Bmatrix} = \sum_i a_i^2 \begin{Bmatrix} \delta_i^2 \\ \Delta_i^2 \end{Bmatrix} \tag{4.32}$$

where the expressions for a_i are given in Appendix D. To determine the terms of practical significance, it is necessary to study the coefficients a_i in Eq. 4.32.

Figures 4.4 and 4.5 show the variation of the gust factor $\overline{G}_D$ and the various a_i with $\overline{f}_o$ and $\overline{\beta}$ for a specified mean wind profile on a building of moderate height. It can be observed that the mean gust factor $\overline{G}_D$ is insensitive to variations in $\overline{f}_o$ and $\overline{\beta}$. This is significant because these quantities are often estimated from empirical expressions. The implication is that refined estimates of the dynamic characteristics of the system will not improve the determination of the gust factor.

Figure 4.6 shows the variation of a_i and $\overline{G}_D$ with the height of a building. For tall, slender buildings, the parameters $\overline{\beta}$, $\overline{U}_o$, $\overline{c}_y$, $\overline{c}_z$, and $\overline{f}_o$ become more significant, and $\overline{\alpha}$ and $\overline{k}$ lose some of their importance. Shorter buildings are more affected by the surface roughness, as reflected in k, and the wind profile. For a lightly damped structure with a

response dominated by resonance, the specification of the natural frequency f_o becomes important. The gust factor decreases as the height increases up to 400 ft (in Fig. 4.6) because the turbulent components of velocity caused by surface roughness become less significant in comparison to the steady-state velocity.

For lightly damped buildings of moderate height, the variations in the gust factor statistics attributable to c_y and c_z are small and can be neglected. Overall variations are dominated by those of k and α, and to a lesser extent U_o. Vickery [57] observed that the gust factor is insensitive to the mode shape; hence, the actual mode shape is usually not too important.

Statistics for U_o are found from existing meteorological information. For example, using Thom's data [54] the annual extreme fastest-mile-wind-speed at 30 ft height for the area around Chicago, Illinois is 80 mph for a return period of 100 years, and 70 mph for a return period of 50 years (for open country exposures). These values must be converted to averages over a time duration t_d suitable for determining the gust factor, and then translated to urban exposures. A suitable averaging time is 20 minutes. [48] The result of this computation gives $\overline{U}_o$ = 37 ft/sec and 33 ft/sec for return periods of 100 and 50 years, respectively. The c.o.v. δ_{U_o} is about 0.15.

The natural frequency f_o may be expressed in terms of the dead and live load, assuming all floors are loaded identically, as

$$f_o \simeq c_f \left(N_s (L + D)\right)^{-\frac{1}{2}} \tag{4.33}$$

where c_f is a constant depending on the stiffness of the fundamental mode. The mean of f_o is estimated approximately from $\overline{f}_o \simeq 10/N_s$, where N_s is the number of stories. From Eq. 4.33, the c.o.v. of f_o is found in terms of δ_D and δ_L as

$$\delta_{f_o} \simeq \frac{1}{2}\left[\left(\frac{\overline{L}/\overline{D}}{1+\overline{L}/\overline{D}}\right)^2 \delta_L^2 + \left(\frac{1}{1+\overline{L}/\overline{D}}\right)^2 \delta_D^2\right]^{1/2} \tag{4.34}$$

The appropriate mean live loads are those for short-term duration.

The variability in the design wind pressure is found from Eq. 4.30 to be

$$\delta_W^2 = \delta_{G_D}^2 + \delta_{\overline{p}}^2 \tag{4.35}$$

in which $\delta_{\overline{p}} = 2\,\delta_{U_o}$, and

$$\delta_{G_D}^2 \simeq a_{U_o}^2\,\delta_{U_o}^2 + a_{f_o}^2\,\delta_{f_o}^2$$

where a_{U_o} and a_{f_o} are the appropriate coefficients in Eq. 4.32.

Additional (prediction) uncertainties may arise from the assumed values of $\overline{k}$ and $\overline{\alpha}$, as well as in the value of $\overline{\beta}$ and the determination of $\overline{f}_o$. In view of these, the prediction error in the calculated wind pressure is

$$\Delta_W^2 = \Delta_{G_D}^2 + \Delta_{\overline{p}}^2 \tag{4.36}$$

where

$$\Delta_{\overline{p}}^2 \simeq \Delta_{c_p}^2 + 4\,\overline{\alpha}^2\,\ln^2\left(\frac{h}{30}\right)\,\Delta_\alpha^2 \tag{4.37}$$

assuming $\Delta_{U_o} \simeq 0$, and

$$\Delta_{G_D}^2 \simeq a_k^2\,\Delta_k^2 + a_\alpha^2\,\Delta_\alpha^2 + a_\beta^2\,\Delta_\beta^2 + a_{f_o}^2\,\Delta_{f_o}^2 \tag{4.38}$$

where uncertainties in c_y and c_z have been ignored. In buildings of moderate height, Eq. 4.38 may be approximated by

$$\Delta_{G_D}^2 \simeq a_k^2\,\Delta_k^2 + a_\alpha^2\,\Delta_\alpha^2$$

Reasonable estimates [57] of the prediction errors are $\Delta_\alpha = 0.10$, $\Delta_k = 0.20$, $\Delta_\beta = 0.25$, $\Delta_{c_p} = 0.10$, and $\Delta_{f_o} = 0.10$. Alternatively, Δ_{f_o} could be computed from Eq. 4.34 by substituting Δ_L and Δ_D for δ_L and δ_D.

The mean wind load effect is

$$\overline{S}_W = \overline{c}_W\,\overline{W} \tag{4.39}$$

where $\overline{W}$ is defined in Eq. 4.30, evaluated at $z = h$, and c_W is an influence coefficient. Its variability is $\delta_{S_W} = \delta_W$, from Eq. 4.35, and the prediction error is

$$\Delta_{S_W}^2 = \Delta_{c_W}^2 + \Delta_W^2 \tag{4.40}$$

where Δ_W is defined in Eq. 4.36, and Δ_{c_W} is the measure of inaccuracy in the structural analysis.

Chapter 5

CRITICAL APPRAISAL OF CURRENT DESIGN CRITERIA

5.1 General Remarks

In this chapter, the resistance and load statistics found in Chapters 3 and 4 are used to evaluate the reliability of designs determined from present ACI provisions. The primary objective is to determine what risk levels are implied in current designs, or associated with designs obtained with existing load factors.

This evaluation is necessary to aid in the adoption of a probability based design format. Code formulation is an evolutionary process, and new provisions seldom reflect abrupt changes from previous codes [49]. It is reasonable to expect that a reliability based code should initially give the same designs as existing code provisions. This means that the current level of safety, or risk, should be maintained. The level of risk implicit in current designs, therefore, must be evaluated.

In the present analysis, the resistance and load effects are assumed to be mutually independent random variables. The study is restricted to consideration of the adequacy of designs where strength is the governing criterion. Beams are examined with regard to their adequacy in flexure and shear, whereas columns are studied from the standpoint of the development in Sec. 3.4. Of particular interest is the comparison of the risk levels implied in the different failure modes, and the effect of concrete quality on the member reliability.

5.2 Appraisal of ACI Design Provisions

5.2.1 Analysis of Loading Provisions

To evaluate the adequacy of existing ACI designs, it is necessary to translate the nominal loads and resistances to their mean values. The ACI code requires that the design load be computed as [5]

$$U' = 1.7\,L + 1.4\,D \tag{5.1}$$

when dead and live loads are considered, and

$$U' = 0.75(1.7\,L + 1.4\,D + 1.7\,W) \tag{5.2}$$

when wind effects are included. A third loading condition, in which the live load is absent, is also required, but this will not be considered here. The internal load effect U_i' dimensionally consistent with the response quantity sought is

$$U_i' = \bar{c}_L L_{nom}(1.7 + 1.4\,K) \tag{5.3}$$

where

$$K = \frac{\bar{c}_D D_{nom}}{\bar{c}_L L_{nom}} \tag{5.4}$$

and $\bar{c}_L$ and $\bar{c}_D$ are influence coefficients for the desired load effects, D_{nom} is the nominal dead load in psf, and L_{nom} is the nominal live load in psf, obtained from the ASA Building Code [7], or similar standards. Introduce factors α_D and α_L such that

$$L_{nom} = \alpha_L \overline{L}$$
$$D_{nom} = \alpha_D \overline{D} \tag{5.5}$$

where $\overline{L}$ and $\overline{D}$ are predicted mean values of live and dead load (e.g., obtained from load surveys). Then

$$U_i' = \overline{c}_L \alpha_L \overline{L} (1.7 + 1.4 K) \tag{5.3a}$$

in which

$$K = \frac{\overline{c}_D \alpha_D \overline{D}}{\overline{c}_L \alpha_L \overline{L}} \tag{5.4a}$$

α_L may be computed by comparing $\overline{L}(A)$ from load survey data [43] to the nominal live load computed from Eq. 4.9. α_D may be found by comparing the 95 percent load value to the mean dead load, assuming D is normally distributed; with $\delta_D \simeq 0.06$, $\alpha_D \simeq 1.10$. Similarly, when wind load effects are included,

$$U_i' = \overline{c}_L \alpha_L \overline{L} (0.75)(1.7 + 1.4 K + 1.7 K_W) \tag{5.6}$$

in which

$$K_W = \frac{\overline{c}_W \alpha_W \overline{W}}{\overline{c}_L \alpha_L \overline{L}} \tag{5.7}$$

$\overline{W}$ is found from Eq. 4.30 evaluated at z = h, and α_W is computed by comparing this value to the standard design wind pressure specified in the Uniform Building Code [56].

5.2.2 Provisions for Flexure

The nominal resistance of a section against flexure is

$$M' = \phi_F \, \bar{b} \, \bar{d}^2 \, \bar{p} \, f'_y \left(1 - 0.59\bar{p} \frac{f'_y}{f'_c}\right) \tag{5.8}$$

where f'_c and f'_y are nominal steel and concrete strengths, and ϕ_F is a flexural capacity reduction factor specified as 0.90. The conventional safety requirement, $M' \geq U'_i$, is then

$$\phi_F \, \bar{b} \, \bar{d}^2 \, \bar{p} f'_y \left(1 - 0.59\bar{p} \frac{f'_y}{f'_c}\right) \geq \bar{c}^F_L \, \alpha_L \, \bar{L} \, (1.7 + 1.4 \, K_F) \tag{5.9}$$

where $\bar{c}^F_L$ is the influence coefficient for flexure, and to find the required design for the section,

$$D_F = \frac{\bar{b} \, \bar{d}^2}{\bar{c}^F_L \, \bar{L}} = \frac{\alpha_L (1.7 + 1.4 \, K_F)}{\phi_F \bar{p} \, f'_y (1 - 0.59\bar{p} \, f'_y / f'_c)} \tag{5.10}$$

D_F represents a flexural design, given in terms of the material properties and the mean load ratio only. A design may be obtained from D_F by multiplying D_F by the mean internal live load effect, i.e., $\bar{b} \, \bar{d}^2 = D_F \, \bar{c}^F_L \, \bar{L}$. When wind effects are included,

$$D_F = \frac{\bar{b} \, \bar{d}^2}{\bar{c}^F_L \, \bar{L}} = \frac{\alpha_L (0.75)(1.7 + 1.4 \, K_F + 1.7 \, K_{WF})}{\phi_F \, \bar{p} \, f'_y (1 - 0.59\bar{p} \, f'_y / f'_c)} \tag{5.11}$$

The nominal values of p, b, and d have been chosen at their respective means.

To compute the underlying risk of failure of a specified design using the alternative risk measure, it is first necessary to determine the equivalent value of $w_F(\bar{\theta}_F)$. From Eq. 2.18, the mean capacity and load effects are related as

$$\overline{b}\,\overline{d}^2 A = w_F(\overline{\theta}_F)\,\overline{c}_L^F\,\overline{L} \tag{5.12a}$$

where

$$A = \overline{p}\,\overline{f}_y(1 - 0.59q) \tag{5.13a}$$

if failure occurs in tension, and

$$A = \overline{p}\,\overline{f}_s\left(1 - 0.59\overline{p}\,\frac{\overline{f}_s}{\overline{f}_c}\right) \tag{5.13b}$$

if failure occurs in compression, where $\overline{f}_s$ is defined in Eq. 3.19. Therefore,

$$w_F(\overline{\theta}_F) = \frac{\overline{b}\,\overline{d}^2}{\overline{c}_L^F\,\overline{L}}\,A = D_F\,A \tag{5.12b}$$

into which D_F may be substituted from Eqs. 5.10 or 5.11. First, a tension failure is assumed; then using Eqs. 5.13a and 5.12b, $w_F(\overline{\theta}_F)$ is determined and the probability of failure is computed from Eqs. 2.25 and 2.26. Next, a compression failure is assumed and the process is repeated using Eqs. 5.13b and 5.12b. Alternatively, the prescriptive lognormal basis may be used instead of Eqs. 2.25 and 2.26 to compute the probabilities of failure in tension and compression. The total probability of failure may then be found from Eq. 3.11.

5.2.3 Provisions for Shear

The adequacy of a design D_F against shear is investigated by checking the shear capacity at a distance d from the beam support, in accordance with present ACI practice. The mean shear capacity of the beam is

given in Eq. 3.36, in which $\overline{v}_{cu}$ is defined in Eq. 3.29. The shear-moment ratio necessary for its evaluation is found from

$$\frac{\overline{V}}{\overline{M}} = \frac{\overline{c}_D^S \overline{D} + \overline{c}_L^S \overline{L} + \overline{c}_W^S \overline{W}}{\overline{c}_D^F \overline{D} + \overline{c}_L^F \overline{L} + \overline{c}_W^F \overline{W}} \tag{5.14}$$

where all influence coefficients are evaluated at a distance $\overline{d}$ from the support. When only gravity loads are considered, $\overline{W} = 0$. Although Eq. 3.27 suggests that the mean shear capacity is a function of the mean loads, the shear resistance and applied load effects will be assumed to be independent in the evaluation of the risk in shear.

The nominal resistance provided by the ACI code against shear is given as

$$V' = \phi_s \, v'_{cu} \, \overline{b} \, \overline{d} \, (1 + \frac{1}{r'_s}) \tag{5.15}$$

where $r'_s = V'_c/V'_{ws}$, ϕ_s is the shear capacity reduction factor specified as 0.85, and v'_{cu} is evaluated from Eq. 3.27. The nominal shear-moment ratio is determined from Eqs. 5.3a or 5.6 for the bending and shear loads at a distance $\overline{d}$ from the support, with the limitation $V'/M' \leq 1/\overline{d}$, as required by the ACI code.

On the basis of the truss analogy, the value of r'_s provided in the ACI code may be found from equating Eq. 5.15 to Eq. 5.3a or 5.6 for shear. This yields

$$r'_s = \frac{v'_{cu} \, \overline{b} \, \overline{d}}{\frac{\alpha_L \, \overline{c}_L^S \, \overline{L}}{\phi_s} (1.7 + 1.4 \, K_S) - v'_{cu} \, \overline{b} \, \overline{d}} \tag{5.16a}$$

for dead and live loads, or

$$r'_s = \frac{v'_{cu}\ \bar{b}\ \bar{d}}{\frac{\alpha_L \bar{c}_L^S\ \bar{L}}{\phi_S}\ (0.75)(1.7 + 1.4\ K_S + 1.7\ K_{WS}) - v'_{cu}\ \bar{b}\ \bar{d}} \qquad (5.16b)$$

when wind load effects are included. To analyze the underlying reliability for shear, it is necessary to translate r'_s to the parameter r_s based on mean values. This is done using the relation

$$r_s = \frac{\bar{v}_{cu}}{v'_{cu}}\ \frac{f'_y}{\bar{f}_y}\ r'_s \qquad (5.17)$$

To insure that every potential diagonal crack is crossed by at least one stirrup, the spacing of the stirrups must be $\bar{s}_{st} \leq \frac{1}{2}\bar{d}$. In terms of r_s, this implies that

$$r_s = \frac{\bar{v}_{cu}\ \bar{b}\ \bar{d}}{\bar{A}_v\ \bar{f}_y\ \bar{d}}\ \bar{s}_{st} \leq \frac{1}{2}\ \frac{\bar{v}_{cu}\ \bar{b}\ \bar{d}}{\bar{A}_v\ \bar{f}_y} \qquad (5.18)$$

To provide against sudden stirrup yielding and the resulting diagonal crack growth, the ACI code specifies a minimum allowable stirrup area

$$\bar{A}_v \geq 50\ \frac{\bar{b}\ \bar{s}_{st}}{f'_y}$$

Translated to ksi units, and in terms of the parameter r_s, this means that

$$r_s = \frac{\bar{v}_{cu}\ \bar{b}\ \bar{d}}{\bar{A}_v\ \bar{f}_y\ \bar{d}}\ \bar{s}_{st} \leq \frac{\bar{v}_{cu}\ \bar{b}\ \bar{d}}{\bar{A}_v\ \bar{f}_y\ \bar{d}}\ 20\ \frac{\bar{A}_v\ f'_y}{\bar{b}} = 20\ \bar{v}_{cu}\ \frac{f'_y}{\bar{f}_y} \qquad (5.19)$$

Equations 5.18 and 5.19 place additional limitations on the value of r_s derived from strength considerations only. The minimum value of r_s computed from Eqs. 5.17, 5.18 and 5.19 should be used to assess the probability of shear failure of a given design.

The mean shear capacity and applied load effect are related, from Eqs. 2.18 and 3.36, as

$$\bar{\phi}_2 \, \bar{v}_{cu} \, \bar{b} \, \bar{d} \, (1 + \frac{1}{r_s}) = w_s(\bar{\theta}_S) \, \bar{c}_L^S \, \bar{L} \tag{5.20}$$

To compute the underlying risk of shear failure of a flexural design, it is necessary to determine its equivalent value of $w_S(\bar{\theta}_S)$ in shear. From Eq. 5.20,

$$w_s(\bar{\theta}_S) = \frac{\bar{b} \, \bar{d}}{\bar{c}_L^S \, \bar{L}} \, \bar{\phi}_2 \, \bar{v}_{cu} \, (1 + \frac{1}{r_s})$$

This may be expressed in terms of D_F as

$$w_s(\bar{\theta}_S) = \left[\frac{\bar{b} \, \bar{d}^{\,2}}{\bar{c}_L^F \, \bar{L}} \right] \frac{\bar{c}_L^F}{\bar{c}_L^S} \, \frac{1}{d} \, \bar{v}_{cu} \, \bar{\phi}_2 \, (1 + \frac{1}{r_s})$$

$$= D_F \, \frac{\bar{c}_L^F}{\bar{c}_L^S} \left(\frac{\overline{b/d}}{D_F \, \bar{c}_L^F \, \bar{L}} \right)^{1/3} \bar{\phi}_2 \, \bar{v}_{cu} \, (1 + \frac{1}{r_s}) \tag{5.21}$$

wherein $\bar{d}$ is found from the flexural solution as

$$\bar{d} = \left(\frac{D_F \, \bar{c}_L^F \, \bar{L}}{\overline{b/d}} \right)^{1/3} \tag{5.22}$$

With $w_s(\overline{\theta}_S)$ given above, the risk of failure in shear may be computed from Eqs. 2.25 and 2.26 as a function of r_s and $\overline{b/d}$.

5.2.4 Provisions for Axial Thrust and Bending

Combined bending and axial thrust is handled in a manner similar to flexure. For a given $\overline{e/t}$, the conventional safety requirement, $P' \geq U_i'$, is

$$\phi_c \, \overline{k}_3 \, f'_c \, \overline{b} \, \overline{t} \, q'_u \geq \alpha_L \, \overline{c}_L^P \, \overline{L} \, (1.7 + 1.4 \, K_C) \qquad (5.23a)$$

when dead and live loads are considered, or

$$\phi_c \, \overline{k}_3 \, f'_c \, \overline{b} \, \overline{t} \, q'_u \geq \alpha_L \, \overline{c}_L^P \, \overline{L} \, (0.75)(1.7 + 1.4 \, K_C + 1.7 \, K_{WC}) \qquad (5.23b)$$

when wind effects are included. q'_u is a dimensionless axial capacity defined in Appendix C, and is dependent on $\overline{e/t}$ and whether a tension or compression failure occurs. ϕ_c is the capacity reduction factor for tied columns, given as 0.70 by ACI 318-63. Thus, a design is determined as

$$D_C = \frac{\overline{b} \, \overline{t}}{\overline{c}_L^P \, \overline{L}} = \frac{\alpha_L (1.7 + 1.4 \, K_C)}{\phi_c \, \overline{k}_3 \, f'_c \, q'_u} \qquad (5.24a)$$

when dead and live loads are considered, or

$$D_C = \frac{\overline{b} \, \overline{t}}{\overline{c}_L^P \, \overline{L}} = \frac{\alpha_L (0.75)(1.7 + 1.4 \, K_C + 1.7 \, K_{WC})}{\phi_c \, \overline{k}_3 \, f'_c \, q'_u} \qquad (5.24b)$$

when wind effects are included. The ACI code places a lower limit on the allowable $\overline{e/t}$ of 0.10; the effect is to prescribe a minimum D_C.

The probability of failure of a design is evaluated by first determining the associated $w_C(\bar{\theta}_C)$ for compression and tension failures, computing the conditional probabilities of failure on the basis of the assumed failure mode, and applying Eq. 3.48 to determine the total probability of failure. The mean capacity and applied load effects are related as

$$\bar{b}\ \bar{t}\ B = w_C(\bar{\theta}_C)\ \bar{c}_L^P\ \bar{L} \tag{5.25}$$

where

$$B = \bar{k}_3\ \bar{f}_c\ \bar{q}_u^C$$

if failure occurs in compression, and

$$B = \bar{k}_3\ \bar{f}_c\ \bar{q}_u^T$$

if failure occurs in tension; $\bar{q}_u^C$ and $\bar{q}_u^T$ are dimensionless mean values of axial capacity defined in Appendix C. Therefore,

$$w_C(\bar{\theta}_C) = \frac{\bar{b}\ \bar{t}}{\bar{c}_L^P\ \bar{L}}\ B = D_C B \tag{5.26}$$

into which the design D_C may be substituted to evaluate its risk of failure under combined thrust and bending.

5.3 Risks Associated With Current ACI Designs

The levels of risk associated with current ACI provisions for the design of beams and columns are determined herein for different loading conditions. For purposes of illustration, elastic analysis is used throughout. Assuming the members are prismatic, and the within-member resistances

are perfectly correlated, the design is, therefore, determined at the point of maximum load effect.

5.3.1 Beams Subjected to Specified Load Effects

Consider a beam of 15 ft span supporting a tributary area of 150 ft^2; the loads consist of dead load and permanent live loads. The dead and live load statistics are found by the methods described in Secs. 4.2 and 4.3. A summary of the pertinent quantities is given in Table 5.1.

TABLE 5.1

Load Statistics for a Beam Supporting a Tributary Area of 150 Ft^2

	Mean(psf)	δ_{S_i}	Δ_{S_i}	α
Dead Load	100	0.06	0.10	1.10
Live Load	45	0.29	0.23	1.78

Figure 5.1 shows probabilities of failure of ACI flexural designs in tension and compression modes, for varying reinforcement ratio $\bar{p}$. These are actually conditional probabilities, in accordance with Eqs. 3.12 and 3.13. However, if $\bar{p}$ = 0.02, with intermediate grade steel, the probability of the occurrence of a compression failure is 0.0378 (0.0567), and the probability of the occurrence of a tension failure is 0.9622 (0.9433); parenthetical quantities refer to poor concrete quality. As a result, the first term in Eq. 3.11 dominates, and the probability of failure of the section in

flexure is approximately equal to its probability of failure in the tension mode. This suggests that if the reinforcement ratio is suitably chosen, the possibility of a compression failure may be ignored in assessing the underlying risk. Commonly, reinforcement ratios are often chosen considerably less than $0.75p_b'$. The total probability of failure computed from Eq. 3.11 is also shown in Fig. 5.1, and indicates the small difference when the possibility of a compression failure is included.

It can be observed from Fig. 5.1 that the risk levels (in tension) are all of the order of 10^{-5}, and are not sensitive to $\bar{p}$, for the range of $\bar{p}$ of interest. The lognormal-prescriptive risk evaluation provides conservative but approximate agreement to that obtained from the alternative risk measure. Poor concrete quality does not have a significant effect on the probability of tension failure. (The probability of failure in the compression mode is significantly affected, but the likelihood of its occurrence is very small). This was foreseen in Fig. 3.5, showing the insensitivity of δ_{M_T} and Δ_{M_T} to $\bar{p}$ and the concrete quality. There is no significant difference when high strength steel is used.

Figure 5.2 illustrates the relative safety against flexural failure when deterministic load factors other than the current values of 1.7 against live load and 1.4 against dead load are used. ACI 318-63 provided values of 1.8 and 1.5. Provisions of ACI 318-71 imply an increase in risk of less than one order of magnitude; the margins of safety for flexural designs are thus not significantly different. If the load factors should decrease to 1.5 and 1.2, the implied risk would increase to about 10^{-4}, about one order of magnitude higher than that of current designs.

To examine the safety against shear failure, the end restraints must be considered, since the V/M ratio is required. For this purpose, simply supported and fully fixed beams are examined.

Figures 5.3 and 5.4 illustrate the probability of failure in shear of ACI beams as a function of the amount of web reinforcement r_s, and the cross sectional parameter $\overline{b/d}$. Large r_s corresponds to light web reinforcement. Figures 5.3 and 5.4 also demonstrate the difference between simply supported and fully fixed end conditions. The probability of shear failure is more sensitive to r_s when the beam is fully restrained, than when it is simply supported; for a given risk level and reinforcement ratio $\overline{p}$, r_s is also smaller for the restrained beam. This is because the flexural sections are smaller with full end restraint; hence, the resulting area for shear resistance is decreased accordingly, and more web reinforcement is needed to resist the same shear force.

Figure 5.5 illustrates the effect of poor concrete quality on the risk of shear failure, with $r_s = 2$. An increase of δ_{f_c} from 0.12 to 0.20 increases the risk of a shear failure only slightly; the reason for this may be seen from Fig. 3.7, wherein δ_{V_T} is nearly the same for both values of δ_{f_c}. For given r_s and $\overline{p}$, beams with a low $\overline{b/d}$ exhibit a greater risk in shear than those where $\overline{b}$ and $\overline{d}$ are about the same.

The failure probability in shear is extremely sensitive to the amount of web reinforcement provided. A 20 percent change in r_s, implying a 20 percent change in stirrup spacing, may change the shear risk level by one or two orders of magnitude. As an example of how the reliability in shear may be assessed, suppose a simply supported beam has been designed for

flexure according to ACI provisions, with $\overline{p} = 0.025$ and $\overline{b/d} = 0.75$; then $D_F = 8.91$, with a probability of flexural failure of 1.14×10^{-5}. From Eq. 5.22, $\overline{d} = 12.2$ inches and $\overline{b} = 9.15$ inches, and from Eq. 3.29, $\overline{v}_{cu} = 0.201$ ksi. If No. 2 bars are used as stirrups, $\overline{A}_v = 0.10$ in.^{2} A summary of the r_s required by different shear design criteria, the stirrup spacing, and the respective probabilities of failure in shear is given in Table 5.2.

TABLE 5.2

Design of Web Reinforcement

Criterion	r_s	$\overline{s}_{st}$ (in.)	p_f (shear)
p_f(Flexure) = p_f(Shear)	2.83	7.3	1.14×10^{-5}
ACI - Truss Analogy	4.55	11.8	9.6×10^{-5}
$s_{st} \leq \frac{1}{2}\overline{d}$	2.36	6.1	3.7×10^{-6}
Minimum Area	3.37	8.72	2.9×10^{-5}

The web spacing is controlled by $\overline{s}_{st} \leq \frac{1}{2}\overline{d}$ in this example.

Figure 5.6 shows the probabilities of failure in flexure and shear of ACI designs for the simply supported beam, when the truss analogy equation governs the design of the web reinforcement. The shear provisions using $\phi_s = 0.85$ are seen to be clearly inadequate to insure that p_f(Shear) < p_f(Flexure), especially when $\overline{p}$ is small. It is necessary to reduce ϕ_s to 0.70 to 0.75 before the risk levels in flexure and shear are approximately equal. Figure 5.7 illustrates the modifying effect that the maximum spacing

and minimum web steel restrictions have on the adequacy of the web in shear. The stirrups are assumed to consist of No. 2 bars. Assuming that $\phi_s = 0.85$ the spacing restriction will govern the design of the web, and is seen to be a necessary additional restriction if adequacy in shear is to be maintained.

Figure 5.8 compares the risks of failure in flexure and shear for the fully fixed beam, when the web design is determined from the truss analogy. Here, the current ACI shear strength provisions are also inadequate to insure a flexural failure, but the disparity in the risk levels is not as pronounced. A reduction in ϕ_s to 0.75 or 0.80 would be sufficient to insure that $p_f(\text{Shear}) < p_f(\text{Flexure})$. Figure 5.9 shows the effect of the minimum spacing requirement. If No. 2 bars are used, the spacing requirement has no effect; if No. 3 bars are chosen, the risk of shear failure is depressed by two orders of magnitude.

The implication that the shear capacity reduction factor should be reduced from its present value of 0.85 should not be unexpected. Tests of beams failing in flexure and shear indicate that the variability in shear capacity is considerably larger than that of flexural strength. In view of this, the decrease from $\phi_F = 0.90$ to $\phi_s = 0.85$, which is the only current reflection of the higher uncertainty, is probably neither consistent nor adequate.

The fully fixed beam appears to be more adequate in shear than the simply supported one, and the risk of a shear failure decreases as the amount of longitudinal reinforcement increases. In general, a large reinforcement ratio and/or a high degree of end restraint implies a smaller

beam cross sectional area. For a given shear effect, this will necessitate heavier web reinforcement; thus r_s will become small, and δ_{V_T} and the associated risk will decrease.

The ACI requirement regarding the maximum allowable shear stress on a section

$$v'_u - v'_{cu} \leq 8\sqrt{f'_c}$$

where $v'_u = V'/bd$ and V' is defined in Eq. 5.15, is not applicable to these examples. However, this requirement implies that

$$r'_s \geq \frac{v'_{cu}}{8\sqrt{f'_c}}$$

If r'_s is less than this value, then the section area must be increased, and r'_s will therefore increase. Since δ_{V_T} will increase with r_s, the probability of failure in shear will also increase.

Rather than placing a lower limit on r_s, a region in which δ_{V_T} is relatively small, it is more consistent to place an upper limit on r_s to insure that δ_{V_T} does not become too large. One way to accomplish this is with a minimum web area requirement, such as that in Eq. 5.19, provided by the ACI code. Figure 5.7 indicates that the present requirement may not be adequate to achieve this objective in all cases, and perhaps should be made somewhat more restrictive.

On the basis of the above analysis, it is clear that the shear strength provision derived from the truss analogy model is inadequate to assure greater safety in shear than in flexure. However, when the additional requirements of minimum web reinforcement and maximum stirrup spacing are

imposed, the probability of a shear failure is greatly reduced, and is generally less than or equal to the risk of flexural failure. Therefore, the intent and purpose of the ACI shear provisions appear to be satisfied.

Beams in a Tall Building

In this example, a beam is designed from a preliminary structural analysis of a twenty story office building. A comparison of the adequacy of the ACI provisions against dead and live loads with those pertaining to combined effects of gravity and wind is made. To obtain the influence coefficients, a STRUDL analysis of the structure was performed for dead and live loads only, and for combined gravity and wind loads. The height of the building is 240 ft and the along-wind and cross-wind dimensions are 60 ft and 100 ft respectively. The main floor beams are 20 ft in the along-wind direction, and support a tributary loaded area of 500 ft^2. The dead and live load statistics are found by the methods described in Secs. 4.2 and 4.3. For purposes of combining the live loads with wind loads, a differentiation must be made between short term and permanent live loads. The wind load statistics are found from Sec. 4.4. The fundamental natural frequency is estimated to have a mean $\overline{f}_o$ = 0.5 cps, and the total damping is assumed to be 0.015, whence $\overline{G_D}$ = 2.77 from Eq. 4.31. A summary of the pertinent statistics is contained in Table 5.3.

Figures 5.10 and 5.11 compare the probabilities of failure of ACI flexural designs for the two loading cases considered. Although the live load statistics and the live load-dead load ratio have changed, the probability measures in Figs. 5.1 and 5.10 are almost the same. With prescribed

TABLE 5.3

Load Statistics for Beams in a Tall Building

	Mean(psf)	δ_{S_i}	Δ_{S_i}	α
Dead Load	100	0.06	0.10	1.10
Permanent Live Load	34.25	0.27	0.19	1.68
Short Term Live Load	15.63	0.54	0.19	3.69
Wind Load	20.37	0.30	0.21	2.21

lognormals, the risk measures are in close agreement with the alternative risk measure, as would be expected. The risk of failure under combined gravity and wind loads is slightly less than for gravity loading only, but not enough to be significant. It may, therefore, be concluded that the levels of safety underlying current ACI flexural requirements are about equal for these two loading conditions.

The ACI code requires that the governing design be determined from the maximum of the two loading conditions. The risk of this design under the noncontrolling load condition may also be computed, e.g., if gravity and wind loads control the design, determine the probability of failure of this design against dead and live loads alone. An illustration of this is given in Table 5.4, where $\bar{p}$ has been assumed to be 0.02. The combined effect of gravity and wind governs the ACI flexural design; its probability of failure under dead and live loads is 2.1×10^{-7}. If the controlling flexural design had been based on the consideration of dead and live loads only, its failure

TABLE 5.4

Flexural Design Risks Under Different Loading Conditions

Loading	D_F	$p_f(D + L)$	$p_f(D + L + W)$
D + L	11.96	1.6×10^{-5}	5.1×10^{-4}
D + L + W	14.83	2.1×10^{-7}	1.1×10^{-5}

probability against combined load effects would have been an order of magnitude higher than for the loading condition for which it was designed, indicating that some care should be exercised in determining the governing load combination.

Figures 5.12 and 5.13 compare the probabilities of failure in flexure and shear of designs obtained according to ACI provisions for these two modes, assuming $\phi_s = 0.85$. The behavior is similar to that previously encountered. These results indicate that present ACI code provisions are reasonably consistent with regard to their treatment of beams with different end conditions and loading effects. If the shear capacity reduction factor is reduced to about 0.75, the shear strength provisions derived from the truss analogy would usually be adequate to insure that beam failure is governed by flexure.

5.3.2 Columns Subjected to Eccentric Loads

A column with an eccentricity from applied loads of 20 inches is studied. It is assumed that the column supports one floor and the loaded

tributary area is 150 ft^2. Dead and live loads are considered, and thus the load statistics are the same as in Table 5.1. $\Delta_{\overline{e}}$ is assumed negligible in this case. This example illustrates the effect that quality control of the concrete, and the amount and strength of the longitudinal reinforcement have of the underlying risk of failure of column designs prescribed by the ACI code.

The parameter $\overline{p}$ has the same interpretation as in the flexural case. The total percentage of longitudinal reinforcement, p_t, may be deduced from $\overline{p}$. For the symmetrically reinforced rectangular section,

$$p_t = \frac{\text{Total Steel Area}}{\text{Section Area}} = 2\,\overline{p}\,\frac{\overline{d}}{\overline{t}}$$

For purposes of illustration, it is assumed that $\overline{d}/\overline{t} = 7/8$, from which $p_t = 1.75\,\overline{p}$.

Figures 5.14 and 5.15 compare the underlying risk of ACI prescribed designs for good and poor concrete quality, with intermediate grade reinforcement. The probability measures increase rapidly when $\overline{e/t}$ is small, and change more gradually as $\overline{e/t}$ becomes large and tension failures are more likely. As $\overline{e/t}$ becomes very large, a state of pure flexure is approached, with the attendant insensitivity to $\overline{p}$ of beams. The probability of failure when $\overline{e/t}$ is large is of the order 10^{-5}, about the same as for a beam; note, however, that a capacity reduction factor of $\phi_c = 0.70$ for tied columns instead of the value of 0.90 for flexure was applied, and the uncertainties in the column capacity are somewhat larger than the uncertainties in flexural capacity. The lower capacity reduction factor and higher uncertainties, therefore, compensate for one another. The increase in ϕ_c allowed by ACI

318-71 when $\overline{e/t}$ is large will cause the probability of failure in Fig. 5.14 to increase further, and does not appear to be consistent with the objective of maintaining a lower risk level for beam-columns.

A comparison of Figs. 5.14 and 5.15 reveals that poor concrete quality control could increase the risk of failure by two or three orders of magnitude when the load eccentricity is small, and compression failure is likely. This sensitivity is particularly noticeable when the section is lightly reinforced; in such cases, the axial capacity is primarily dependent on the compressive strength of the concrete. For larger values of $\overline{e/t}$, the sensitivity disappears, as in the flexural case. There is a clear implication that when an analysis suggests that a column is close to being concentrically loaded, particular care should be exercised to insure high standards of control in its construction.

The irregularity in p_f in the mid range of $\overline{e/t}$ is particularly noticeable for small reinforcement ratios and for poor concrete quality. It has been observed that this irregularity occurs in the vicinity of the mean balanced point for the value of $\overline{p}$ selected. It seems likely that this behavior is due to the use of the approximate expression, Eq. 3.46, to define the axial capacity when failure is governed by compression.

The significance of high strength reinforcement is illustrated in Fig. 5.16. The probability measures are not much different from those in Fig. 5.14 signifying, therefore, that the level of safety implicit in the ACI code is uniform for the two grades of reinforcing steel used.

The ACI safety provisions attempt to assign a greater reliability to members in which failure may occur suddenly and have catastrophic

consequences. It is clear from the present statistical analysis that this objective has been satisfied. Assuming a similar level of quality control throughout, the probability of compression failure in a column is two or three orders of magnitude less than the probability of flexural failure. As the load eccentricity increases and the column behavior becomes more ductile, the difference in the risk levels decreases.

Columns in a Twenty Story Office Building

Two columns from the twenty story office building described in Sec. 5.3.1 are considered. A STRUDL analysis was used to determine the load influence coefficients for dead and live loads, and combined gravity and wind loads. One column is chosen from the first level, and supports twenty loaded floors; the other column is chosen having six loaded floors above it. The loadings on each floor are assumed identically distributed. The loaded area tributary to the interior columns is 500 ft^2. This example illustrates how the levels of safety implied by the ACI provisions compare for the two columns, and compares the risks underlying the provisions on gravity loads, herein denoted loading I, and gravity and wind loads combined, herein denoted loading II.

The dead and wind load statistics have already been defined. The variability of the column live load intensity must include the second order reduction dependent on the number of stories the column supports, as discussed in Sec. 4.3. A summary is presented in Table 5.5. From Eq. 4.20, $\Delta_L \simeq 0.24$. The prediction error in the load eccentricity is assumed to be 15 percent. For illustrative purposes, it is assumed that f'_y = 40 ksi and

TABLE 5.5

Live Load Statistics for Columns
in a Twenty Story Building

	Mean (psf)	Variability
Long Term Live Load		
Lower Story	34.25	0.12
Upper Story	34.25	0.20
Short Term Live Load		
Lower Story	15.63	0.23
Upper Story	15.63	0.39

and f'_c = 3000 psi; Figs. 5.14 and 5.16 suggest that the level of reliability would be about the same, regardless of the strength of the materials chosen.

The STRUDL analysis indicates the mean eccentricity of applied axial force on the lower story column is 0.02 inch under loading I, and is 1.62 inch under loading II. The column is nearly concentrically loaded, and the ACI requirement that $\overline{e/t} \geq 0.10$ may be expected to govern the deterministic design. This restriction significantly increases the safety margin provided when $\overline{e/t}$ is actually less than 0.10, as shown in Fig. 5.17, because D_C is forced to increase to its value corresponding to $\overline{e/t} = 0.10$. The increase in the margin of safety becomes more pronounced as the amount of longitudinal reinforcement provided increases, as illustrated in Fig. 5.18. The additional margin of safety provided is about the same for both loading configurations.

Suppose that a column is designed with $\bar{p} = 0.03$, corresponding to $p_t = 5.25$ percent, and it is desired that the column be desinged with $\bar{b} = \bar{t}$. For loading I, the STRUDL analysis and Eqs. 5.24 yield $\bar{b} = \bar{t} \simeq 31$ inches. The probability of failure of this design, $p_f^I(D_C^I)$, with $\overline{e/t} \simeq 0.02/31 \simeq 0$, is of the order 10^{-13}. Under loading II, $\bar{b} = \bar{t} \simeq 27.2$ inches; with $\overline{e/t}$ $= 1.62/27.2 \simeq 0.06$, $p_f^{II}(D_C^{II}) \simeq 1.75 \times 10^{-9}$. These probabilities may be taken from Eq. 5.17. From a deterministic standpoint, loading I will govern the design. The probability of failure of D_C^I under loading II, $p_f^{II}(D_C^I)$, is also shown in Fig. 5.17; with $\overline{e/t} = 1.62/31 = 0.052$, $p_F^{II}(D_C^I)$ is of the order 10^{-13} also. Thus although the ACI design is governed by loading I, the risk of failure of this controlling design is about the same for both load configurations.

This example points out the difficulty with a strict interpretation of risk measures. The probabilities are of such small magnitude that it is impossible to assign any physical meaning to them. Such measures should be interpreted on a comparative basis only, i.e., it was shown that the design risk levels are about the same for loading I and loading II.

Without the restriction $\overline{e/t} \geq 0.10$, for loading I, $\bar{b} = \bar{t} = 27.5$ inches, and $p_f^I(D_C^I) = 9 \times 10^{-10}$. The probability of failure of D_C^I against loading II, with $\overline{e/t} = 1.62/27.5 = 0.06$, is $p_f^{II}(D_C^I) = 1.75 \times 10^{-9}$, about the same magnitude.

For the loadings considered in this example, the minimum eccentricity ratio restriction imposed by the ACI code forces the designs for small $\overline{e/t}$ to be excessively conservative. Without this restriction, designs have underlying failure risks of the order 10^{-9} - 10^{-10}, which should furnish

adequate safety in most circumstances. In reliability based design, it would be more reasonable to account for possible uncertainties in the load eccentricity by adjusting the prediction error $\Delta_{\overline{e}}$ than to place an arbitrary lower bound on $\overline{e/t}$.

The STRUDL analysis of the upper story column indicates that the mean eccentricity of applied axial force is 1.08 inches under loading I and 3.20 inches under loading II. Results of the risk analysis are presented in Fig. 5.19. If $\overline{p} = 0.03$ and $\overline{b} = \overline{t}$, the requirement $\overline{e/t} \geq 0.10$ will again govern the design against loading I, and loading I will govern the deterministic design. The probabilities of failure for the upper story column will be larger becasue the load eccentricities are larger. With $\overline{b} = \overline{t}$ = 17.3 inches, and $\overline{e/t}$=1.08/17.3 = .0625, $p_f^I(D_C^I) = 1.3 \times 10^{-10}$ from Fig. 5.19. The risk of failure of D_C^I under loading II is also shown in Fig. 5.19; with $\overline{e/t}$ = 3.2/17.3 = 0.185, $p_f^{II}(D_C^I) = 5.1 \times 10^{-8} > p_f^I(D_C^I)$. It is therefore conceivable that the risk of failure of a "governing" design may be higher for nongoverning load configurations than for the loading for which it was designed. The dimensions of a design must be selected with care to insure adequacy against other possible load configurations; in the above case, reducing $\overline{b/t}$ would cause $p_f^{II}(D_C^I)$ to decrease relative to $p_f^I(D_C^I)$.

Chapter 6

FORMULATION OF RELIABILITY-BASED DESIGN CRITERIA

6.1 General Remarks

This chapter is devoted to the formulation of design criteria on the basis of specified acceptable risk measures, with special reference to reinforced concrete members. The form of the traditional design equations may remain unchanged; however, the determination of the appropriate factors in these equations is based on the specified design risk. In this manner, the significance of uncertainties can be reflected properly in design, and the load factors will vary with the degree of uncertainty and the level of risk. Uncertainties in current designs and their implied risk levels have been evaluated in order to furnish a starting point for this reevaluation.

This formulation should enable future code revisions to be made in a more rational manner. The objectives of the ACI safety provisions may be satisfied more consistently if design criteria are developed on a risk basis, e.g., this furnishes a basis for the design of beams in which the level of safety in shear is higher than that in flexure; this objective is not always achieved by the current provisions of the ACI code. If fabrication and construction practices change or improve, or if more accurate modeling and analysis techniques become available, their effect on the design safety may be properly reflected by modifying the uncertainty measures. Moreover, in future code revisions, the level of

design safety may be increased or decreased by adjusting the risk levels relative to those currently considered acceptable. The level of safety implied by the design provisions, therefore, may be quantitatively defined and carefully controlled.

The required strength may be found from any one of several alternative but equivalent design formats. The true measure of safety in reliability-based design is the probability of failure. In this regard, when several loads are involved, it is the safety against the total load effect that is relevant. Accordingly, in the load-factor format of design, it is the overall load factor that is important. In other words, the required design (in terms of mean values) is

$$\overline{R} = \gamma \overline{S} \tag{6.1}$$

in which $\overline{S}$ is the total mean load effect, and γ is the appropriate load factor. This may be evaluated on the basis of prescribed lognormals or using the alternative risk measure, corresponding to a specified risk.

However, in order to comply with current code formats, a multiple load factor format including a capacity reduction factor may also be used. Suitable values may be obtained when Eq. 2.18 is rewritten to include a capacity reduction factor ϕ. In terms of mean values, when dead and live loads are considered,

$$\phi \overline{R} = \gamma_L \overline{S}_L + \gamma_D \overline{S}_D \tag{6.2a}$$

and when wind effects are included,

$$\phi \overline{R} = \gamma_L \overline{S}_L + \gamma_D \overline{S}_D + \gamma_W \overline{S}_W \tag{6.2b}$$

One appropriate value of ϕ is suggested by Eqs. 2.22 and 2.22a, i.e., $\phi = 1 - \beta_o \alpha \delta_R$, in which α is defined in Eq. 2.22a, and is commonly about 2/3. Theoretically, α is a function of the resistance and load statistics; hence, ϕ will depend on the loads as well as the resistance. Another way of defining ϕ is to assume that the "equivalent" resistance, $\phi \bar{R}$, occurs at some cumulative probability level p_ϕ of R; if $\phi \bar{R}$ is set equal to the nominal value R' defined in the ACI code, then $\phi = 1 - \beta_\phi \delta_R$. This specification of ϕ is then independent of the load effects.

Alternatively, if the probability levels for the resistance and loads are specified, the required strength may be determined in terms of nominal (e.g., characteristic) resistance and loads. Under dead and live loads,

$$\phi' R' = \gamma_L' S_L' + \gamma_D' S_D' \tag{6.3a}$$

and when wind effects are included,

$$\phi' R' = \gamma_L' S_L' + \gamma_D' S_D' + \gamma_W' S_W' \tag{6.3b}$$

in which

$$\phi' = \frac{\phi}{1 - \beta_R \delta_R}$$

$$\gamma_k' = \frac{\gamma_k}{1 + \beta_k \delta_k}, \quad k = D, L, W \tag{6.3c}$$

and β_k depend on the probability levels chosen.

6.2 Flexure

To insure a tension mode of flexural failure, the maximum allowable tensile reinforcement ratio $\bar{p}$ for beams may be found by requiring that

$$\Pr\ (p_b < p) \lesssim \alpha_b \tag{6.4}$$

where suitable values of α_b range from 0.01 to 0.05. Assuming $\delta_{f_c} = 0.12$, $\bar{p} \lesssim 0.45\ \bar{p}_b$ when $\alpha_b = 0.01$, and $\bar{p} \lesssim 0.57\ \bar{p}_b$ when $\alpha_b = 0.05$; $\bar{p}_b$ is computed from Eq. 3.9. This requirement makes a tension failure nearly certain. It also implies that the member cross section will be large enough that serviceability will be a lesser consideration.

In Chapter 5, it was found that the probability of failure of flexural designs was of the order of 10^{-5}, and the designs were virtually independent of the longitudinal reinforcement ratio, and of the quality of concrete. Initially, then, the design criterion for flexure should be based on a risk level of 10^{-5}.

Table 6.1 compares overall load factors for flexure, corresponding to different risk levels, computed on the basis of lognormal prescription and with the alternative risk basis. The two risk bases show close agreement.

TABLE 6.1

Mean Overall Load Factors for Flexure

p_f	Lognormal Prescription		Alternative Risk	
	D + L	D + L + W	D + L	D + L + W
10^{-4}	2.19	2.26	2.24	2.29
10^{-5}	2.46	2.55	2.54	2.61
10^{-6}	2.72	2.84	2.85	2.94
10^{-7}	2.99	3.13	3.16	3.29

In terms of mean values, the multiple load and capacity reduction factors for flexure, obtained from the alternative risk basis, are given in Table 6.2.

TABLE 6.2

Mean Load Factors for Flexure

	Dead and Live Loads						Dead, Live and Wind Loads							
	$\phi = 1 - \beta_\phi \delta_M$			$\phi = 1 - \beta_o \alpha \delta_M$			$\phi = 1 - \beta_\phi \delta_M$				$\phi = 1 - \beta_o \alpha \delta_M$			
P_f	ϕ	γ_L	γ_D	ϕ	γ_L	γ_D	ϕ	γ_L	γ_D	γ_W	ϕ	γ_L	γ_D	γ_W
10^{-4}	.84	2.25	1.76	.83	2.23	1.73	.84	2.70	1.68	2.19	.82	2.64	1.64	2.14
10^{-5}	.84	2.62	1.97	.80	2.50	1.87	.84	3.20	1.87	2.54	.79	3.02	1.76	2.39
10^{-6}	.84	3.01	2.18	.77	2.76	2.00	.84	3.74	2.07	2.90	.76	3.38	1.87	2.63
10^{-7}	.84	3.42	2.41	.75	3.06	2.15	.84	4.30	2.27	3.28	.74	3.79	2.00	2.89

β_ϕ has been found to be 1.37 for flexure by solving $1 - \beta_\phi \delta_M = M'/\overline{M}$ for β_ϕ, using nominal 40 ksi reinforcement and nominal 3000 psi concrete. Table 6.3 illustrates the required factors for nominal loads and strength, where an acceptance level of 10 percent on R and exceedance levels of 95 percent on dead load and 99 percent on live load and wind load have been selected.

From a reliability standpoint, it is advantageous to use mean values and corresponding load factors. The exceedance values for the nominal quantities depend on the distributions of the load and resistance variables. In addition, the necessary statistical information is usually available in terms of mean values and variances. Designs given in terms of mean values, therefore, are more convenient to obtain; moreover, they are more directly associated with risk, and thus are less ambiguous.

We might emphasize that the load factors are functions of the uncertainty measures; the factors given in the above tables correspond to the uncertainty measures determined in Chapters 3 and 4. However, if these uncertainties should change, either as a result of change in the basic variabilities or the prediction errors, the load factors ought to be reevaluated.

A comparison of the flexural designs, i.e., D_F, that would be obtained for various risk levels with those obtained from current ACI provisions for flexure is shown in Fig. 6.1 for dead and live loads. The decrease in D_F with $\overline{p}$ reflects the smaller beam cross sections that would result when larger amounts of longitudinal reinforcement are provided.

TABLE 6.3

Nominal Load Factors for Flexure

	Dead and Live Loads						Dead, Live and Wind Loads							
	$\phi = 1 - \beta_\phi \delta_M$			$\phi = 1 - \beta_o \alpha \delta_M$			$\phi = 1 - \beta_\phi \delta_M$				$\phi = 1 - \beta_o \alpha \delta_M$			
P_f	ϕ	γ_L	γ_D	ϕ	γ_L	γ_D	ϕ	γ_L	γ_D	γ_W	ϕ	γ_L	γ_D	γ_W
10^{-4}	.99	1.38	1.60	.97	1.37	1.57	.99	1.20	1.53	1.29	.96	1.17	1.49	1.26
10^{-5}	.99	1.61	1.79	.94	1.53	1.70	.99	1.42	1.70	1.49	.93	1.34	1.60	1.41
10^{-6}	.99	1.85	1.98	.90	1.69	1.82	.99	1.66	1.88	1.71	.89	1.50	1.70	1.55
10^{-7}	.99	2.10	2.19	.88	1.88	1.96	.99	1.90	2.06	1.93	.87	1.68	1.82	1.70

The load factors are insensitive to the mean load ratios (see Figs. 2.7 and 2.8) and, therefore, $\overline{L}/\overline{D}$ need not be considered as a design parameter. As the live load statistics depend on the tributary loaded area, [43] the load factors may be expected to vary with the tributary area. This is indicated in Table 6.4 for a risk level of 10^{-5} (with mean load factors).

TABLE 6.4

Mean Load Factors in Flexure As Functions of the Tributary Loaded Area

$$p_f = 10^{-5}$$

Tributary Area (ft^2)	$\phi = 1 - \beta_\phi \delta_M$			$\phi = 1 - \beta_o \alpha \delta_M$		
	ϕ	γ_L	γ_D	ϕ	γ_L	γ_D
25	.84	3.34	2.36	.80	3.18	2.25
56	.84	2.81	2.12	.80	2.67	2.02
151	.84	2.72	2.00	.80	2.59	1.90
336	.84	2.63	1.97	.80	2.51	1.88
624	.84	2.62	1.97	.80	2.50	1.87

Higher values for small tributary areas are indicated because δ_L and Δ_L are larger in this case. Further reductions when $A \geq 625$ ft^2 are not necessary. For tributary areas that are normally encountered in design, the load factors are relatively insensitive to A.

6.3 Shear

To insure that failure of a beam will be in a flexural mode rather than the shear mode, the risk of shear failure should be prescribed to be at least one order of magnitude less than the risk of failure in flexure. On this basis, the required r_s may be determined, from which the size of the stirrups $\overline{A}_v$ and their spacing $\overline{s}_{st}$ are obtained from Eq. 3.38. To insure that each potential diagonal crack is crossed by at least one stirrup, the provision that $\overline{s}_{st} \leq \frac{1}{2}\overline{d}$ should be retained.

For a given risk level, r_s depends on the amount of longitudinal reinforcement $\overline{p}$ and the cross sectional aspect ratio $\overline{b/d}$; as indicated in Figs. 5.3 and 5.4, a small change in r_s could result in a large change in the risk of failure in shear. The required amount of web reinforcement for a specified risk of shear failure may be found by equating Eqs. 5.21 and 2.21 and solving for r_s. The relationship is complicated, and the complexity of this procedure makes it unsuitable for design purposes.

It is therefore not possible to prescribe one overall risk-based design criterion for shear, as is done in the ACI code. At this time, it seems that to insure a risk-consistent treatment of shear, the designer must be permitted to choose the necessary r_s (or load factors) directly from curves of the type illustrated in Figs. 5.3 and 5.4. To allow sufficient flexibility in design, a large number of such curves, encompassing sufficient variations in $\overline{p}$ and $\overline{b/d}$ as well as different resistance and load statistics, must be furnished as part of the code format. Since present design formats are given by prescriptive equations, such a suggestion may not be very practical.

Any direct requirement for shear, therefore, would be exceedingly complex. Simplified risk-based design provisions for shear ought to be investigated further. One immediate improvement that may be made in the current ACI code, suggested by the results of Chapter 5, is to reduce the present shear capacity reduction factor from 0.85 to 0.75. The current factor of 0.85 appears to be too high to maintain a lower risk of shear failure than that in flexure; reducing this to 0.75 should achieve this objective for the majority of design conditions.

6.4 Axial Thrust and Bending

As the eccentricity ratio increases, the probability of failure of ACI designs for combined bending and thrust increases rapidly when $\overline{e/t}$ is small, and changes more gradually as $\overline{e/t}$ becomes large (see Fig. 5.14). It is therefore proposed that beam-column designs be based on an acceptable risk increasing exponentially from 10^{-9} (when $\overline{e/t} \simeq 0$) to 10^{-6} (when $\overline{e/t} \gtrsim \overline{e_b/t}$), or

$$\log_{10} p_f = \frac{3}{\overline{e_b/t}} (\overline{e/t}) - 9, \qquad \overline{e/t} < \overline{e_b/t}$$

$$p_f = 10^{-6}, \qquad \overline{e/t} \gtrsim \overline{e_b/t} \tag{6.5}$$

where p_f is the acceptable risk. The restriction $\overline{e/t} \gtrsim 0.10$ has been removed; this condition seems overly conservative. A more consistent way of accounting for unexpected eccentricity is to increase the associated prediction error Δ_e when necessary. The risk of 10^{-6} when $\overline{e/t} \gtrsim \overline{e_b/t}$ is prescribed at one order of magnitude less than the allowable

risk in flexure to reflect the generally higher consequence of a beam-column failure. It is reasonable that the risk should be less when $\overline{e/t}$ is small, since such members will exhibit little ductility prior to failure; notwithstanding that spiral columns can have considerable ductility.

As indicated in previous analysis, the reliability of a beam-column is a function of $\overline{p}$ and $\overline{e/t}$; accordingly, the load factors would depend on these parameters. An illustration of this is presented in Table 6.5 for dead and live loads and intermediate grade reinforcement; the capacity reduction factor has been computed from $\phi = 1 - \beta_o \alpha \delta_P \cdot \Delta_{\overline{e}}$ was assumed to be 10 percent, replacing the ACI requirement of $\overline{e/t} \geq 0.10$.

TABLE 6.5

Mean Load Factors for
Combined Bending and Thrust

	$\overline{p} = 0.02$ ($p_t = 3.5\%$)			$\overline{p} = 0.04$ ($p_t = 7\%$)		
$\overline{e/t}$	ϕ	γ_L	γ_D	ϕ	γ_L	γ_D
0.10	0.77	3.55	2.40	0.80	3.38	2.29
1.0	0.68	3.58	2.50	0.69	3.40	2.36
2.0	0.59	3.88	2.65	0.61	3.75	2.56

A comparison with Table 6.2 for flexure shows that the strength reduction factor ϕ is smaller, whereas the load factors γ_L and γ_D are larger; these are due to the smaller risk level required of beam columns, as well as the larger uncertainties underlying such members.

It should be apparent from the three failure modes considered that the load factors depend on the degree of uncertainty and the specified level of risk. However, except for the flexural case, in which the load factors remain virtually constant for a given risk, there is no simple way of prescribing risk-based design requirements, e.g., for shear. One alternative may be to furnish a number of curves or tables for γ_k and ϕ. This implies that while it is possible to maintain Eq. 6.2 as the design equation, it may not always be advantageous to do so in a reliability-based format. In some cases, it would be more reasonable to allow the designer to compute the required resistance directly from an expression such as Eq. 2.7, arising from the prescriptive-lognormal basis, wherein the uncertainties Ω_R and Ω_S would be furnished by the code writing group for different failure modes and load combinations. As another example, it would be easier to assure adequacy in shear by choosing a value of r_s directly from a curve of the type illustrated in Fig. 5.3, rather than to compute the required load factors.

Chapter 7

SUMMARY AND CONCLUSIONS

A model is developed for formulating designs on the basis of acceptable risks, requiring only the first and second moments of the design variables. Errors arising from uncertainties in prediction and modeling are recognized by introducing a factor of engineering judgment into the risk analysis. Variabilities in the design parameters are estimated from data, whenever possible. A systematic combination of the available information results in a comparative estimate of the underlying design risk which is consistent with the state of present knowledge.

The levels of risk implied by current ACI design provisions for beams in flexure and shear and for eccentrically loaded columns are evaluated. Based on these levels of risk, specific suggestions are made for developing risk-based design criteria. These criteria permit a consistent treatment of uncertainties, and quantitative definition and control of the level of design safety. Difficulties arising in the practical implementation of such a design concept are also discussed.

On the basis of this study, the following conclusions and recommendations can be made:

1. Current design provisions can be appraised in terms of risk measures. This requires a careful evaluation of the basic variabilities and prediction errors associated with the design variables and the resistance and load models. This evaluation can be performed systematically using first-order

statistical analysis. Available data and reported experience provide valuable information, and should be used to determine realistic measures of uncertainties required for the evaluation of risk.

2. Practical reliability-based design criteria can be developed; such criteria (specifically, design based on acceptable risk) can be cast in the format of current design provisions. These criteria ought to be specified in terms of mean values, as they are more convenient from a statistical standpoint. Although the multiple load factor format can be retained, there is no theoretical basis for such multiple factors. A single load factor applied to the total multiple load effects is sufficient from a reliability standpoint; in fact, this format is simpler and more directly consistent with statistical analysis.
3. The implied risk of flexural failure in a beam designed according to ACI provisions is normally of the order of 10^{-5}, regardless of the reinforcement ratio, concrete quality, and load configuration. Risks associated with existing designs, or conversely, designs based on specified risks, may be determined from consideration of the tension failure mode, provided that the longitudinal reinforcement ratio is small.
4. The likelihood of a compression flexural failure may be controlled with a probabilistic statement regarding the design reinforcement ratio. The uncertainty in flexural capacity is primarily a function of uncertainties in the reinforcement yield stress and the effective depth to the reinforcement;

the quality of the concrete is not significant, except when the section is very heavily reinforced. A statistical analysis of shear capacity based on the modified truss analogy indicates that concrete quality is not significant in determining the shear capacity except when the web is very lightly reinforced. The variability in shear capacity may be expected to be considerably larger than the variability in flexural capacity.

5. Current ACI provisions for shear usually insure that the risk of a shear failure is less than the risk of a flexural failure. However, the strength requirement derived from the truss analogy is insufficient to accomplish this objective; provisions for the maximum spacing and minimum area of the web reinforcement are usually necessary. To provide sufficient additional safety against shear failure, risk-based shear provisions should therefore be based on an acceptable risk of 10^{-6} or less; to achieve this in the context of the present ACI format, the capacity reduction factor for shear should be about 0.75.

6. The implied risk of ACI designs for eccentrically loaded columns increases from less than 10^{-9} when $\overline{e/t}$ is very small up to the order of 10^{-5} when $\overline{e/t}$ becomes large. This is compatible with ACI intentions of providing a greater margin of safety when there is less ductility. The risk is less than that for beams when $\overline{e/t}$ is small, reflecting the greater

importance attached to column reliability. The minimum eccentricity requirement (i.e., $\overline{e/t} \geq 0.10$) seems to be excessively conservative.

7. Uncertainty in the capacity of an eccentrically loaded column depends on the eccentricity of the applied load. When the load eccentricity is small, implying that failure occurs in a compression mode, the concrete quality and uncertainties in dimensions are significant to the overall uncertainty of a beam-column. When the eccentricity ratio is large, implying that failure will occur in a tension mode, the factors important to flexure dominate. In all cases, good workmanship is essential.

LIST OF REFERENCES

1. D. E. Allen, "Probabilistic Study of Reinforced Concrete in Bending," Tech. Paper No. 311, National Research Council of Canada, Div. of Bldg. Research, January 1970.

2. ACI-ASCE Committee 326, "Shear and Diagonal Tension," ACI Journal, Proc. Vol. 59, January, February, and March 1962.

3. ACI Standard 214-65, "Recommended Practice for Evaluation of Compression Test Results of Field Concrete," ACI Journal, Proc. Vol. 61, No. 9, September 1964.

4. ACI Standard 318-63, "Building Code Requirements for Reinforced Concrete, and Commentary," 1963.

5. ACI Standard 318-71, "Building Code Requirements for Reinforced Concrete, and Commentary," 1971.

6. ASTM Standard A615-68, "Deformed Billet Steel Bars for Concrete Reinforcement," 1968.

7. American Standard Building Code, "Minimum Design Loads in Buildings and Other Structures," ANSI A58.1, 1955.

8. A. H.-S. Ang, "Probability Considerations in Design and Formulation of Safety Factors," Symposium on Concepts of Safety of Structures and Methods of Design, I.A.B.S.E., London, 1969.

9. A. H.-S. Ang and M. Amin, "Safety Factors and Probability in Structural Design," Journal of the Structural Division, ASCE, Vol. 95, No. ST7, July 1969.

10. A. H.-S. Ang and M. Amin, "Formulation of Wind-Resistant Design Based on Acceptable Risk," Proc. Third Int. Conf. on Wind Effects on Buildings and Structures, Tokyo, 1971.

11. A. H.-S. Ang and B. R. Ellingwood, "Critical Analysis of Reliability Principles Relative to Design," Conf. of Applications of Statistics and Probability to Soil and Structural Engineering, Hong Kong, 1971.

12. A. H.-S. Ang, "Development of a Probabilistic Basis for Evaluating Structural Safety and Design of Deep Submersibles," Final Report of Contract N00014-69-C-0436, Naval Ship Research and Development Center, Washington, D. C., April 1972.

13. J. F. Baker, M. R. Horne, and J. Heyman, The Steel Skeleton, Vol I and II, Cambridge University Press, 1956.

14. M. J. Baker, "The Evaluation of Safety Factors in Structures," CIRIA Research Project 72, Final Report, Department of Civil Engineering, Imperial College, London, 1970.

15. D. L. Bloem, "Concrete Strength in Structures," ACI Journal, Proc. Vol. 65, No. 3, March 1968.

16. J. A. Blume, N. M. Newmark, and L. H. Corning, Design of Multistory Reinforced Concrete Buildings for Earthquake Motions, Portland Cement Association, 1961.

17. V. V. Bolotin, Statistical Methods in Structural Mechanics, Holden-Day, San Francisco, Calif., 1969.

18. J. F. Borges and M. Castanheta, Structural Safety, LNEC, Lisbon, Portugal, March 1971.

19. B. Bresler and J. G. MacGregor, "Review of Concrete Beams Failing in Shear," Journal of the Structural Division, ASCE, Vol. 93, No. ST1, February, 1967.

20. J. O. Bryson and D. Gross, "Techniques for the Survey and Evaluation of Live Floor Loads and Fire Loads in Modern Office Buildings," Building Science Series 16, National Bureau of Standards, December 1968.

21. Building Research Advisory Board, "Dimensional Tolerances for Cast-In Place Concrete," Federal Construction Council Tech. Report 49, National Academy of Sciences, National Research Council, 1964.

22. W. Y. Chow and N. J. Gardner, "Statistical Variability and Probability of Failure of Reinforced Concrete Members," Conf. on Applications of Statistics and Probability to Soil and Structural Engineering, Hong Kong, September 1971.

23. W. G. Corley, "Rotational Capacity of Reinforced Concrete Beams," Journal of the Structural Division, ASCE, Vol. 92, No. ST5, October 1966.

24. C. A. Cornell, "Structural Safety Specifications Based on Second Moment Reliability Analysis," Symposium on Concepts of Safety of Structures and Methods of Design, I.A.B.S.E., London, 1969.

25. C. A. Cornell, "A Probability-Based Structural Code," ACI Journal, Proc. Vol. 66, No. 12, December 1969.

26. J. F. Costello and Kuang-han Chu, "Failure Probabilities of Reinforced Concrete Beams," Journal of the Structural Division, ASCE, Vol. 95, No. ST10, October 1969.

27. H. Cramer, The Elements of Probability Theory, John Wiley and Sons, New York, 1955.

28. H. Cramer and M. Leadbetter, Stationary and Related Stochastic Processes, John Wiley and Sons, Inc., 1967.

29. A. G. Davenport, "Gust Loading Factors," Journal of the Structural Division, ASCE, Vol. 93, No. ST3, June 1967.

30. J. W. Dunham, "Design Live Loads on Buildings," Transactions ASCE, Paper No. 2311, Vol. 112, 1947.

31. A. M. Freudenthal, J. M. Garrelts, and M. Shinozuka, "The Analysis of Structural Safety," Journal of the Structural Division, ASCE, Vol. 92, No. ST1, February 1966.

32. A. M. Freudenthal, "Critical Appraisal of Safety Criteria and their Basic Concepts," Prleiminary Publication, Eighth Congress, I.A.B.S.E., September 1968.

33. J. R. Gaston, C. P. Siess, and N. M. Newmark, "An Investigation of the Load-Deformation Characteristics of Reinforced Concrete Beams up to the Point of Failure," Structural Research Series No. 40, Department of Civil Engineering, University of Illinois, December 1952.

34. A. M. Hasofer, "Statistical Model for Live Floor Loads," Journal of the Structural Division, ASCE, Vol. 94, No. ST10, October 1968.

35. E. Hognestad, N. Hanson, and D. McHenry, "Concrete Stress Distribution in Ultimate Strength Design," ACI Journal, Proc. Vol. 27, December 1955.

36. A. Johansson and B. Warris, "Deviations in the Location of Reinforcement," Proc. No. 40, Swedish Cement and Concrete Research Institute, Royal Institute of Technology, Stockholm, 1969.

37. A. I. Johnson, "Strength, Safety, and Economical Dimensions of Structures," Bulletin of Division of Building Statics and Structural Engineering, Royal Institute of Technology, Stockholm, 1953.

38. O. G. Julian, "Synopsis of First Progress Report of Committee on Factors of Safety," Journal of the Structural Division, ASCE, Vol. 83, No. ST4, July 1957.

39. T. Karman, "Statistical Investigations on Live Loads on Floors," International Council for Building Research, Studies and Documentation, Madrid, 1969.

40. A. Laupa, C. P. Siess, and N. M. Newmark, "Strength in Shear of Reinforced Concrete Beams," University of Illinois Engineering Experiment Station Bulletin No. 428, Vol 52, No. 55, March 1955.

41. Y. K. Lin, Probabilistic Theory of Structural Dynamics, McGraw-Hill, 1967.

42. A. H. Mattock, L. B. Kriz, and E. Hognestad, "Rectangular Concrete Stress Distribution in Ultimate Strength Design," ACI Journal, Proc. Vol. 57, No. 8, February 1961.

43. G. R. Mitchell and R. W. Woodgate, "A Survey of Floor Loadings in Office Buildings," CIRIA Report 25, London, August 1970.

44. J. C. Peir, "A Stochastic Live Load Model for Buildings," Department of Civil Engineering, Massachusetts Institute of Technology, September 1971.

45. E. O. Pfrang, M. A. Sozen, and C. P. Siess, "Load-Moment-Curvature Characteristics of Reinforced Concrete Cross Sections," ACI Journal, Proc. Vol. 61, No. 7, July 1964.

46. H. Raiffa, Decision Analysis, Addison Wesley, Massachusetts, 1968.

47. M. K. Ravindra, A. C. Heaney, and N. C. Lind, "Probabilistic Evaluation of Safety Factors," Symposium on Concepts of Safety of Structures and Methods of Design, I.A.B.S.E., London, 1969.

48. L. E. Robertson and P. W. Chen, "Effects of Environmental Loads on Tall Buildings," Proc. of USA-Japan Research Seminar on Wind Loads on Structures, University of Hawaii, Honolulu, October 1970.

49. E. Rosenblueth and L. Esteva, "Reliability Basis for Some Mexican Codes," ACI Conference, Denver, 1971.

50. H. Rüsch, "Reserches Toward a General Flexural Theory for Structural Concrete," ACI Journal, Proc. Vol. 32, No. 1, July 1960.

51. R. G. Sexsmith, "Reliability Analysis of Concrete Members," ACI Journal, Proc. Vol. 66, No. 5, May 1969.

52. H. C. Shah, "Regression Analysis of Reinforced Concrete Columns," Journal of the Structural Division, ASCE, Vol. 90, No. ST1, February 1964.

53. C. P. Siess, Private Communication.

54. H. C. S. Thom, "New Distributions of Extreme Winds in the United States," Journal of the Structural Division, ASCE, Vol. 94, No. ST7, July 1968.

55. M. Tichy and M. Vorlicek, "Statistical Theory of Interaction Diagrams," Acta Technica, CSAV, No. 1, Prague, 1964.

56. Uniform Building Code, 1967 edition.

57. B. J. Vickery, "On the Reliability of Gust Loading Factors," Proc. of Tech. Meeting Concerning Wind Loads on Buildings and Structures, National Bureau of Standards, Washington D. C., January 1969.

58. J. Warwaruk, M. A. Sozen, and C. P. Siess, "Strength and Behavior in Flexure of Prestressed Concrete Beams," University of Illinois Engineering Experiment Station Bulletin No. 464, Vol. 60, No. 5, August 1962.

FIGURE 2.1

VARIATION OF γ WITH p_f FOR VARIOUS DISTRIBUTIONS OF R AND S

$R = \gamma S$

$p_f = Pr(R < NS)$

$\delta_R = 0.20$ $\delta_S = 0.20$ $\Delta = 0.20$

N/N - Normal R and S
LN/LN - Lognormal R and S
EX3/EX1 - Weibull R and Gumbel S
EX3/EX2 - Weibull R and Frechet S

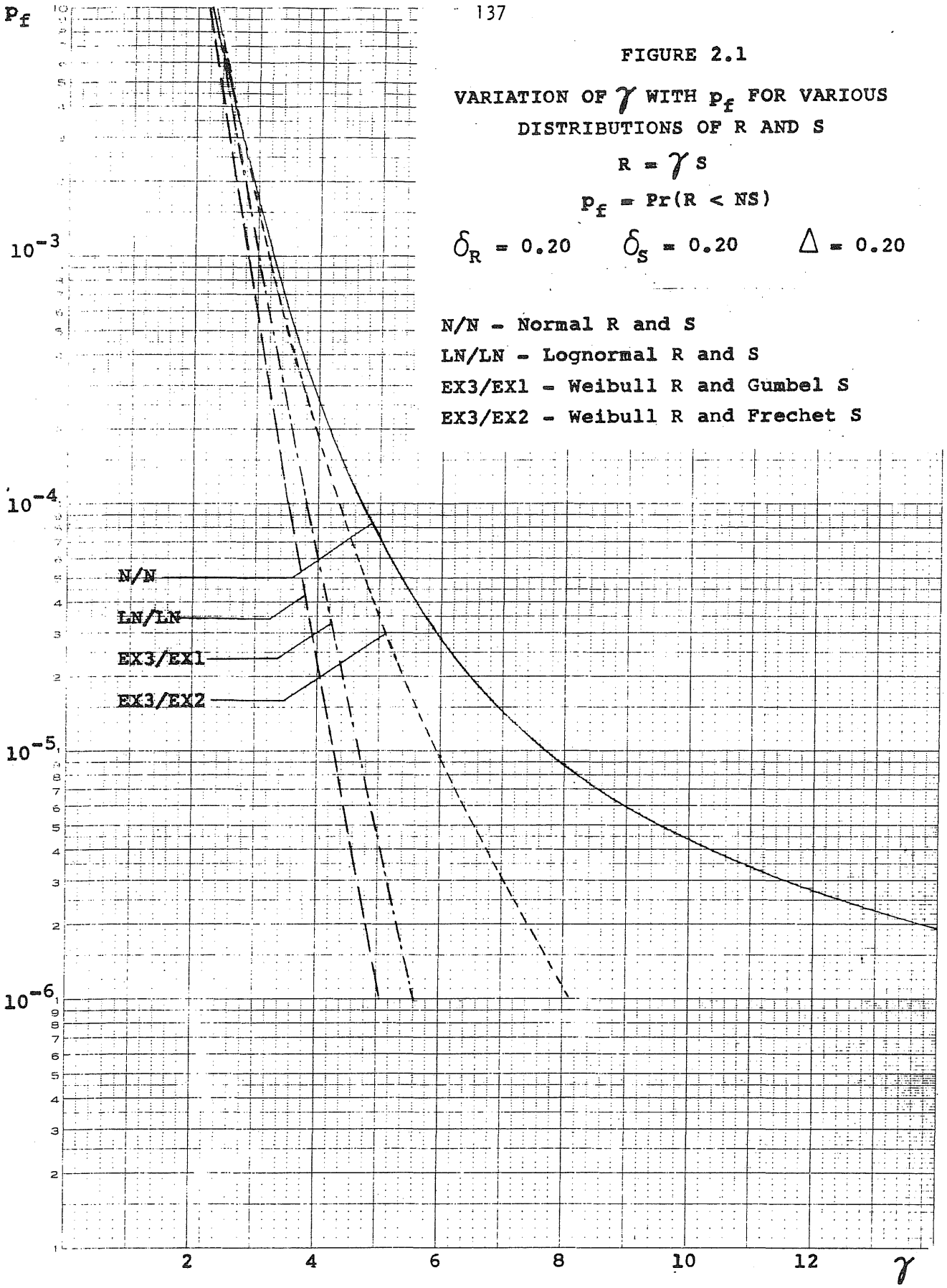

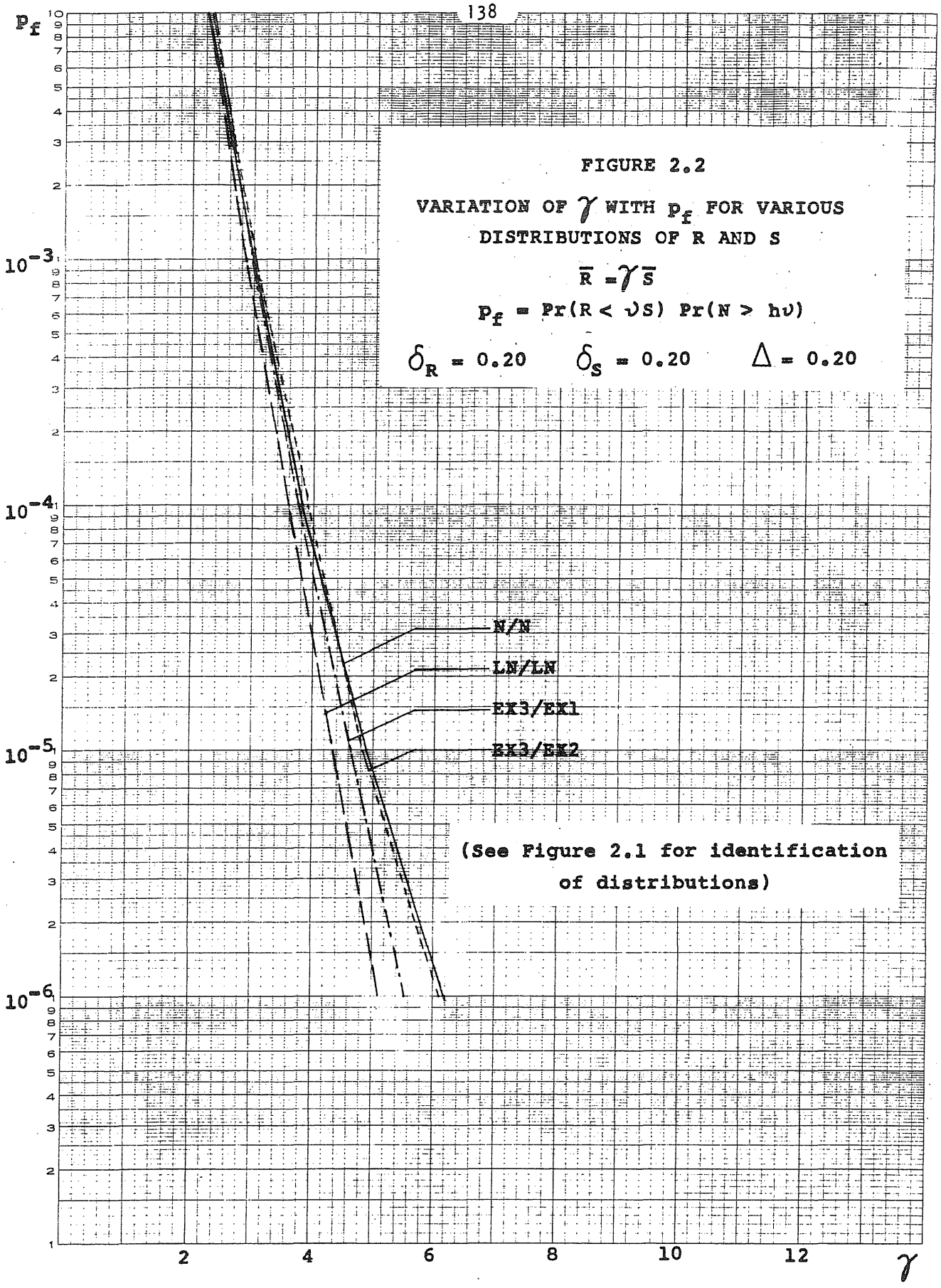

FIGURE 2.2

VARIATION OF γ WITH p_f FOR VARIOUS DISTRIBUTIONS OF R AND S

$\bar{R} = \gamma \bar{S}$

$p_f = Pr(R < \nu S)\ Pr(N > h\nu)$

$\delta_R = 0.20 \quad \delta_S = 0.20 \quad \Delta = 0.20$

(See Figure 2.1 for identification of distributions)

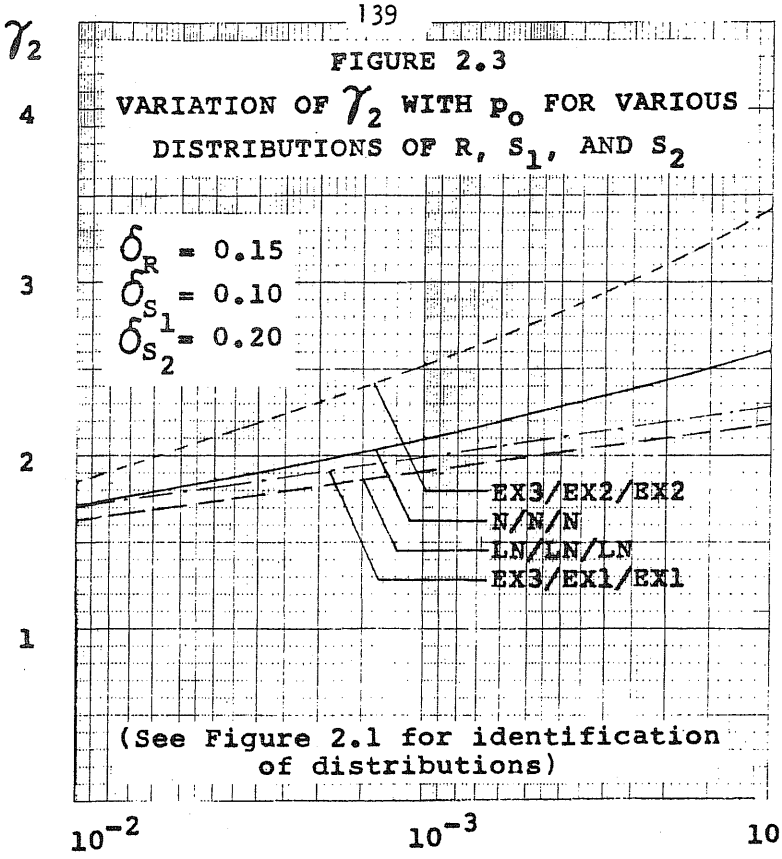

FIGURE 2.3

VARIATION OF γ_2 WITH p_o FOR VARIOUS DISTRIBUTIONS OF R, S_1, AND S_2

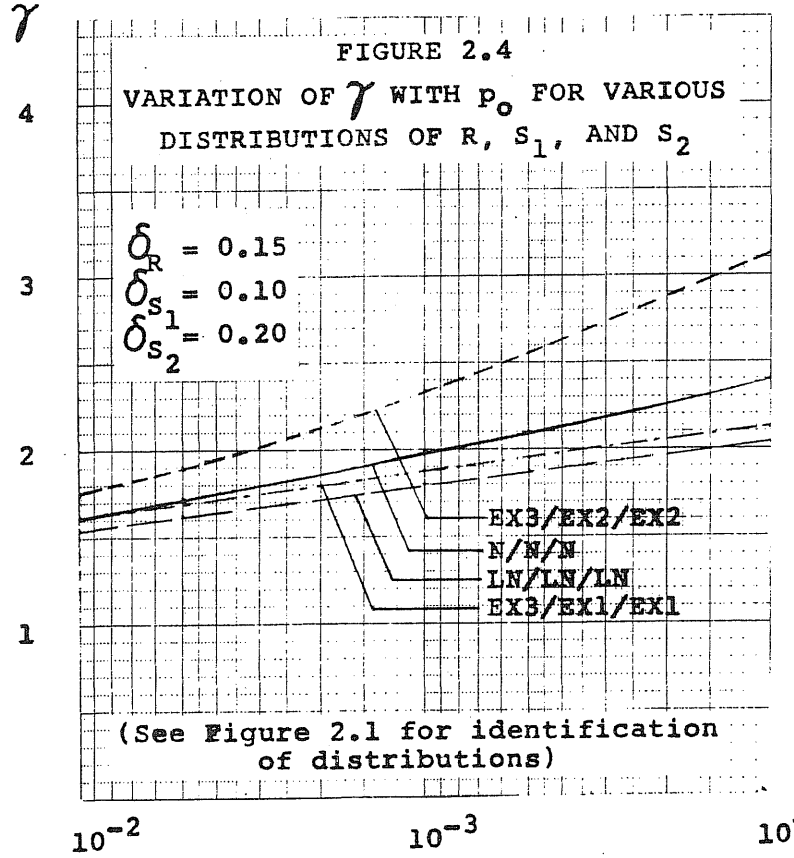

FIGURE 2.4

VARIATION OF γ WITH p_o FOR VARIOUS DISTRIBUTIONS OF R, S_1, AND S_2

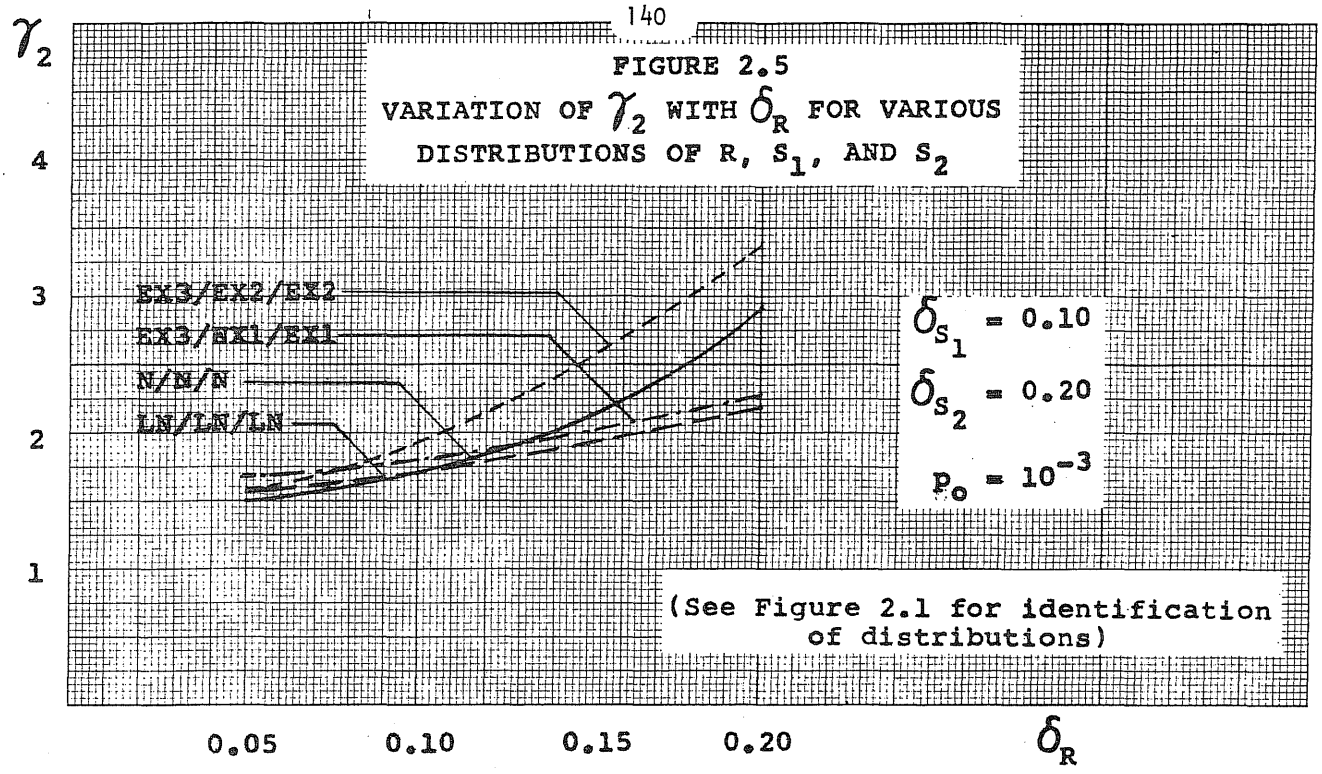

FIGURE 2.5
VARIATION OF γ_2 WITH δ_R FOR VARIOUS DISTRIBUTIONS OF R, S_1, AND S_2

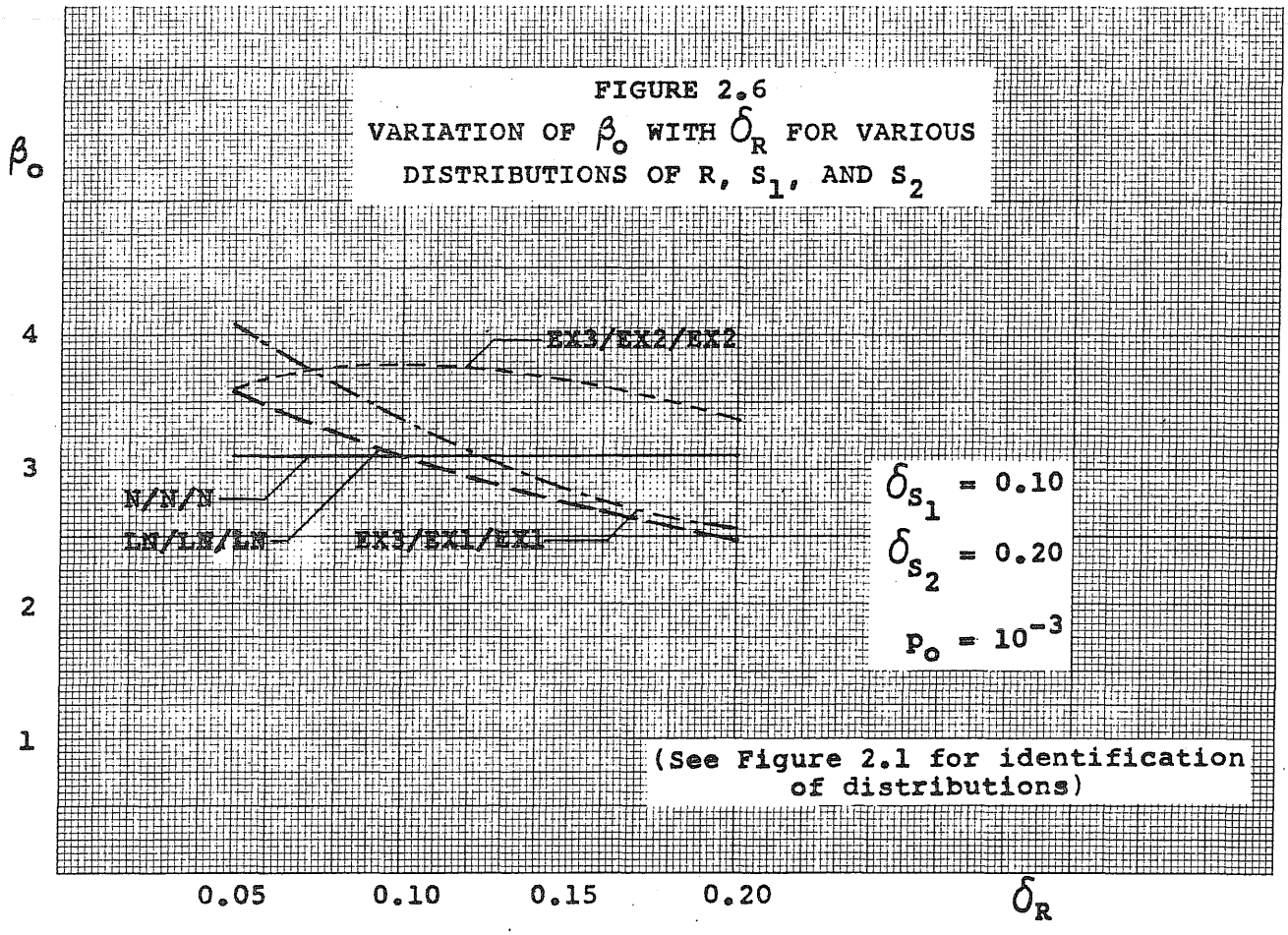

FIGURE 2.6
VARIATION OF β_o WITH δ_R FOR VARIOUS DISTRIBUTIONS OF R, S_1, AND S_2

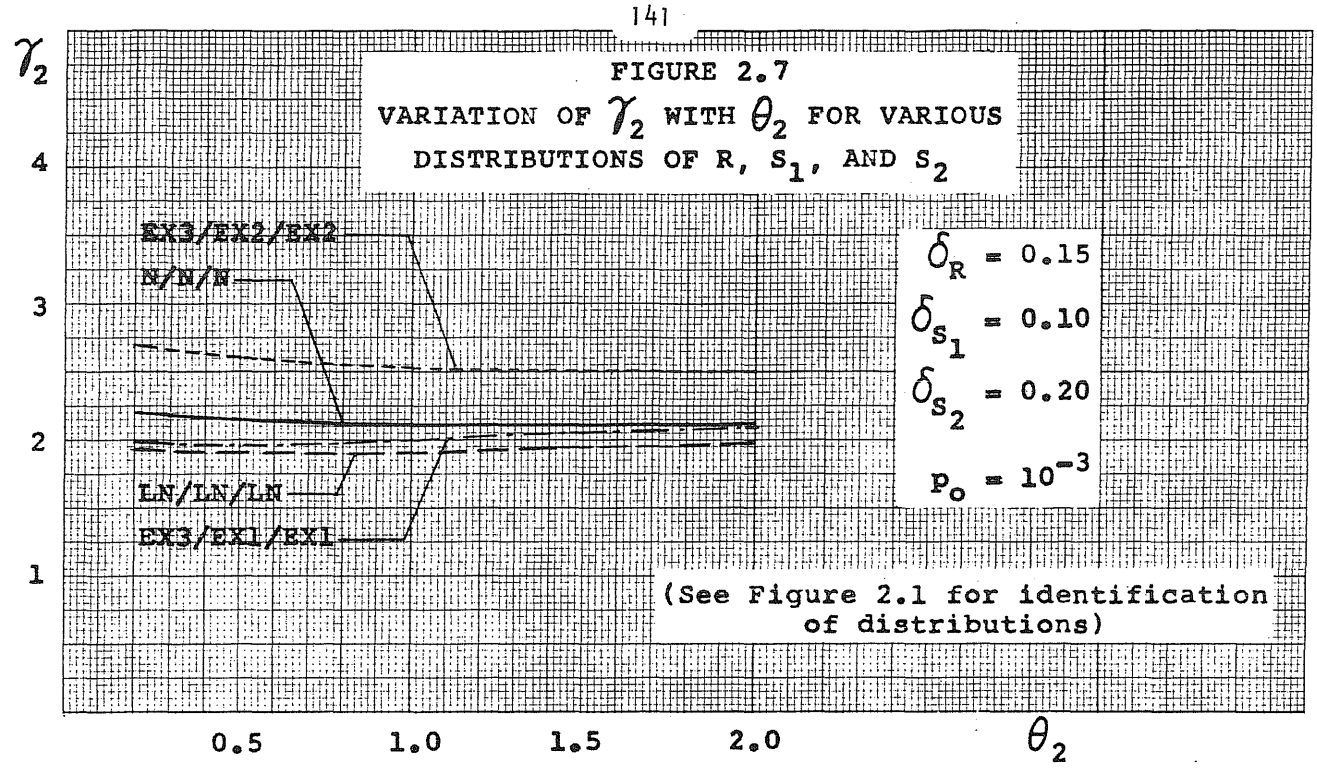

FIGURE 2.7
VARIATION OF γ_2 WITH θ_2 FOR VARIOUS DISTRIBUTIONS OF R, S_1, AND S_2

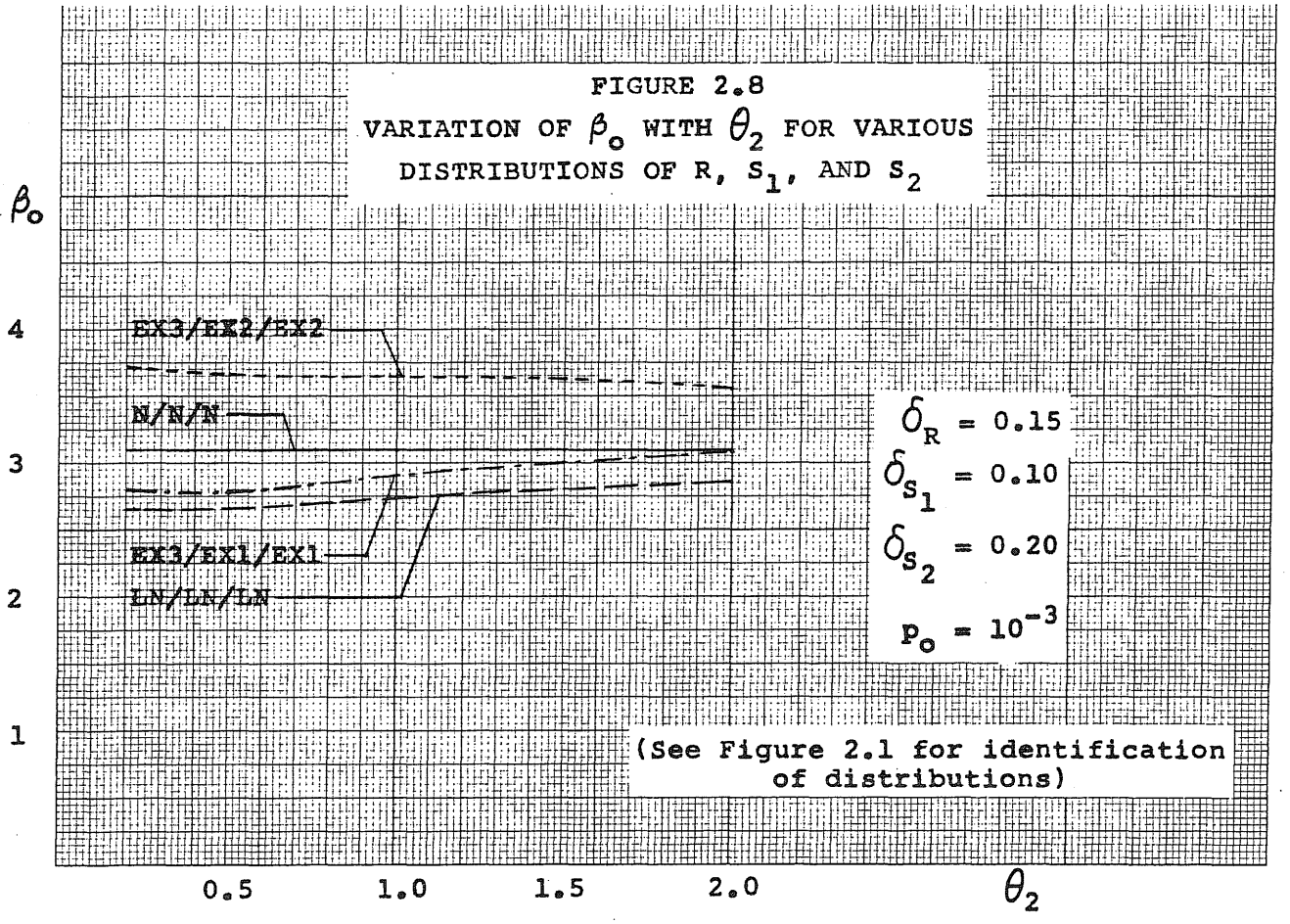

FIGURE 2.8
VARIATION OF β_o WITH θ_2 FOR VARIOUS DISTRIBUTIONS OF R, S_1, AND S_2

FIGURE 2.9

CENTRAL FACTORS OF SAFETY, JUDGMENT FACTOR, AND SAFETY INDEX WHEN R, S_L, AND S_D ARE NORMAL

$\delta_L = 0.20 \quad \delta_D = 0.05 \quad \bar{L}/\bar{D} = 0.40$

$p_f = 10^{-6}$

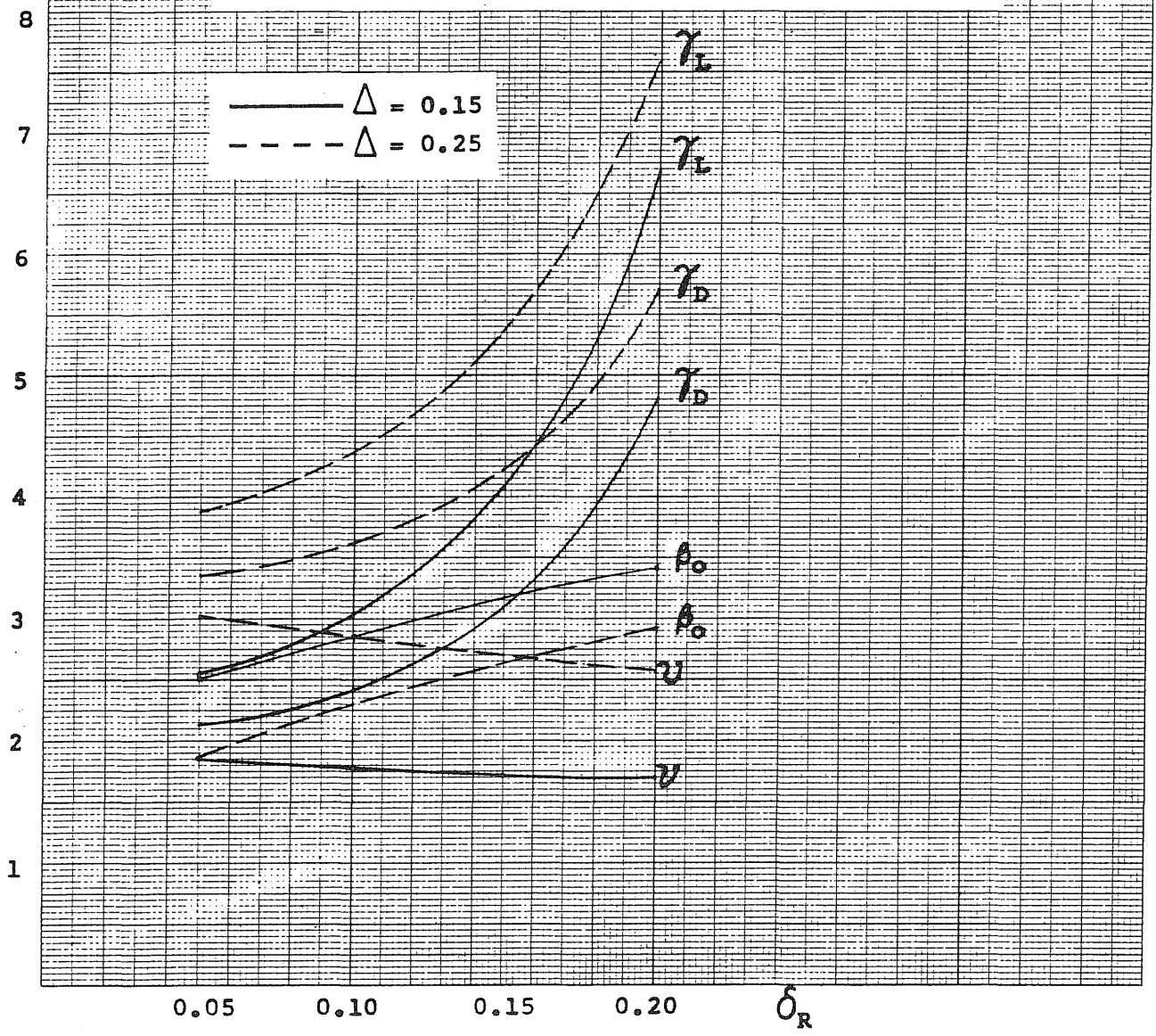

FIGURE 2.10

CENTRAL FACTORS OF SAFETY, JUDGMENT FACTOR, AND SAFETY INDEX WHEN R, S_L, AND S_D ARE NORMAL

$\delta_R = 0.10 \quad \delta_D = 0.05 \quad \bar{L}/\bar{D} = 0.40$

$p_f = 10^{-6}$

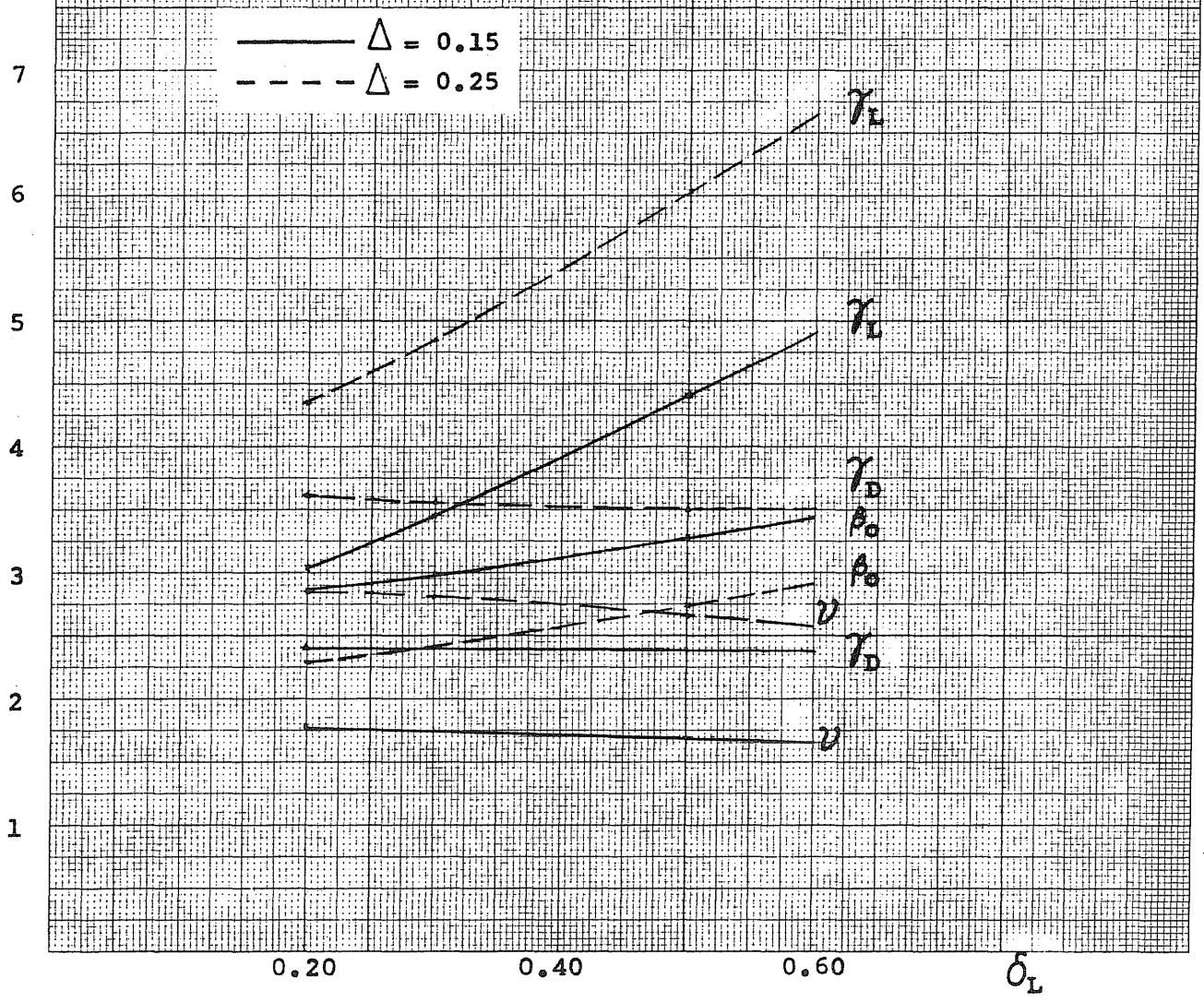

FIGURE 2.11

CENTRAL FACTORS OF SAFETY, JUDGMENT FACTOR, AND SAFETY INDEX WHEN R, S_L, AND S_D ARE NORMAL

$\delta_R = 0.10 \quad \delta_L = 0.20 \quad \delta_D = 0.05$

$p_f = 10^{-6}$

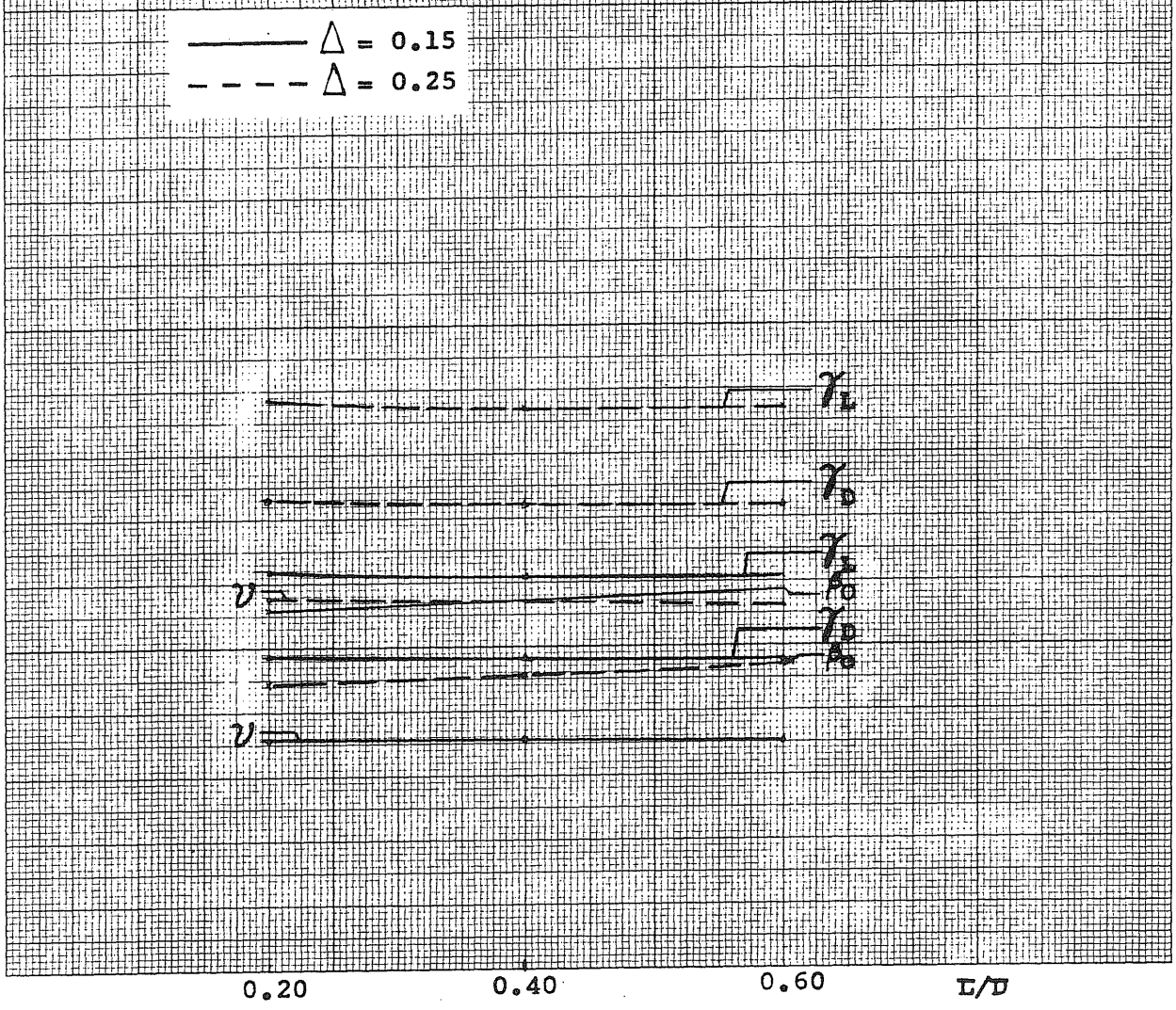

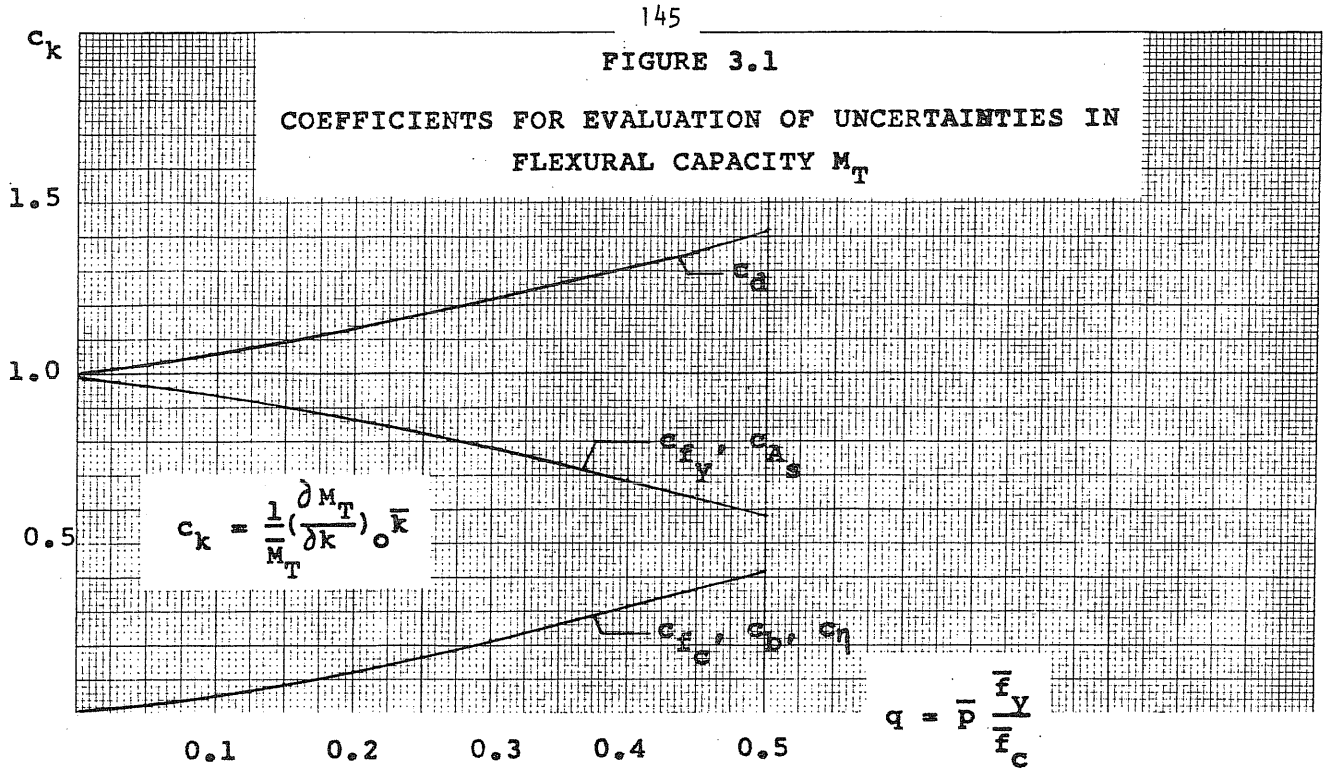

FIGURE 3.1

COEFFICIENTS FOR EVALUATION OF UNCERTAINTIES IN FLEXURAL CAPACITY M_T

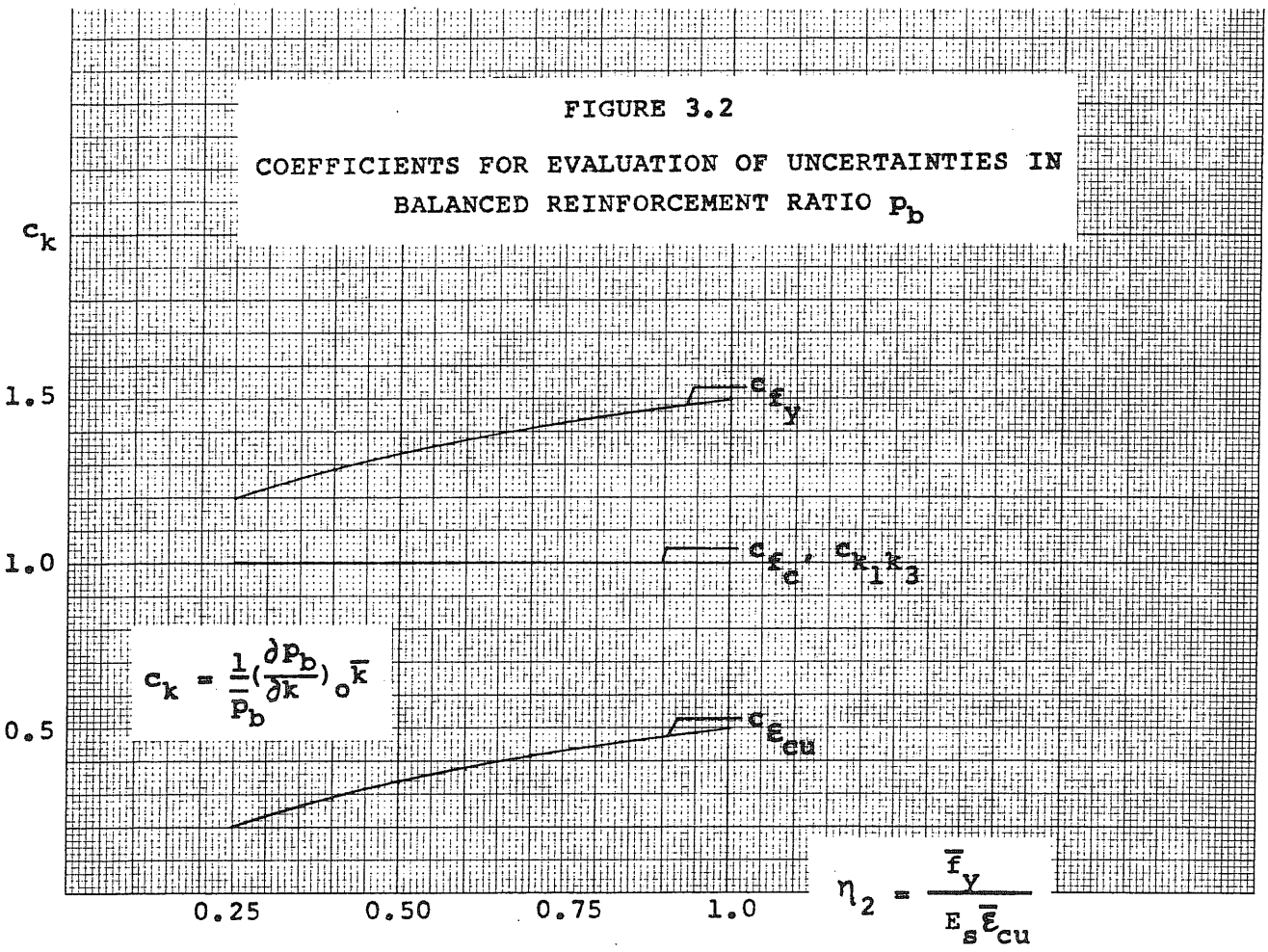

FIGURE 3.2

COEFFICIENTS FOR EVALUATION OF UNCERTAINTIES IN BALANCED REINFORCEMENT RATIO p_b

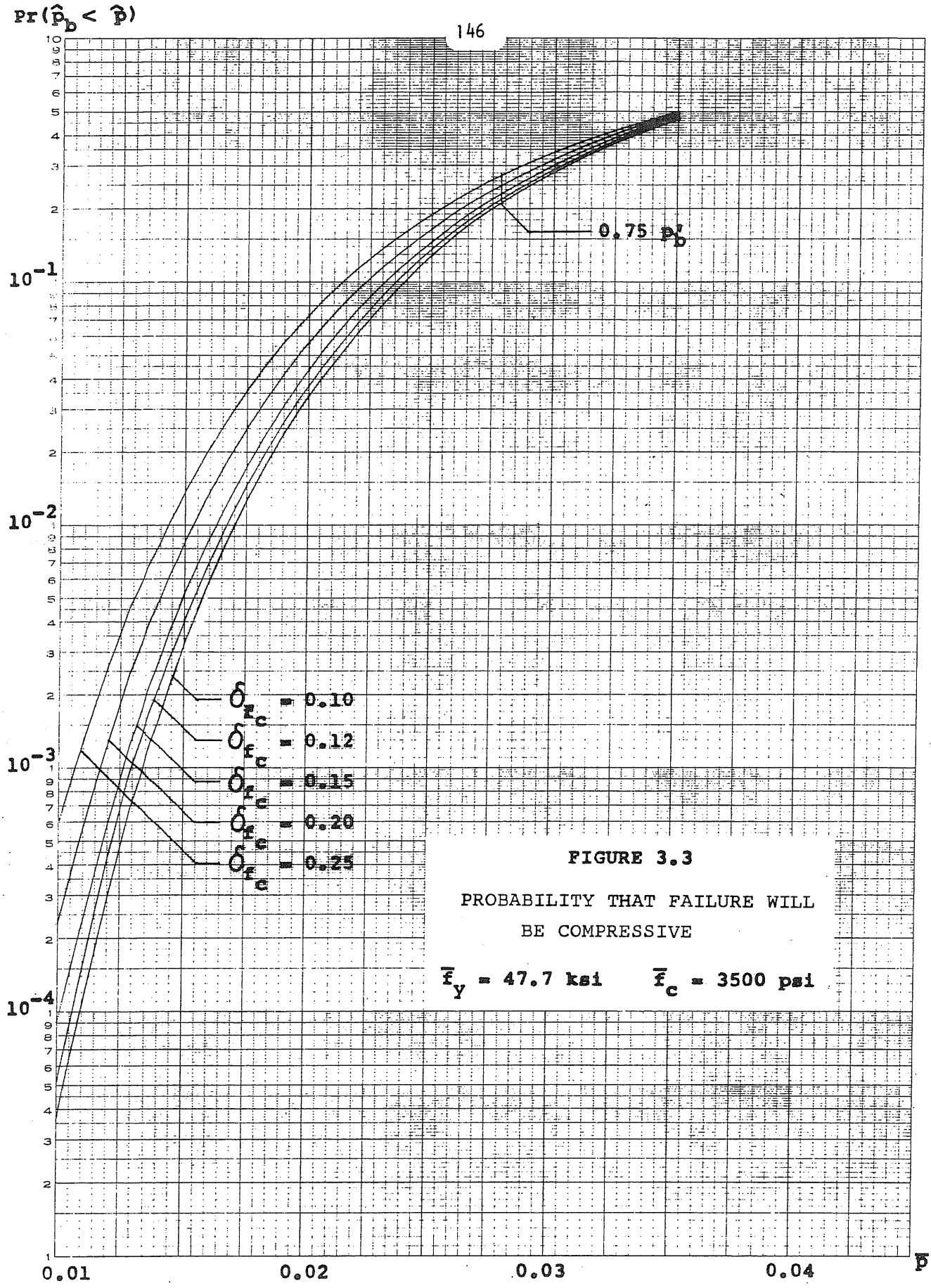

FIGURE 3.3

PROBABILITY THAT FAILURE WILL BE COMPRESSIVE

$\bar{f}_y$ = 47.7 ksi $\bar{f}'_c$ = 3500 psi

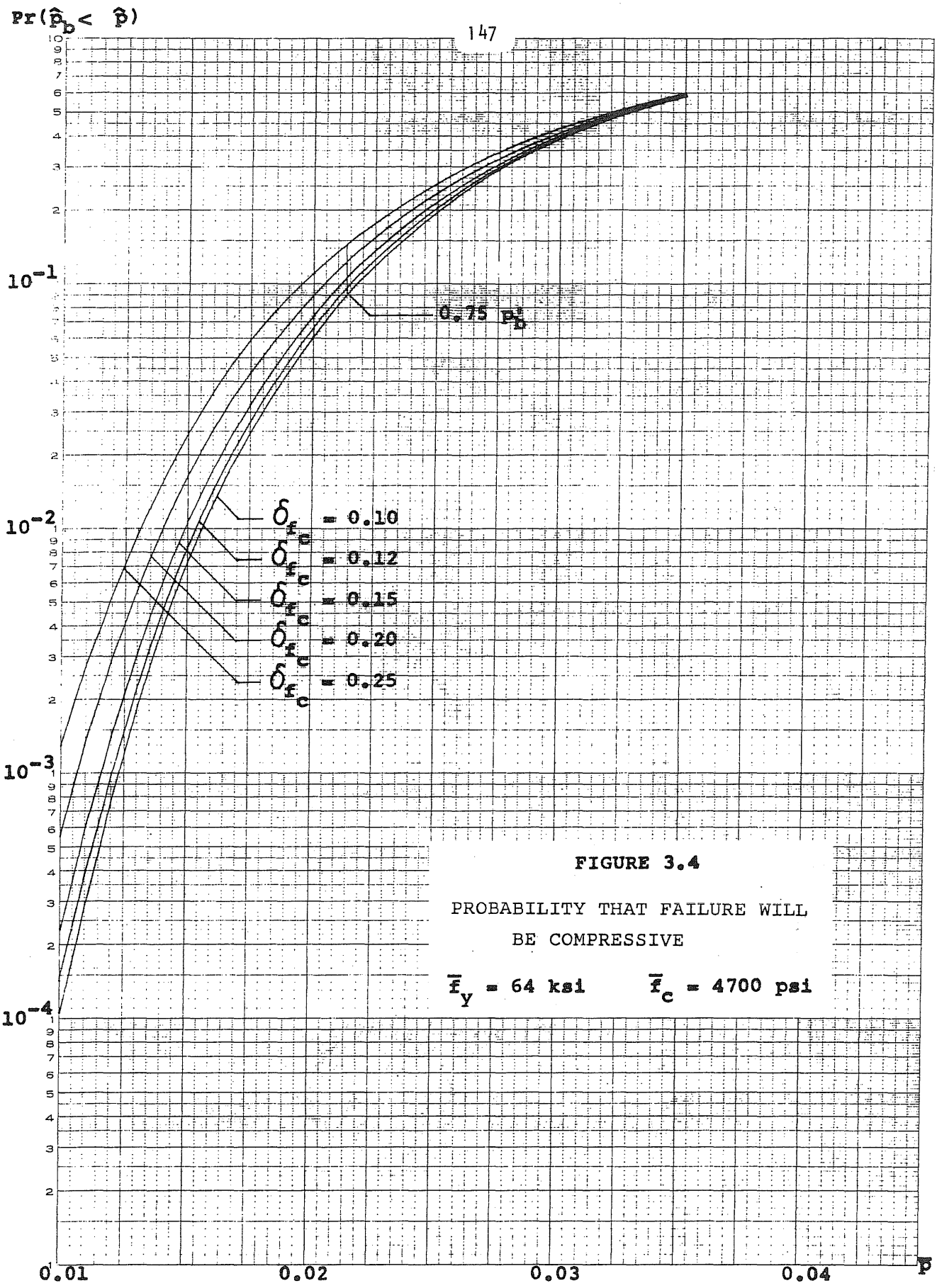

FIGURE 3.4

PROBABILITY THAT FAILURE WILL BE COMPRESSIVE

$\bar{f}_y$ = 64 ksi $\bar{f}_c$ = 4700 psi

FIGURE 3.5

UNCERTAINTIES IN FLEXURAL CAPACITY

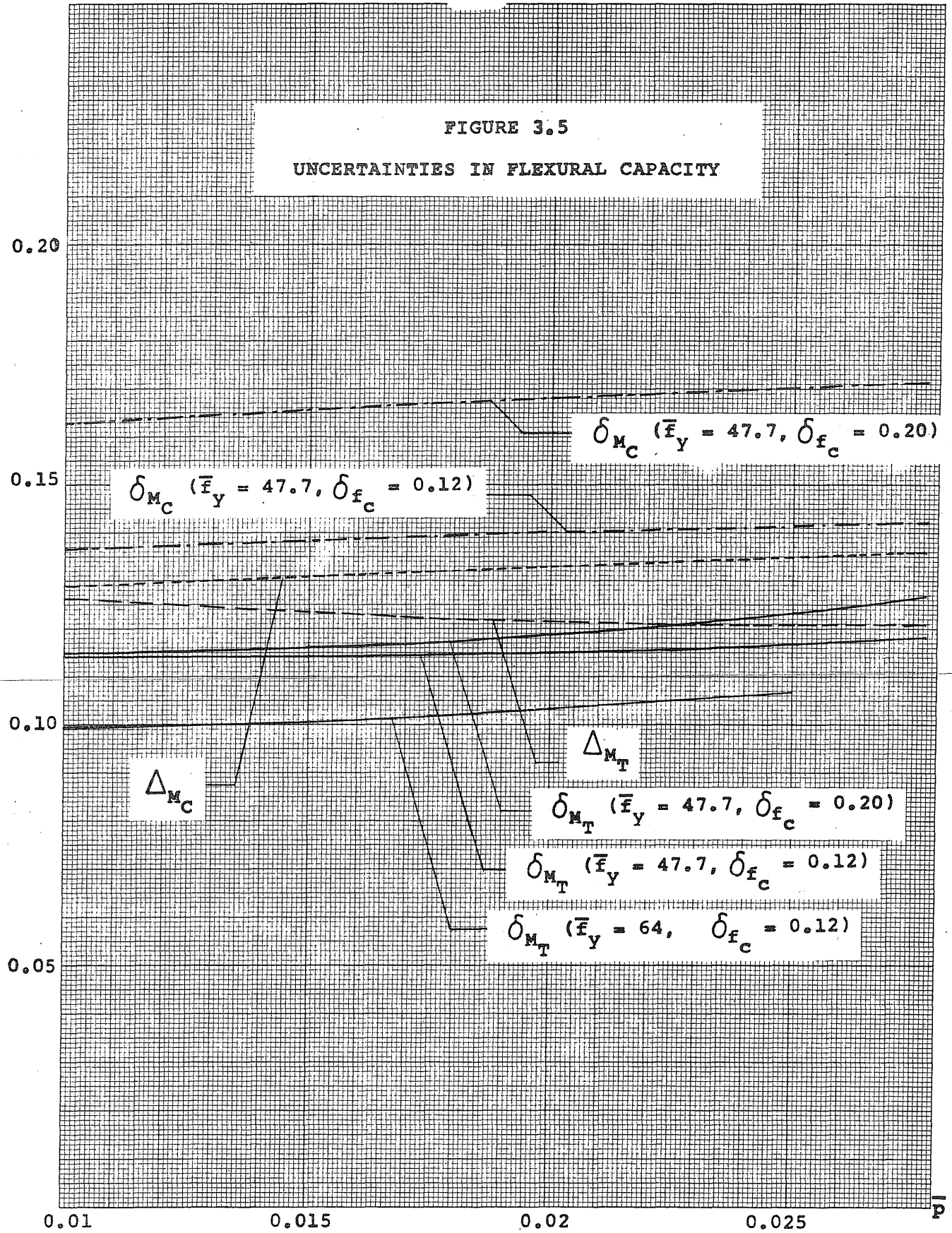

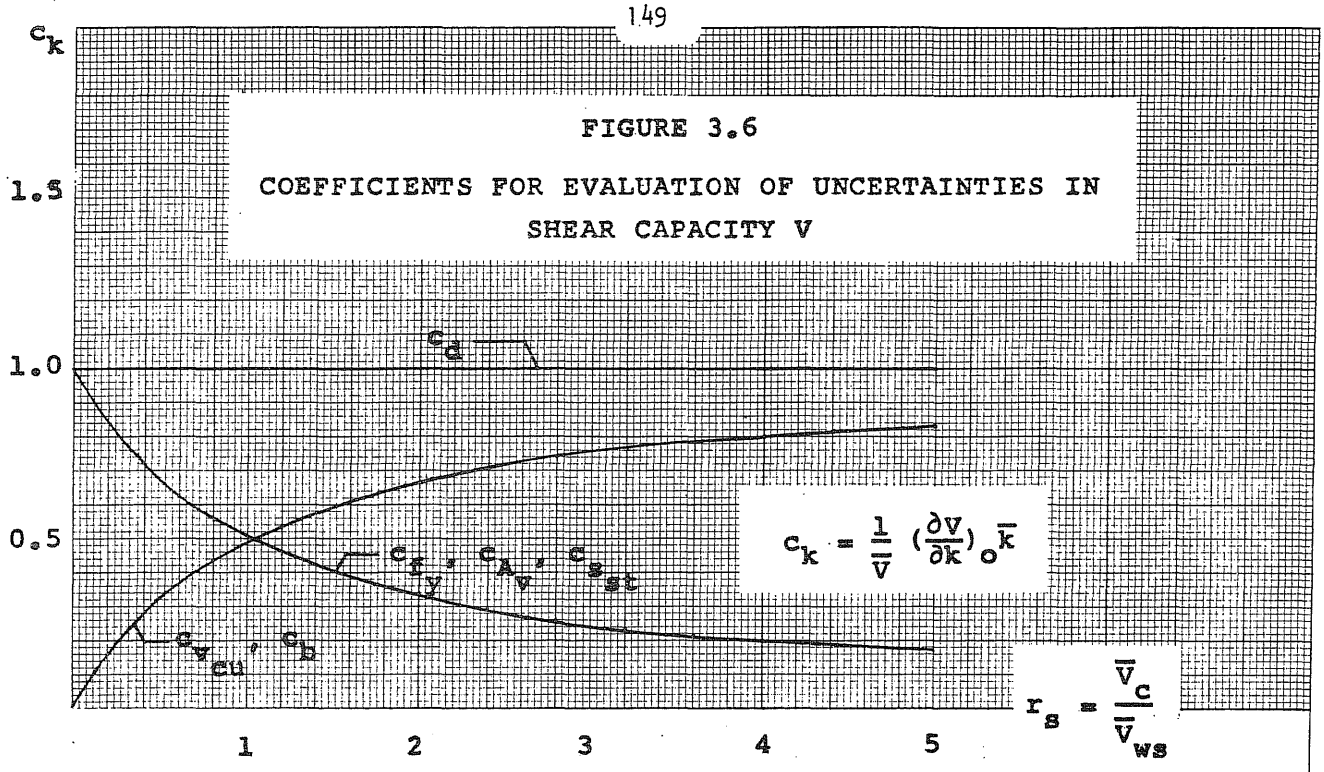

FIGURE 3.6

COEFFICIENTS FOR EVALUATION OF UNCERTAINTIES IN SHEAR CAPACITY V

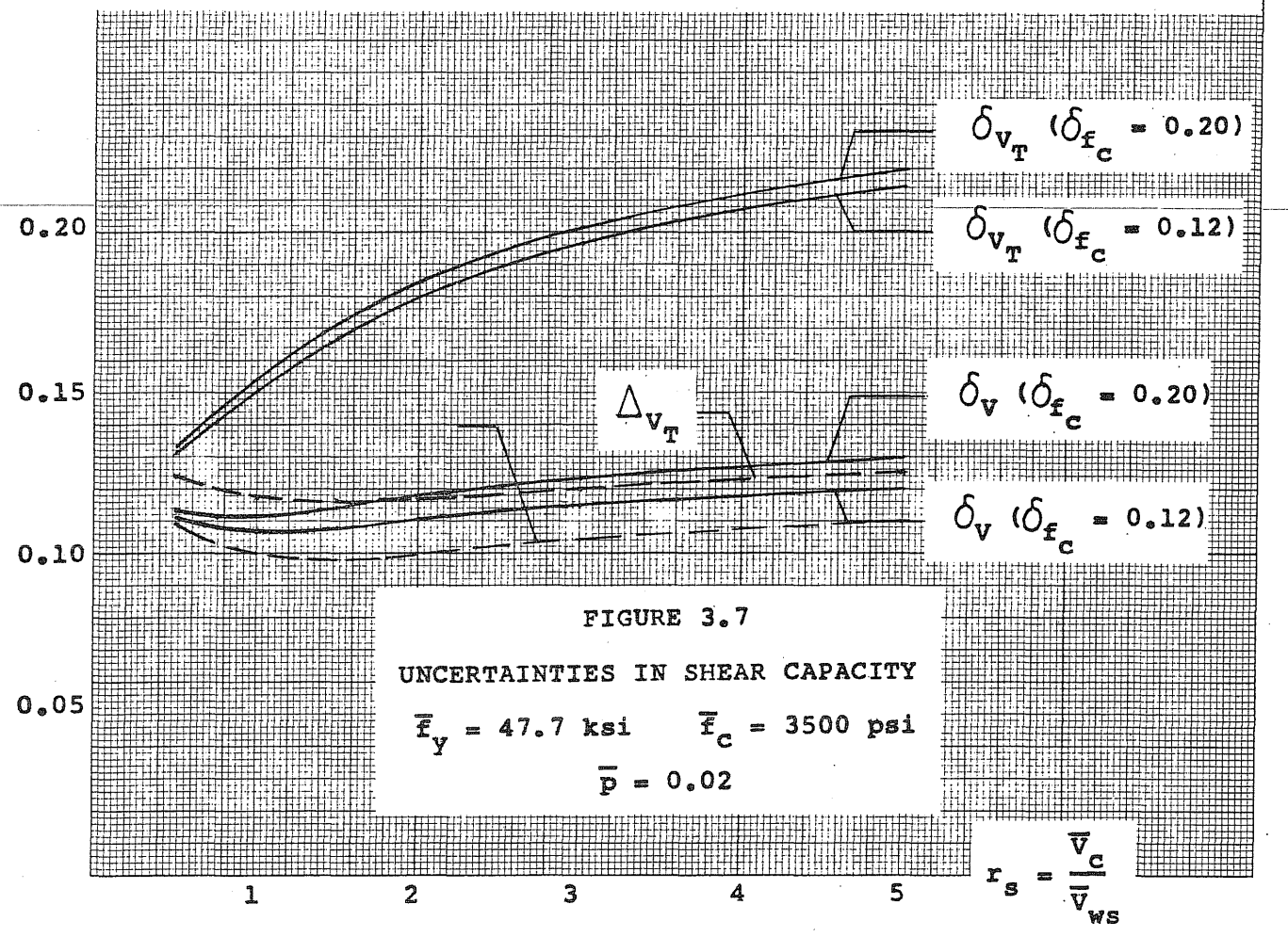

FIGURE 3.7

UNCERTAINTIES IN SHEAR CAPACITY

$\bar{f}_y$ = 47.7 ksi $\bar{f}_c$ = 3500 psi

$\bar{p}$ = 0.02

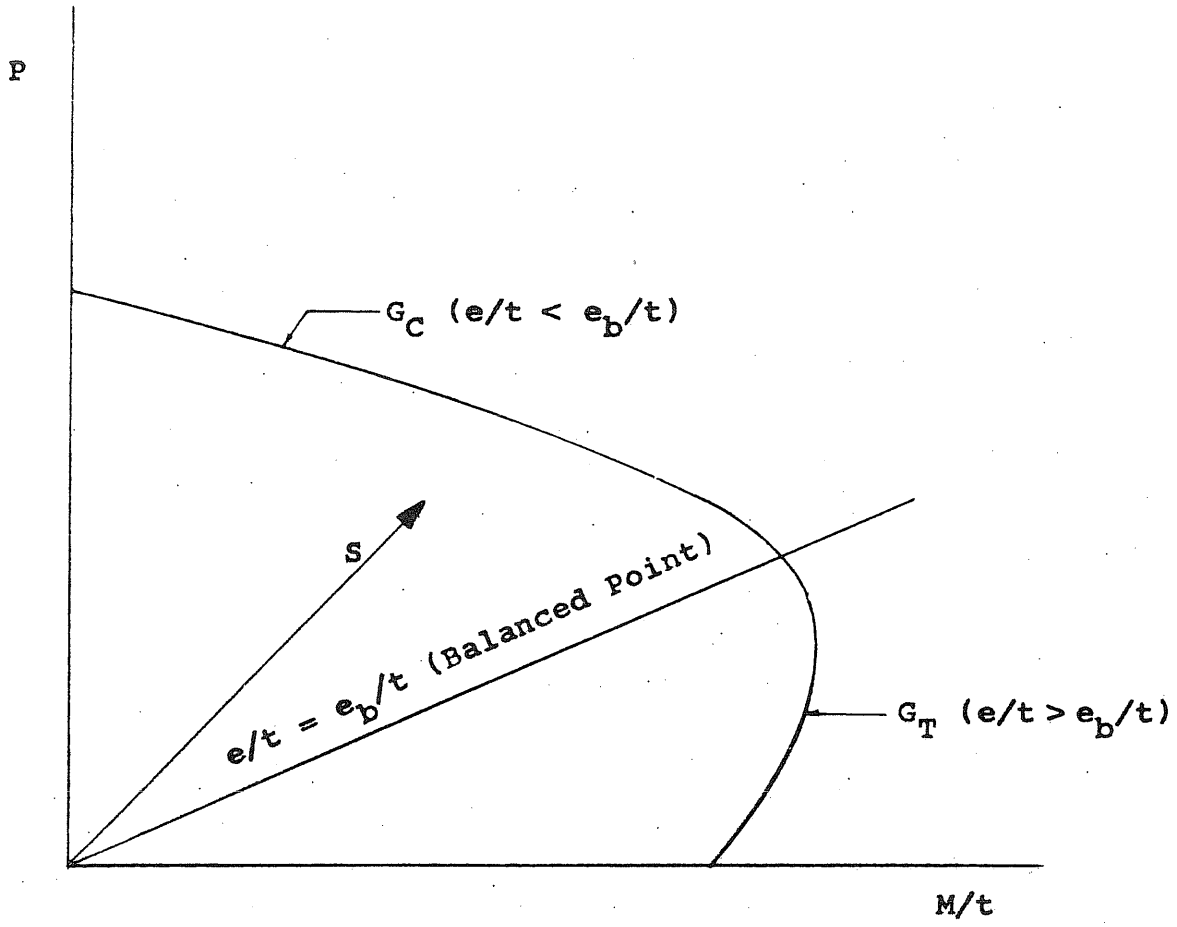

FIGURE 3.8
INTERACTION CURVE FOR A REINFORCED CONCRETE SECTION

FIGURE 3.9

COEFFICIENTS FOR EVALUATION OF UNCERTAINTIES IN BALANCED ECCENTRICITY RATIO e_b/t

$\bar{f}_y$ = 47.7 ksi $\bar{f}_c$ = 3500 psi

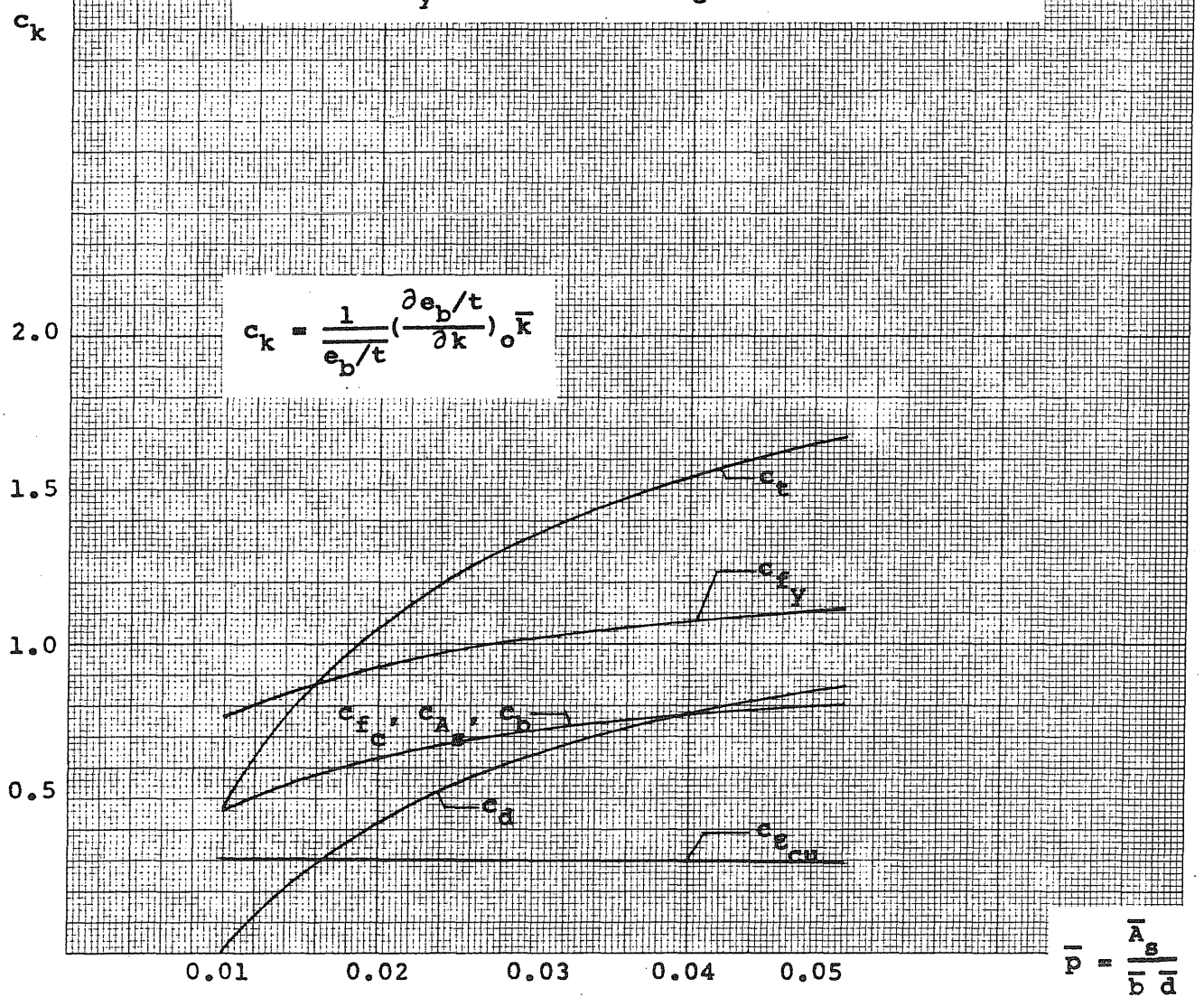

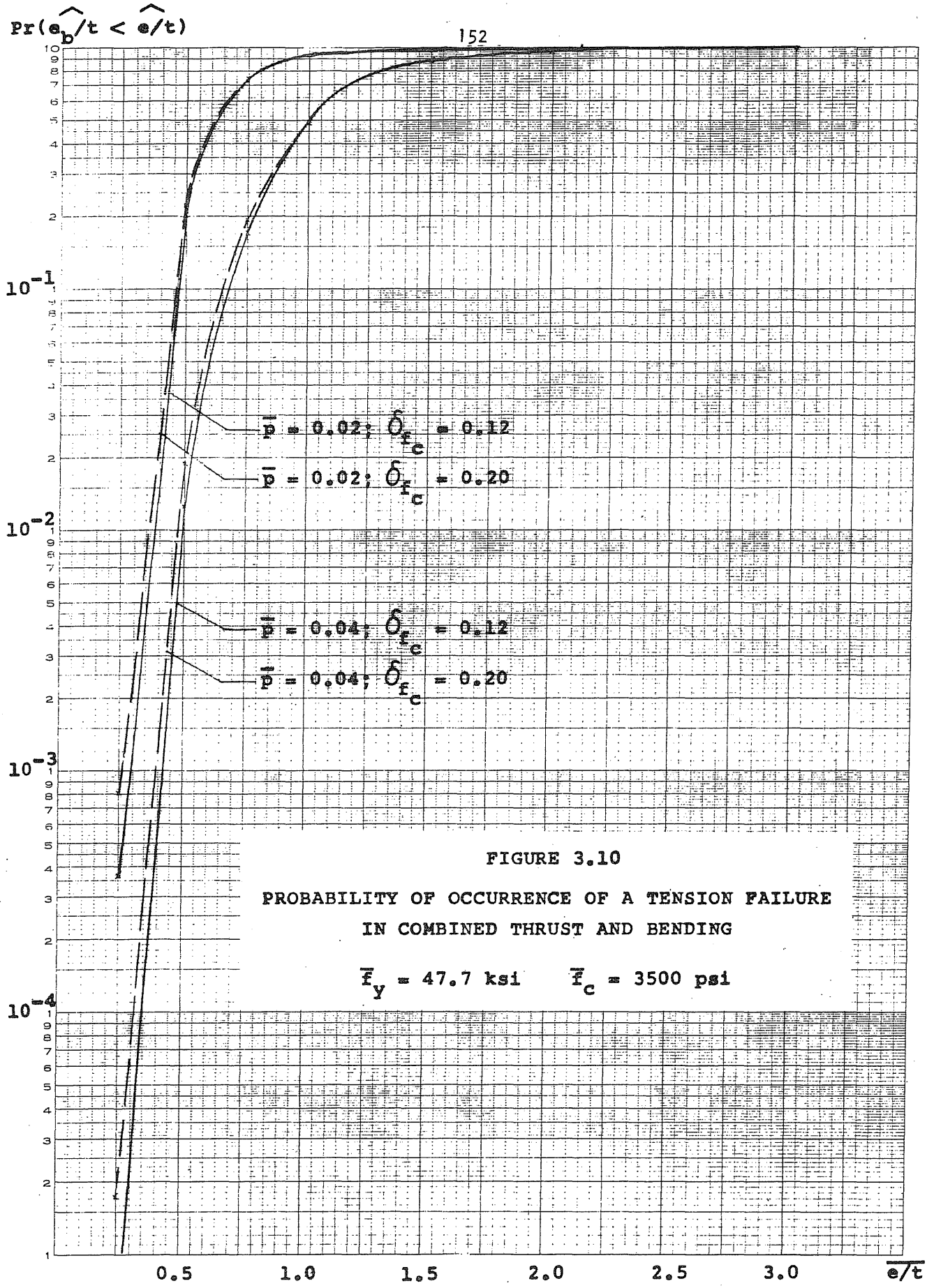

FIGURE 3.10

PROBABILITY OF OCCURRENCE OF A TENSION FAILURE IN COMBINED THRUST AND BENDING

$\bar{f}_y = 47.7$ ksi $\quad \bar{f}_c = 3500$ psi

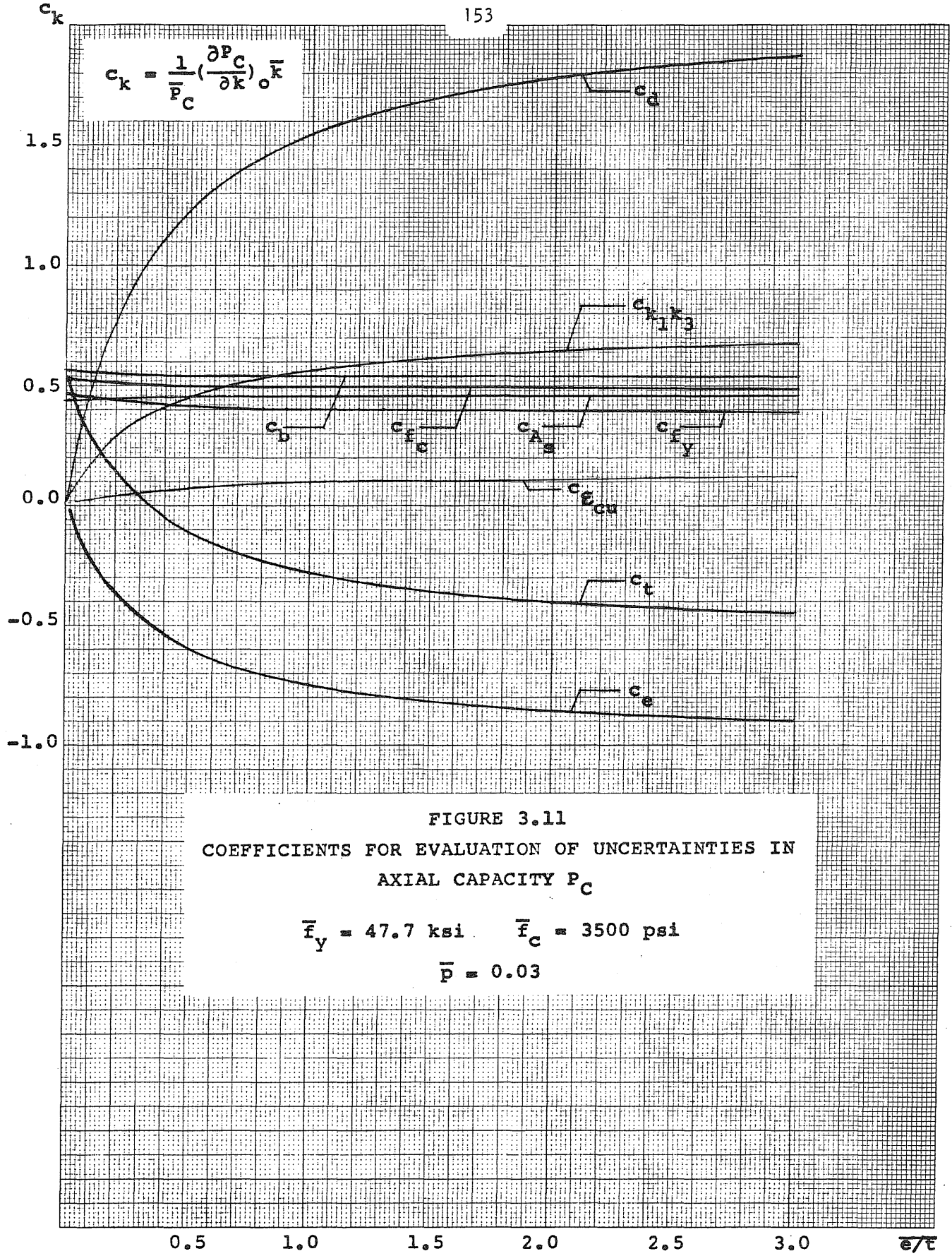

FIGURE 3.11

COEFFICIENTS FOR EVALUATION OF UNCERTAINTIES IN AXIAL CAPACITY P_C

$\bar{f}_y = 47.7$ ksi $\quad \bar{f}_c = 3500$ psi

$\bar{p} = 0.03$

FIGURE 3.12

COEFFICIENTS FOR EVALUATION OF UNCERTAINTIES IN AXIAL CAPACITY P_T

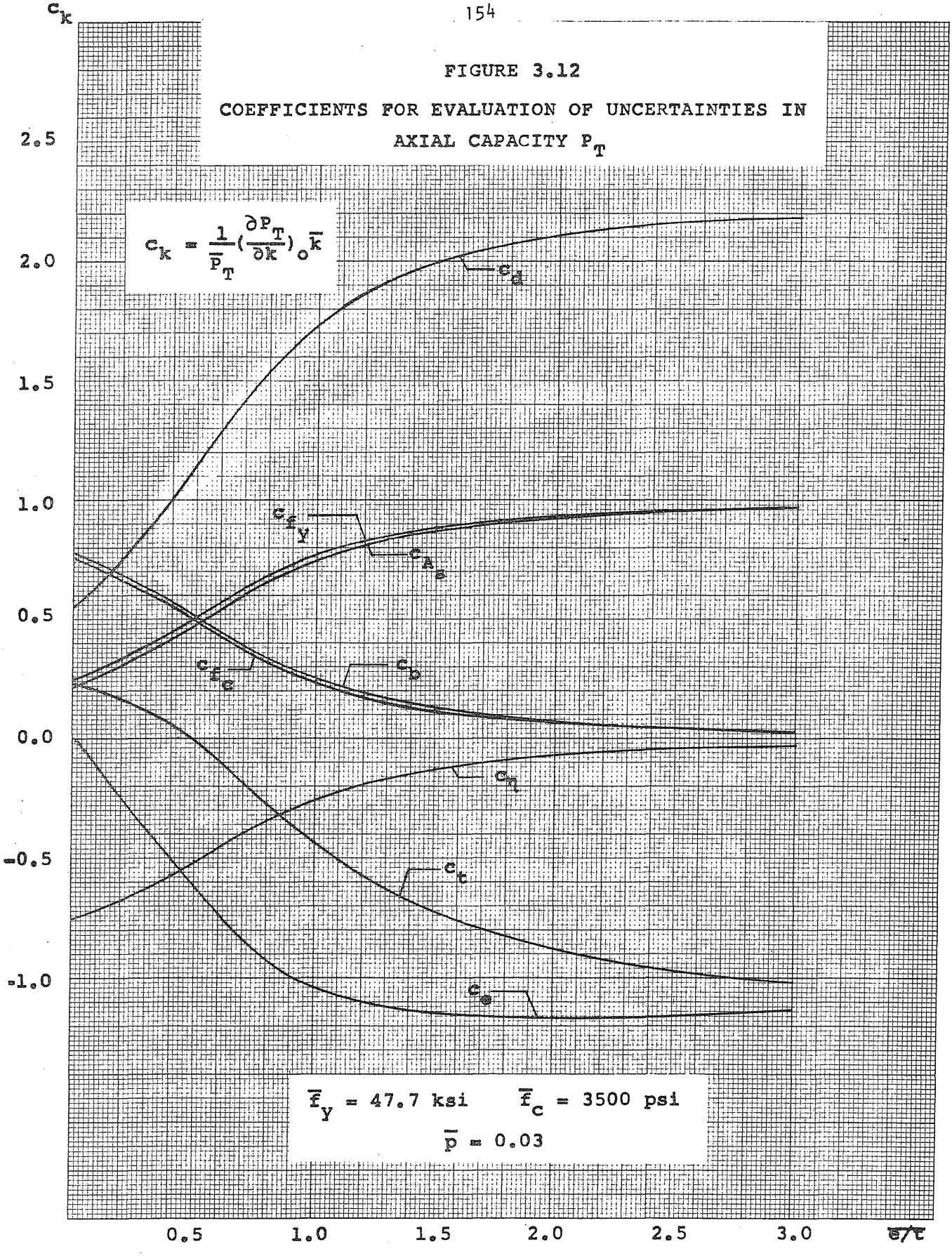

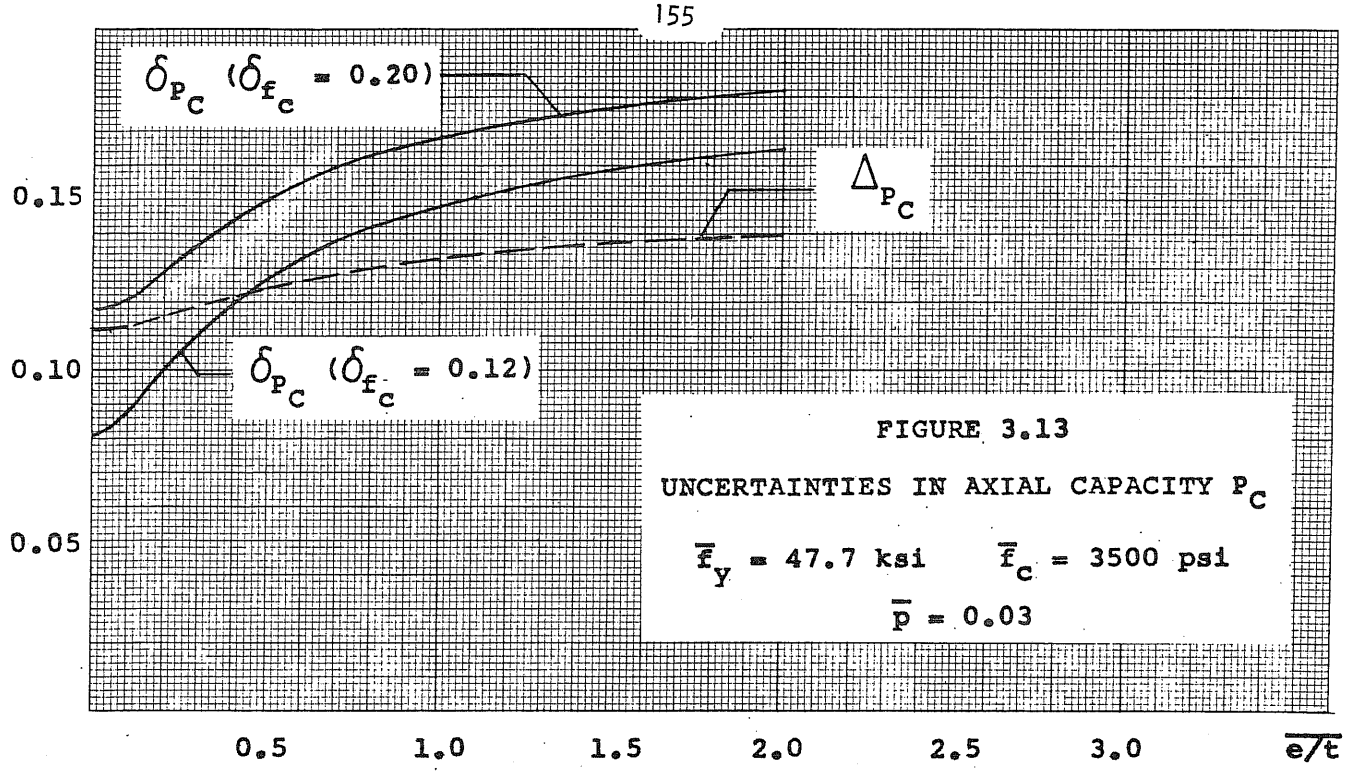

FIGURE 3.13

UNCERTAINTIES IN AXIAL CAPACITY P_C

$\bar{f}_y$ = 47.7 ksi $\bar{f}_c$ = 3500 psi

$\bar{p}$ = 0.03

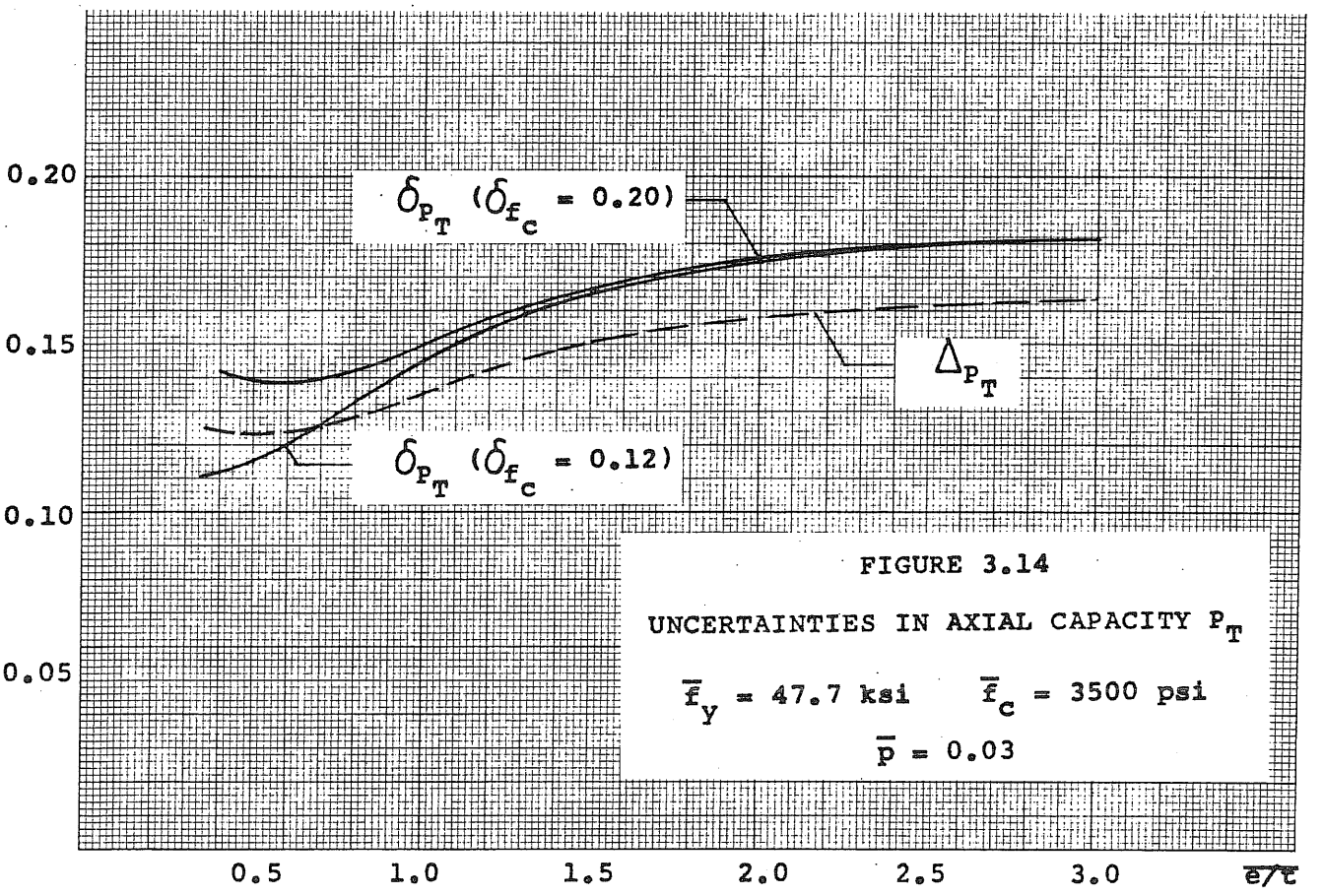

FIGURE 3.14

UNCERTAINTIES IN AXIAL CAPACITY P_T

$\bar{f}_y$ = 47.7 ksi $\bar{f}_c$ = 3500 psi

$\bar{p}$ = 0.03

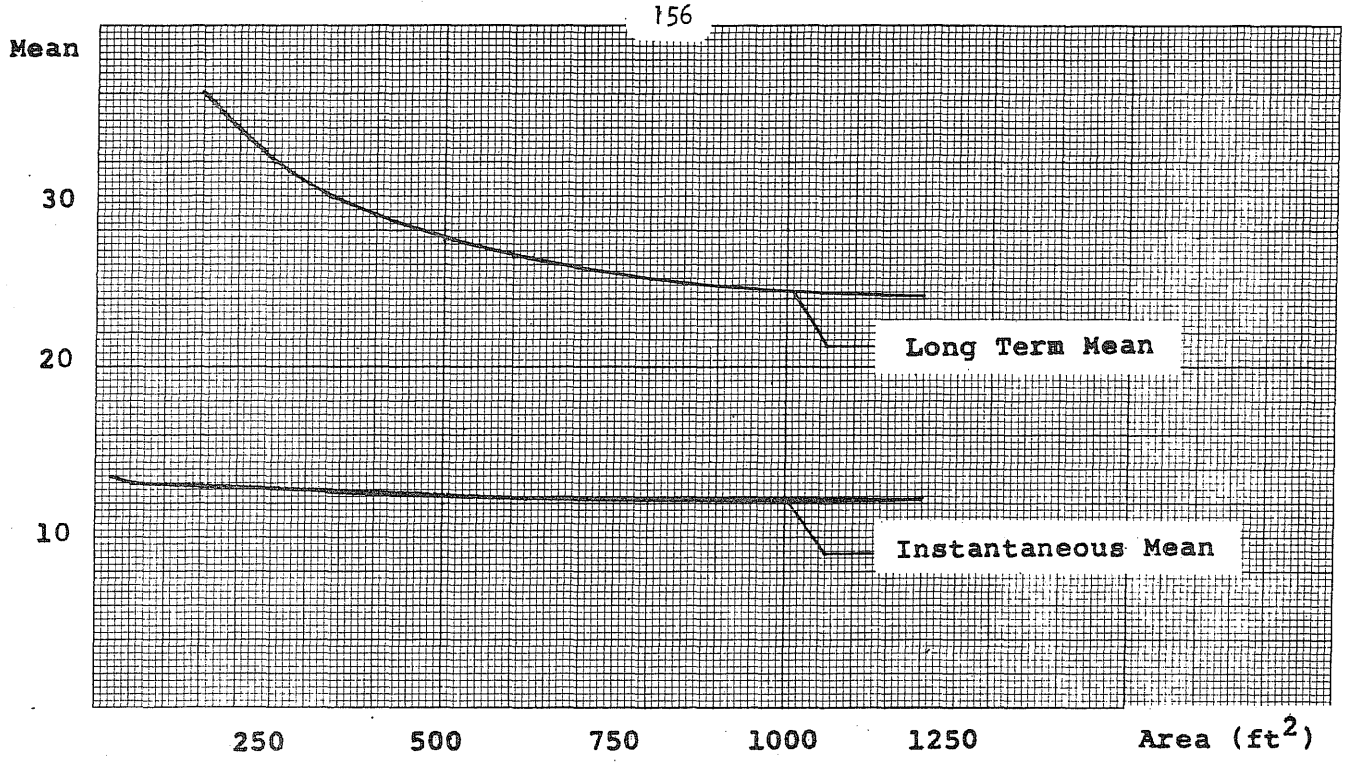

FIGURE 4.1

STATISTICS OF LIVE LOAD INTENSITY

Source: Mitchell and Woodgate (43)

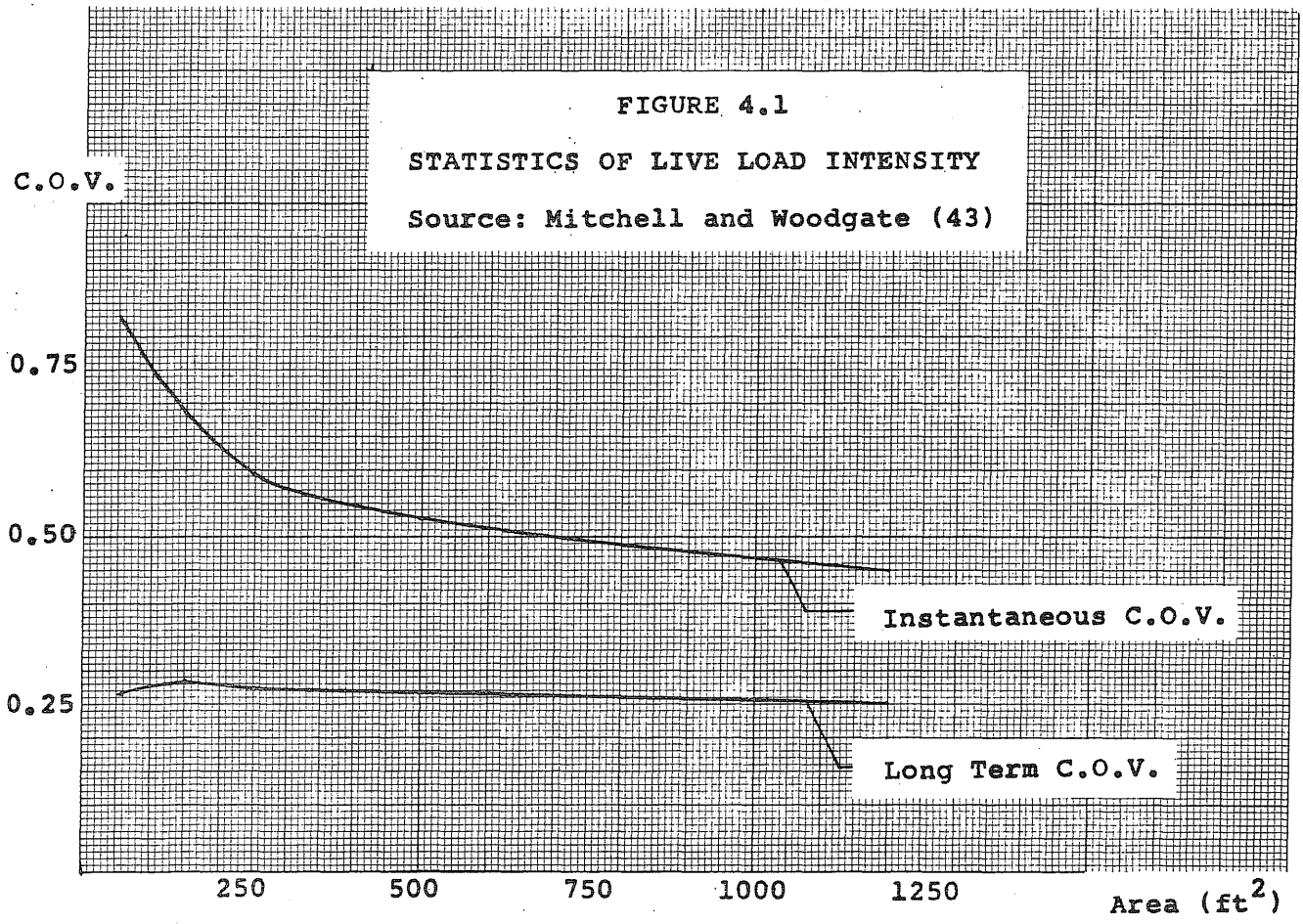

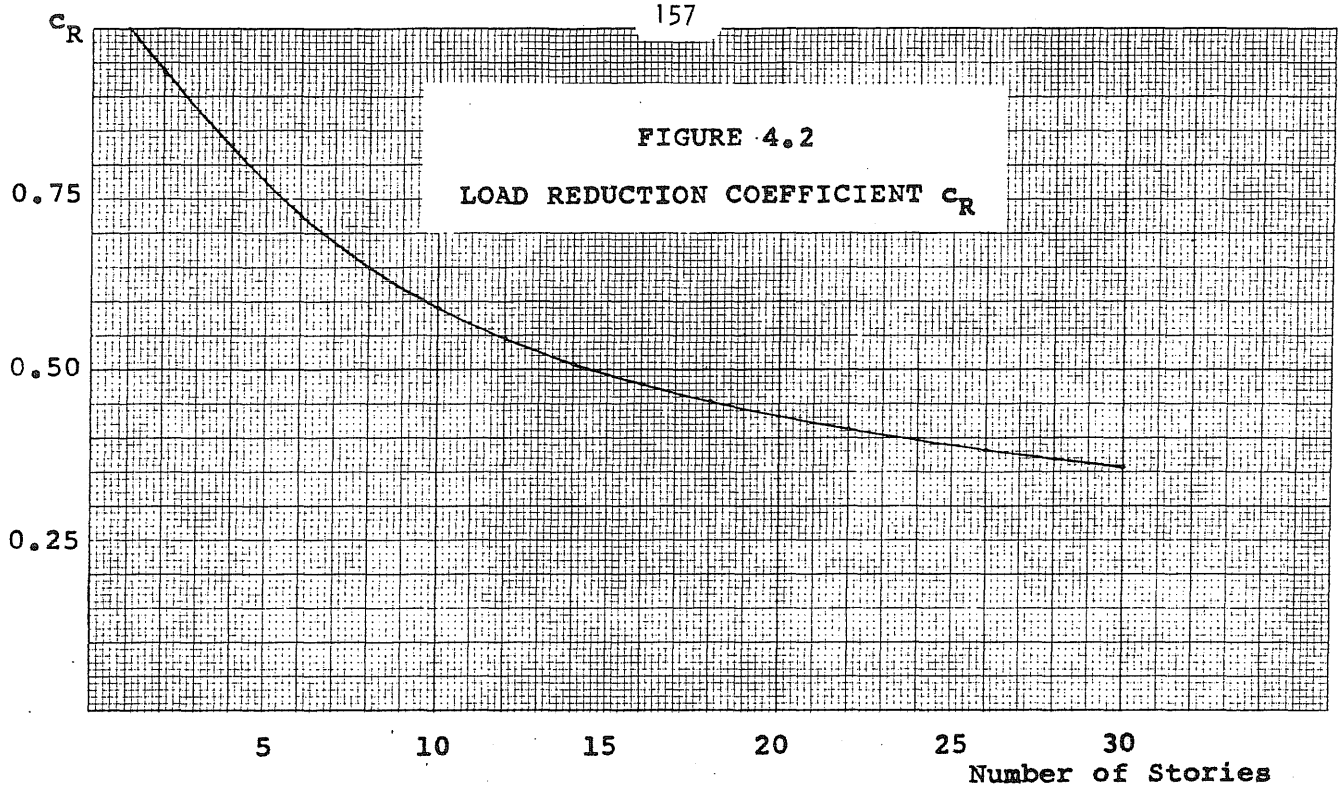

FIGURE 4.2

LOAD REDUCTION COEFFICIENT c_R

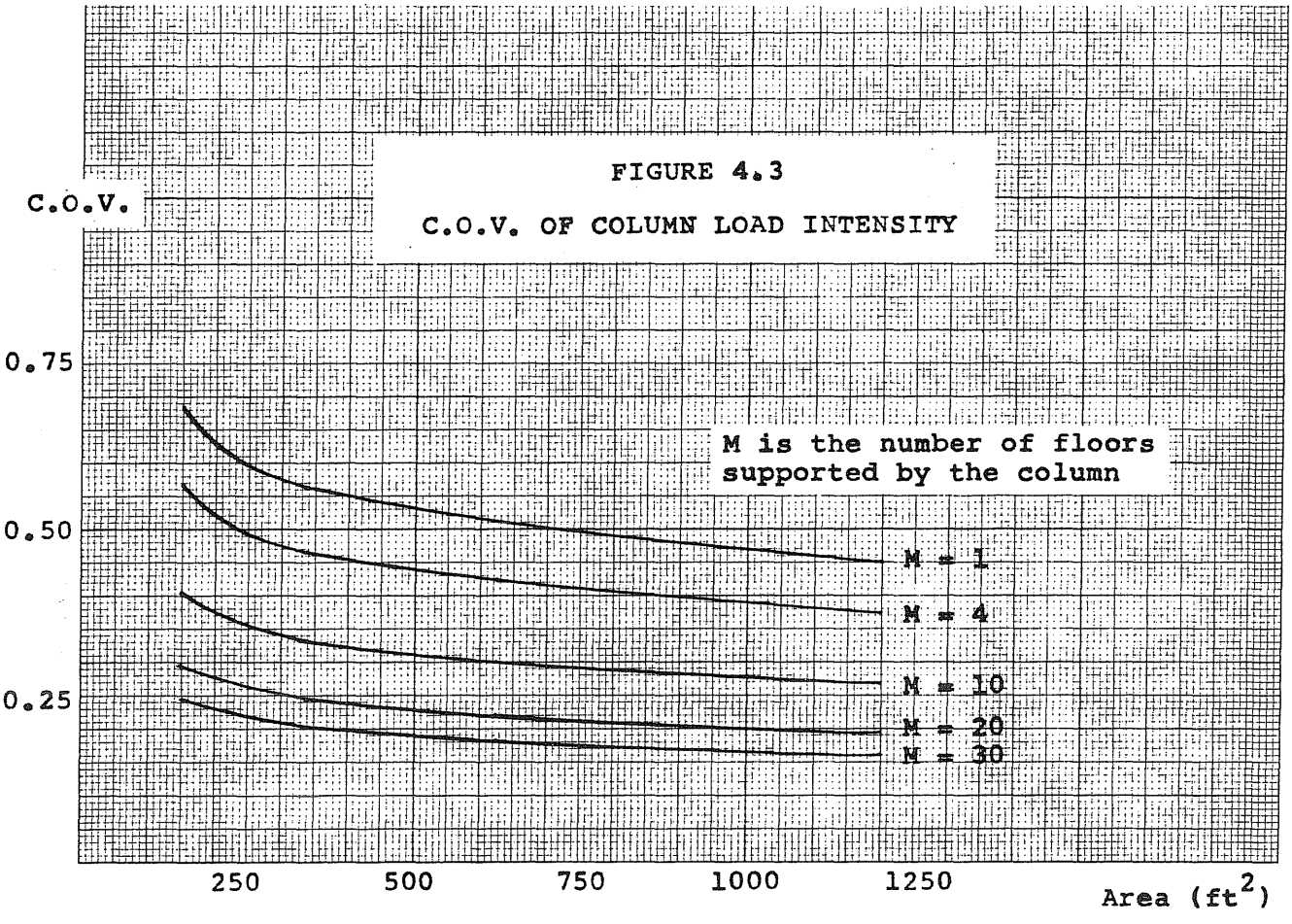

FIGURE 4.3

C.O.V. OF COLUMN LOAD INTENSITY

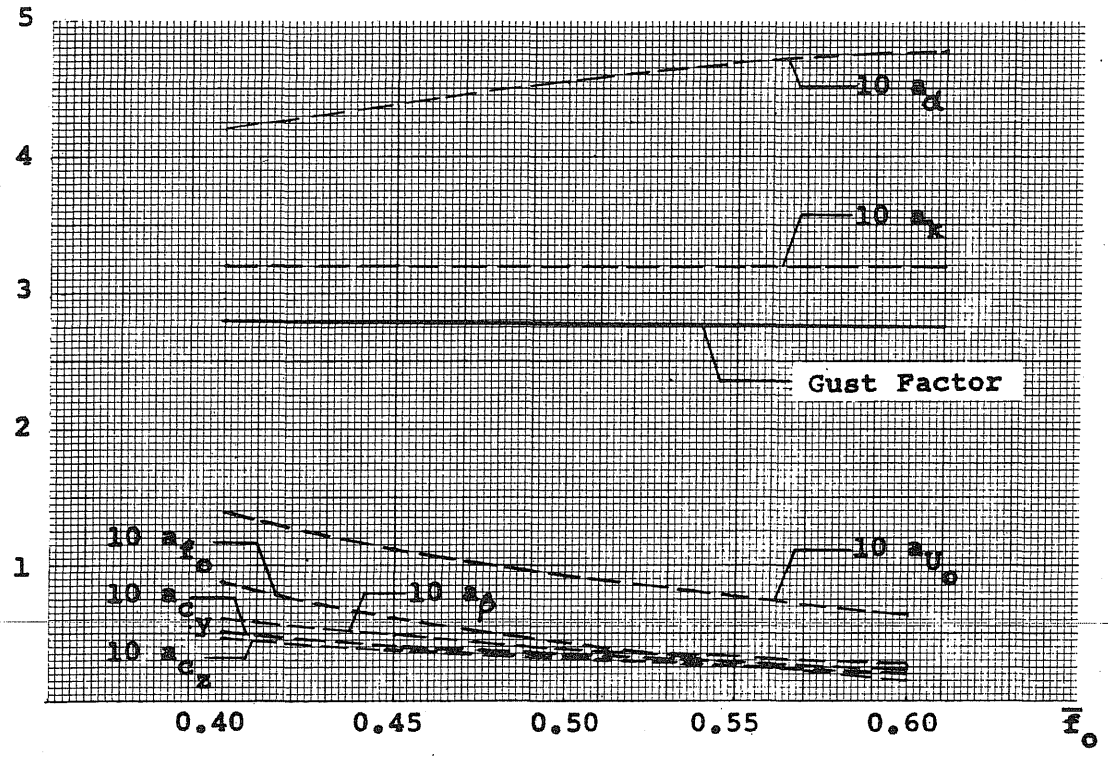

FIGURE 4.4

SENSITIVITY OF GUST FACTOR AND ITS STATISTICS TO FUNDAMENTAL NATURAL FREQUENCY

$\bar{U}_o$ = 33 fps t_d = 20 min.

$\bar{k}$ = 0.05 $\bar{\alpha}$ = 0.4 $\bar{\beta}$ = 0.015

b = 100 ft. h = 240 ft.

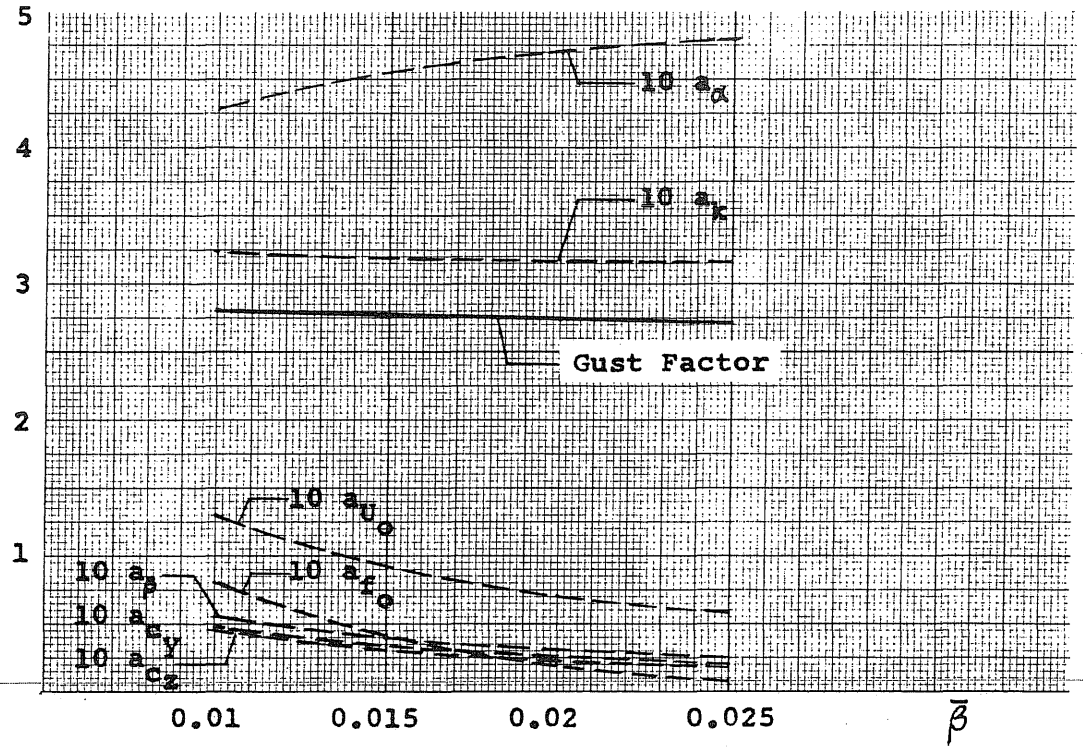

FIGURE 4.5

SENSITIVITY OF GUST FACTOR AND ITS STATISTICS TO DAMPING

$\bar{U}_o$ = 33 fps t_d = 20 min.

$\bar{k}$ = 0.05 $\bar{\alpha}$ = 0.4 $\bar{f}_o$ = 0.5

b = 100 ft. h = 240 ft.

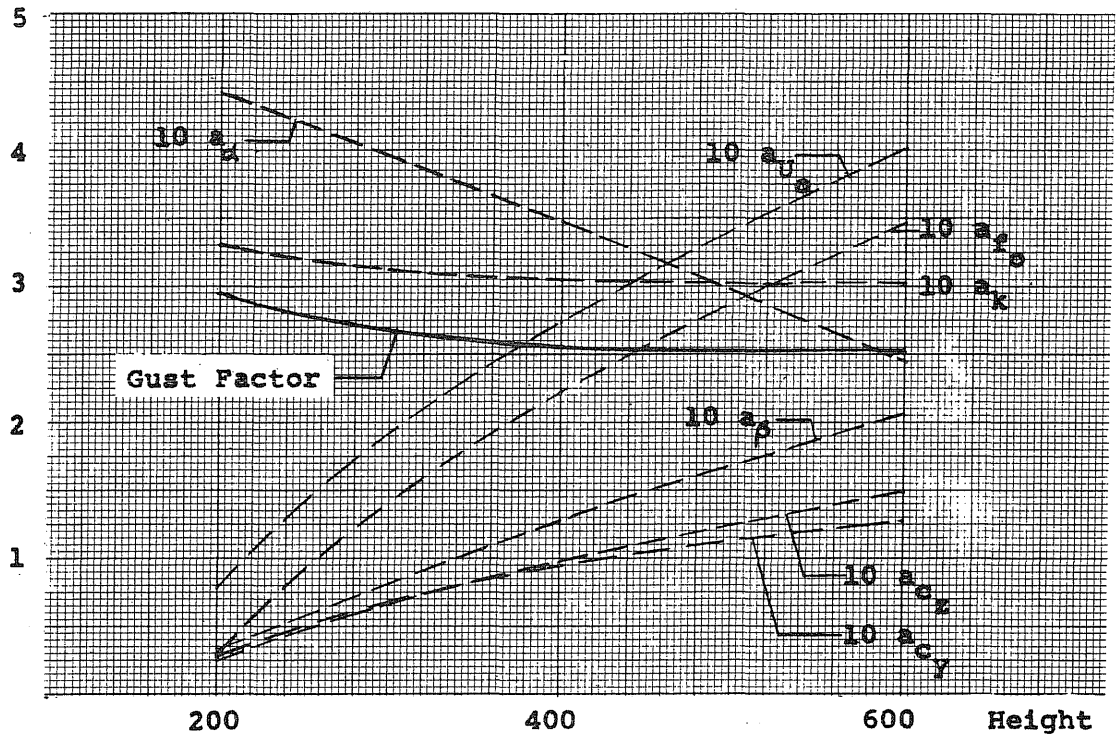

FIGURE 4.6

SENSITIVITY OF GUST FACTOR AND ITS STATISTICS

TO HEIGHT OF BUILDING

$\bar{U}_o$ = 33 fps t_d = 20 min.

$\bar{k}$ = 0.05 $\bar{\alpha}$ = 0.4 $\bar{\beta}$ = 0.015

b = 100 ft.

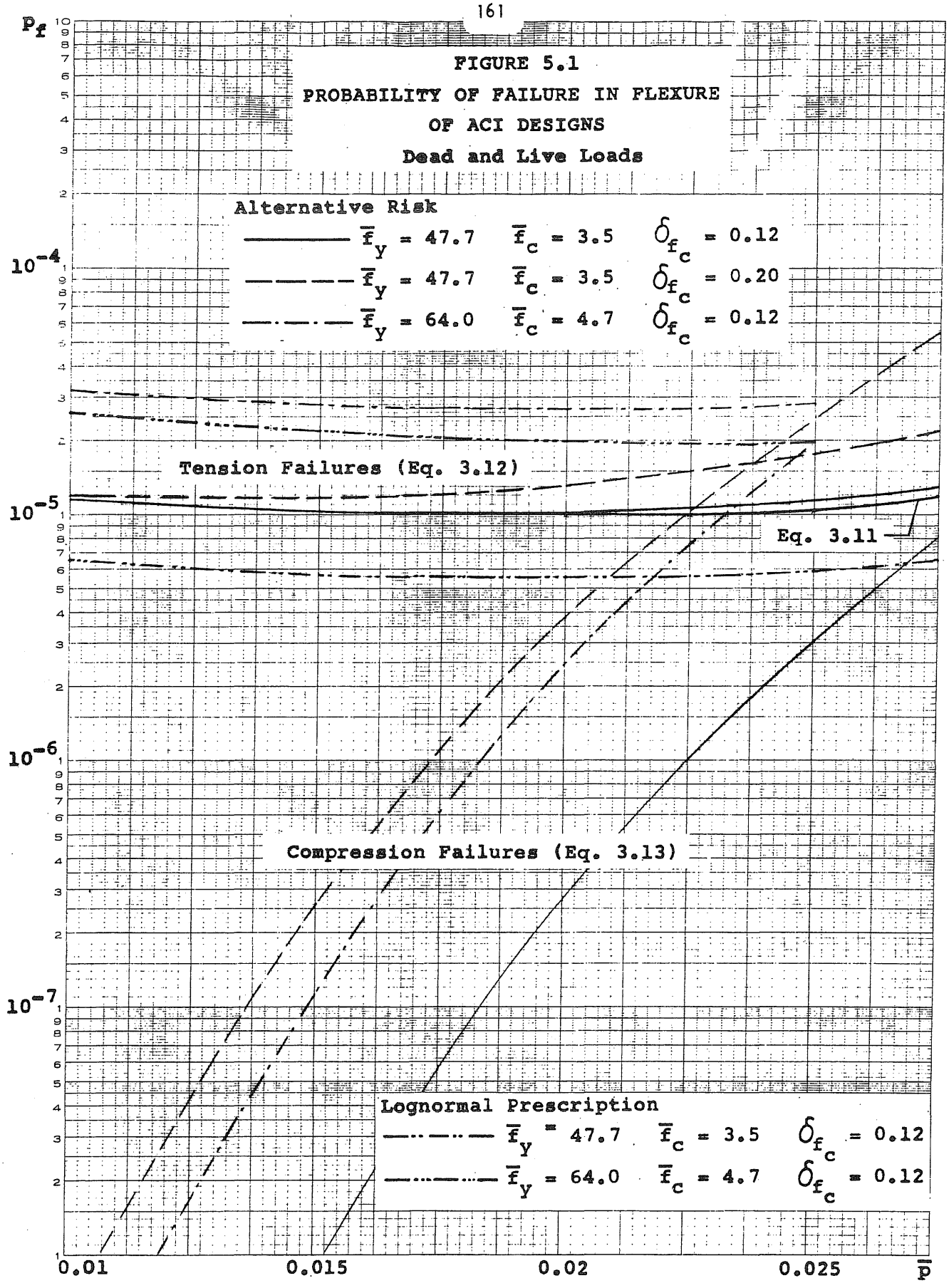
P_f
FIGURE 5.1
PROBABILITY OF FAILURE IN FLEXURE
OF ACI DESIGNS
Dead and Live Loads
Alternative Risk
$\bar{f}_y$ = 47.7 $\bar{f}_c$ = 3.5 δ_{f_c} = 0.12
$\bar{f}_y$ = 47.7 $\bar{f}_c$ = 3.5 δ_{f_c} = 0.20
$\bar{f}_y$ = 64.0 $\bar{f}_c$ = 4.7 δ_{f_c} = 0.12
Tension Failures (Eq. 3.12)
Eq. 3.11
Compression Failures (Eq. 3.13)
Lognormal Prescription
$\bar{f}_y$ = 47.7 $\bar{f}_c$ = 3.5 δ_{f_c} = 0.12
$\bar{f}_y$ = 64.0 $\bar{f}_c$ = 4.7 δ_{f_c} = 0.12
10^{-4}
10^{-5}
10^{-6}
10^{-7}
0.01
0.015
0.02
0.025
$\bar{p}$

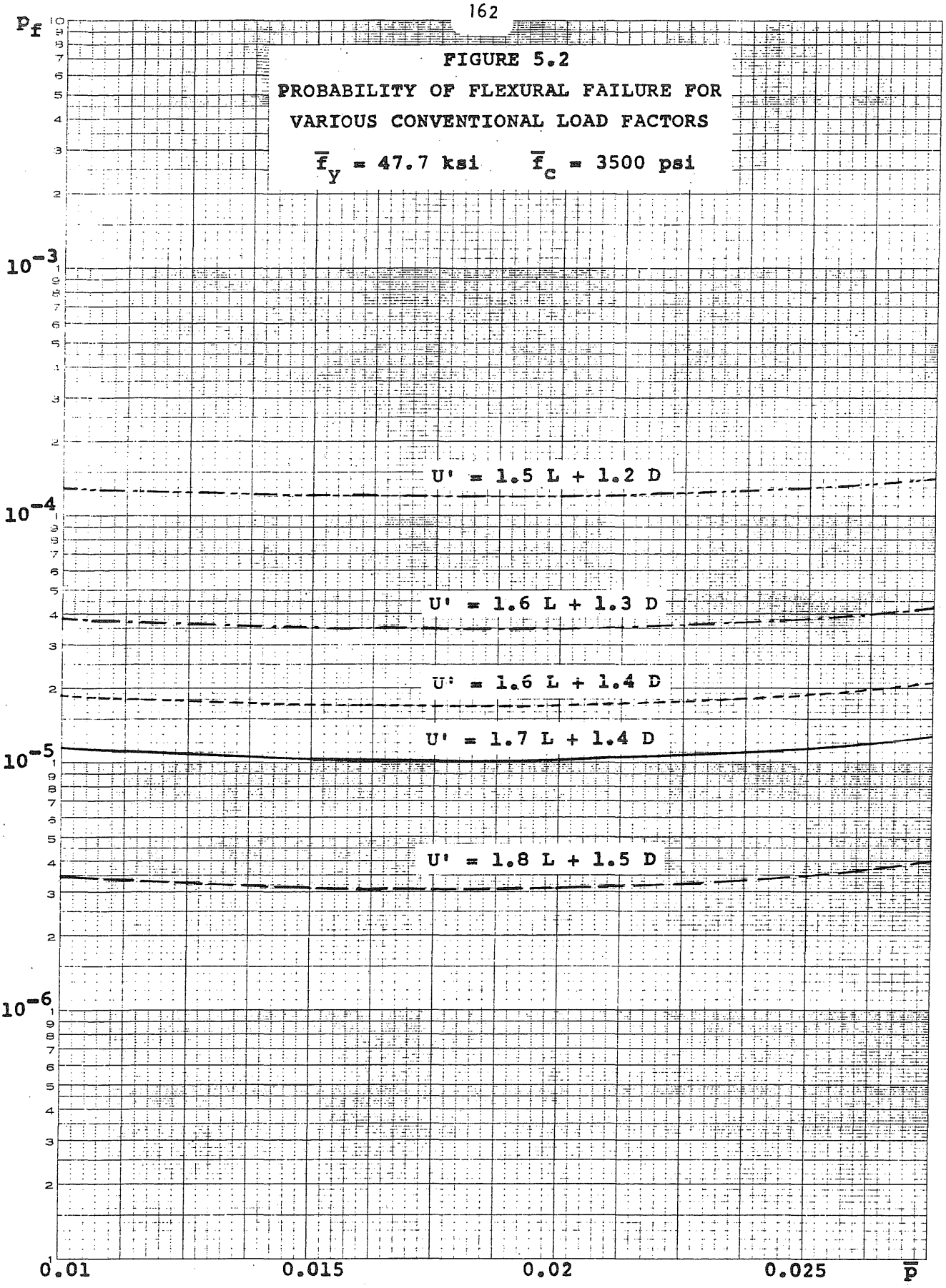

FIGURE 5.2

PROBABILITY OF FLEXURAL FAILURE FOR VARIOUS CONVENTIONAL LOAD FACTORS

$\bar{f}_y$ = 47.7 ksi $\bar{f}_c$ = 3500 psi

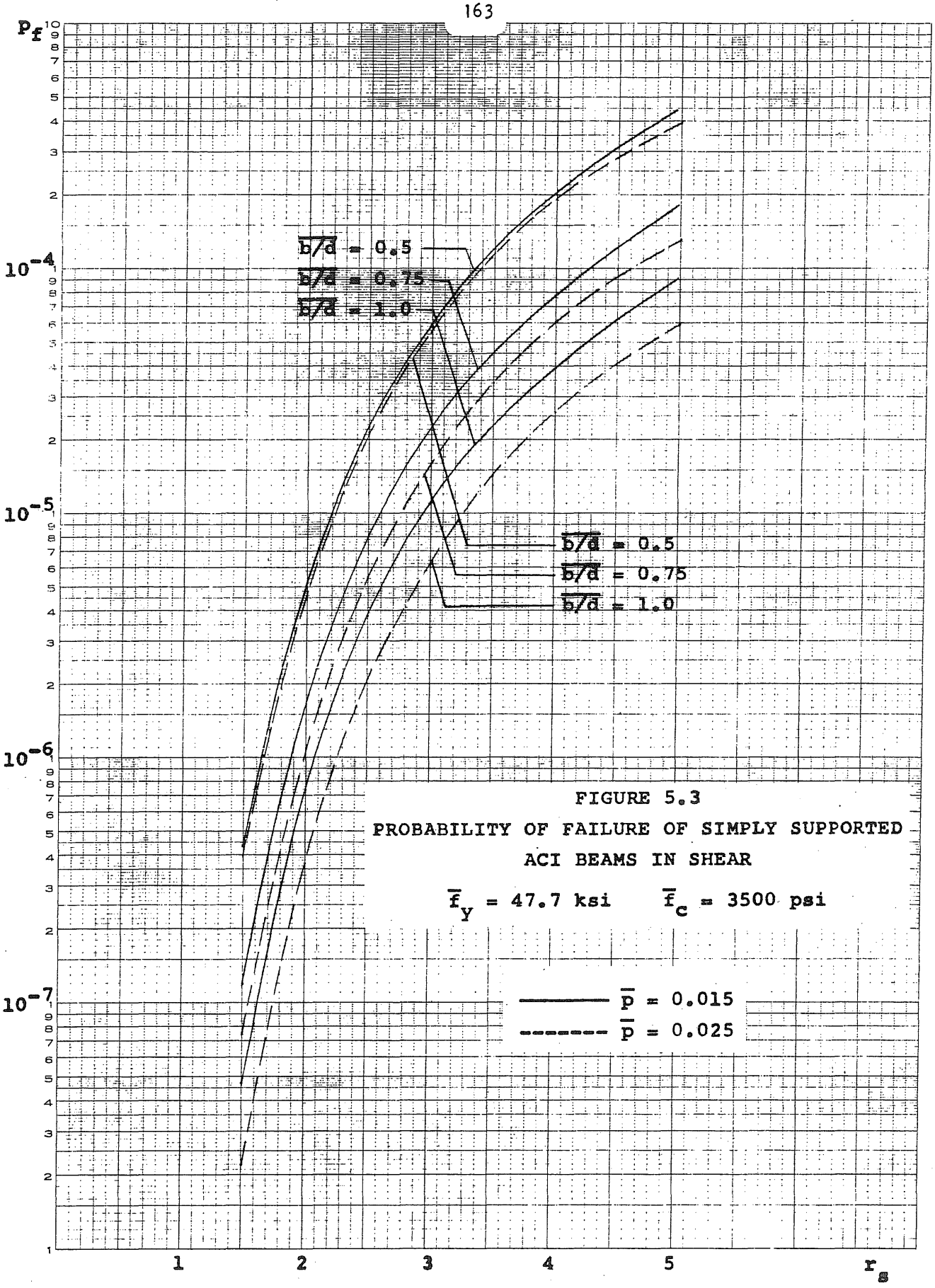

FIGURE 5.3

PROBABILITY OF FAILURE OF SIMPLY SUPPORTED ACI BEAMS IN SHEAR

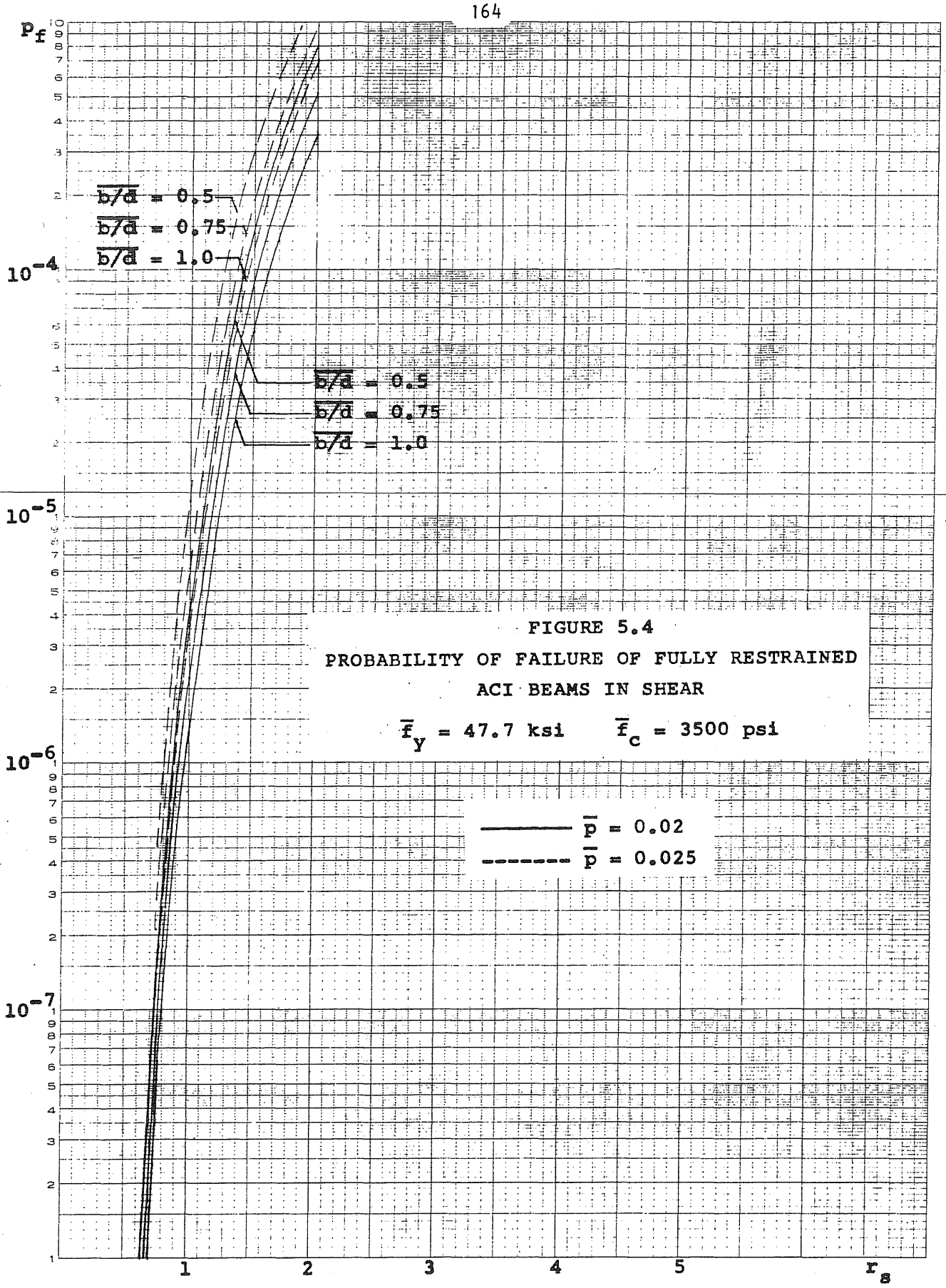

FIGURE 5.4

PROBABILITY OF FAILURE OF FULLY RESTRAINED ACI BEAMS IN SHEAR

$\overline{f}_y$ = 47.7 ksi $\overline{f}_c$ = 3500 psi

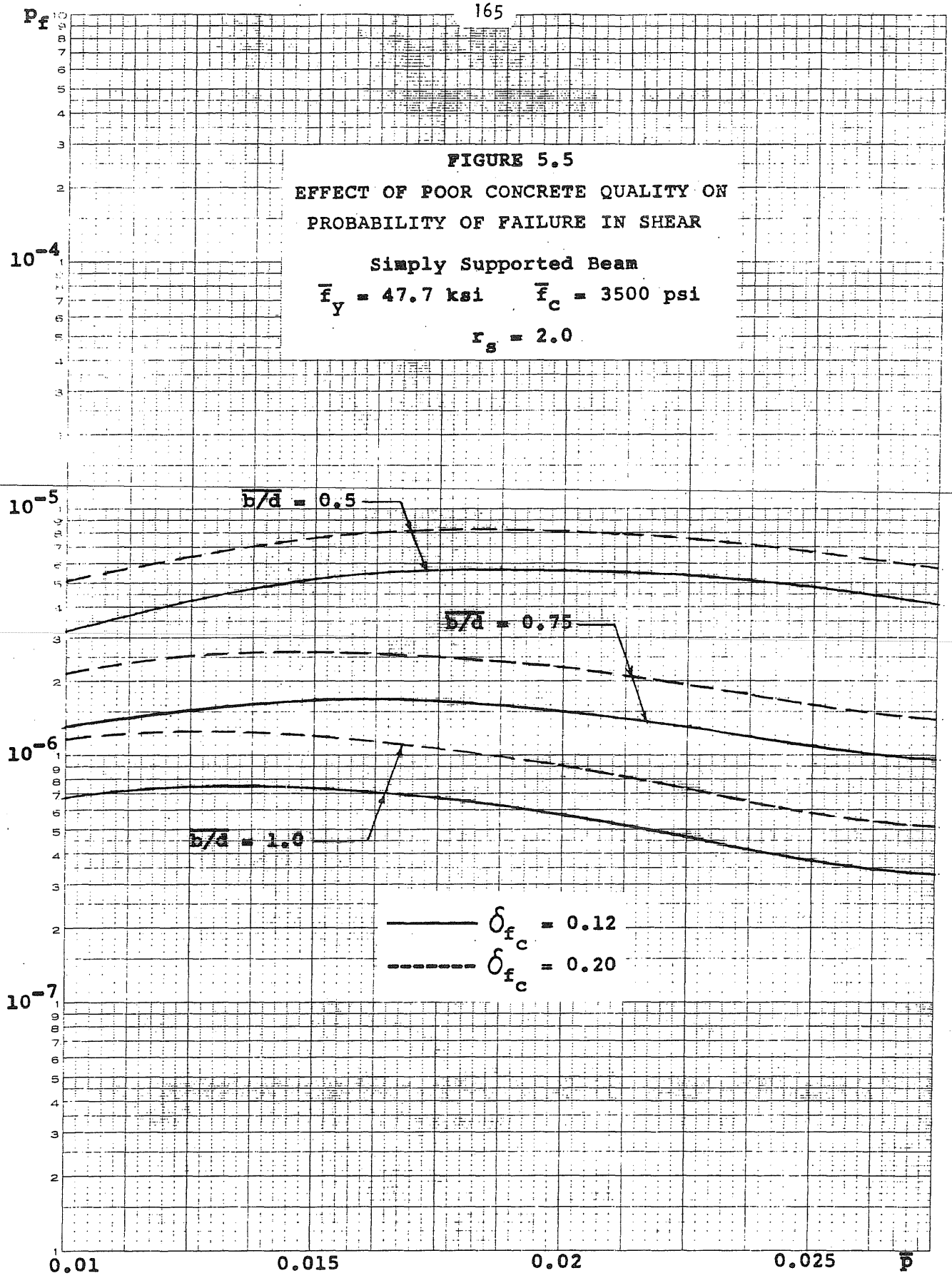

FIGURE 5.5

EFFECT OF POOR CONCRETE QUALITY ON PROBABILITY OF FAILURE IN SHEAR

Simply Supported Beam

$\overline{f}_y$ = 47.7 ksi $\overline{f}_c$ = 3500 psi

r_s = 2.0

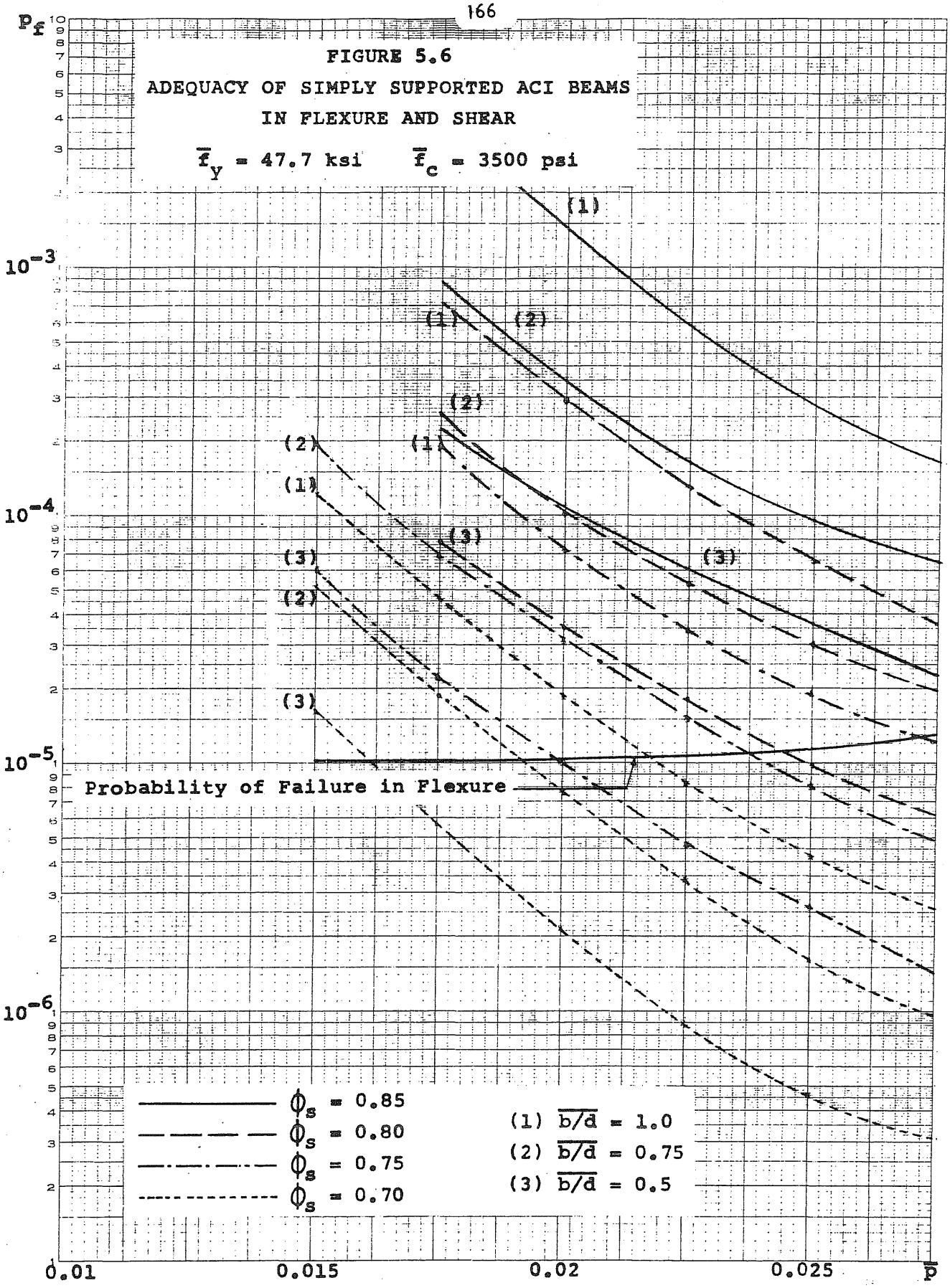

FIGURE 5.6

ADEQUACY OF SIMPLY SUPPORTED ACI BEAMS IN FLEXURE AND SHEAR

$\overline{f}_y$ = 47.7 ksi $\overline{f}_c$ = 3500 psi

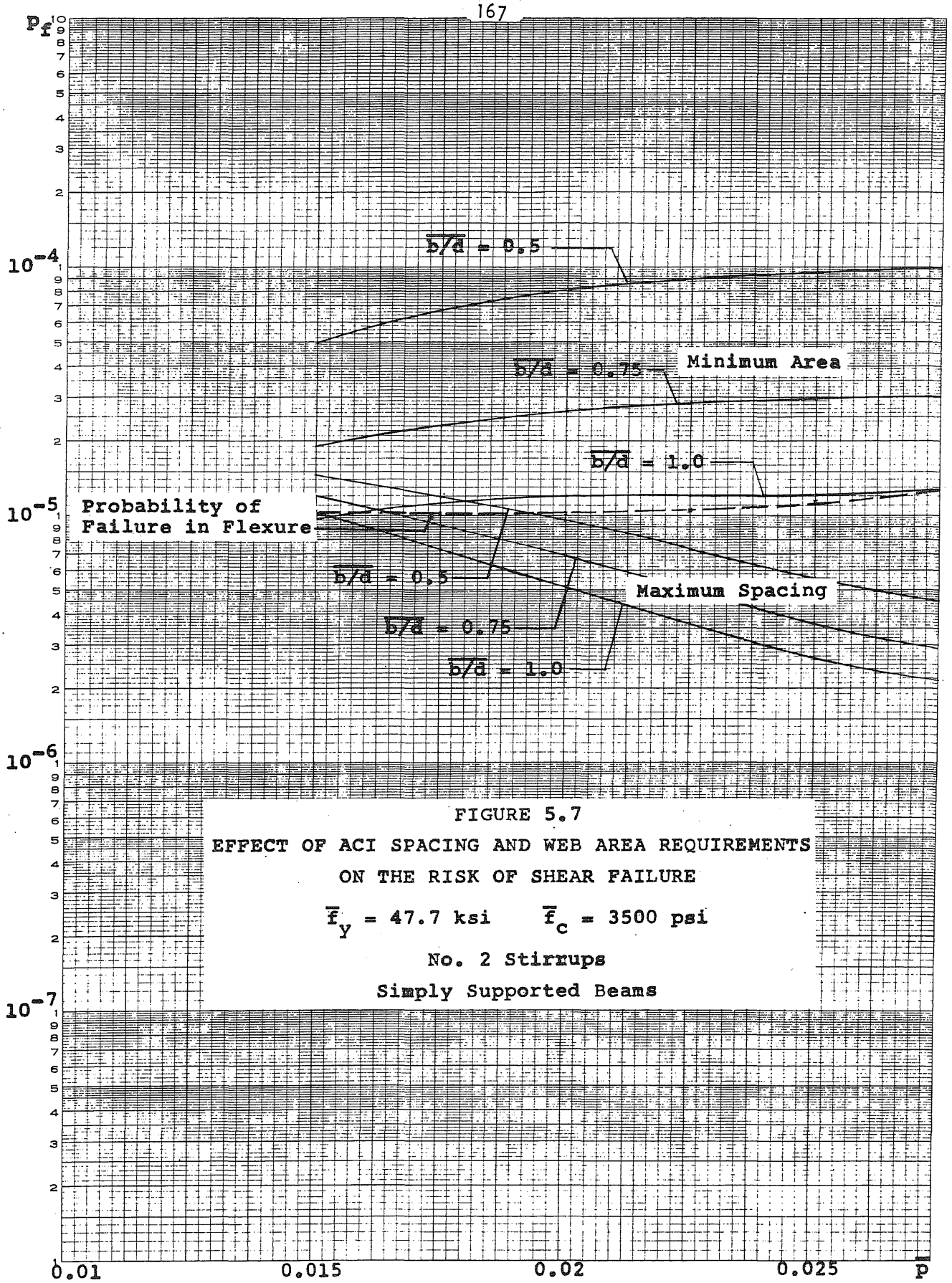

FIGURE 5.7

EFFECT OF ACI SPACING AND WEB AREA REQUIREMENTS ON THE RISK OF SHEAR FAILURE

$\overline{f}_y$ = 47.7 ksi $\overline{f}_c$ = 3500 psi

No. 2 Stirrups

Simply Supported Beams

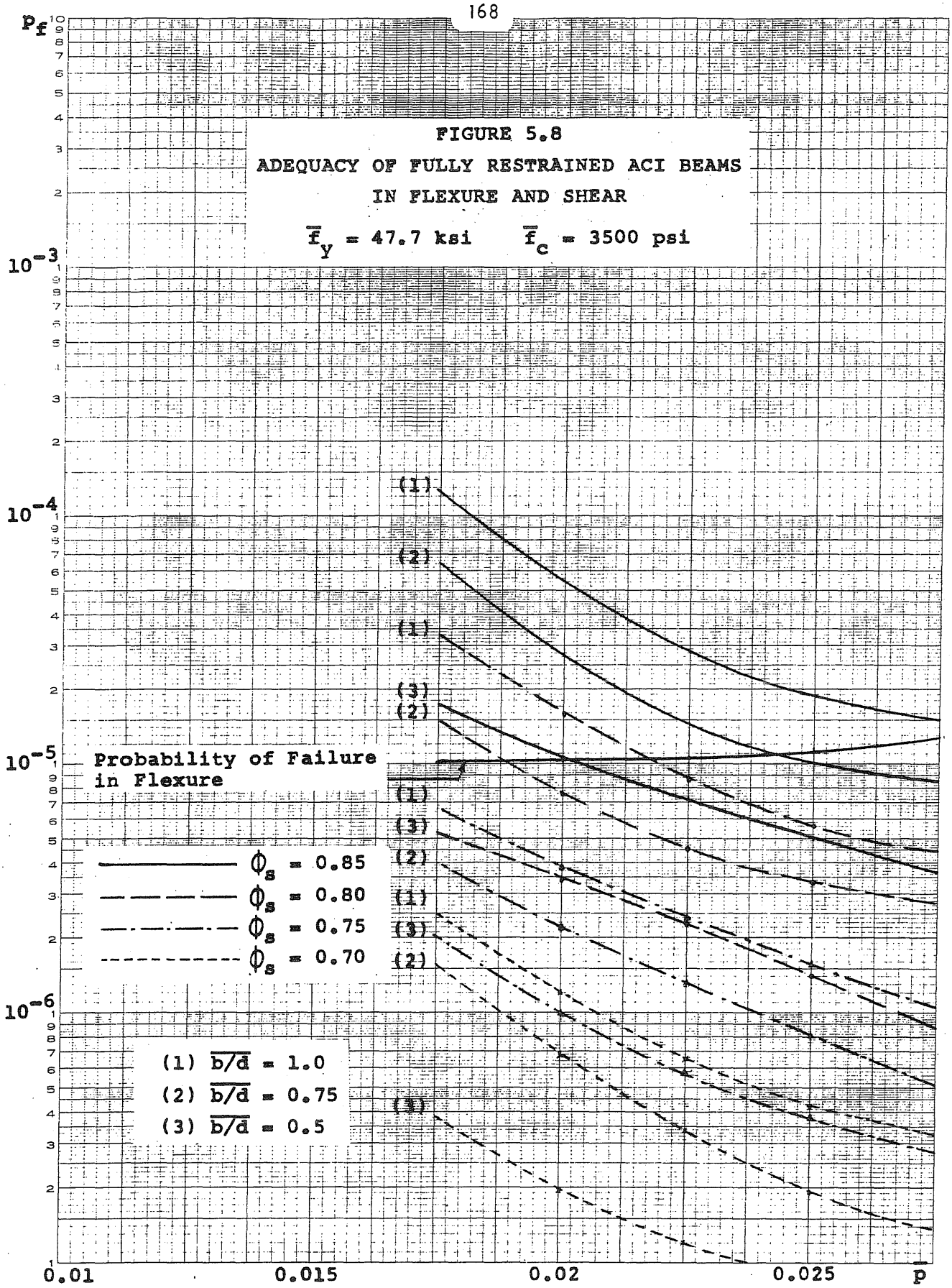

FIGURE 5.8

ADEQUACY OF FULLY RESTRAINED ACI BEAMS IN FLEXURE AND SHEAR

$\overline{f}_y$ = 47.7 ksi $\overline{f}_c$ = 3500 psi

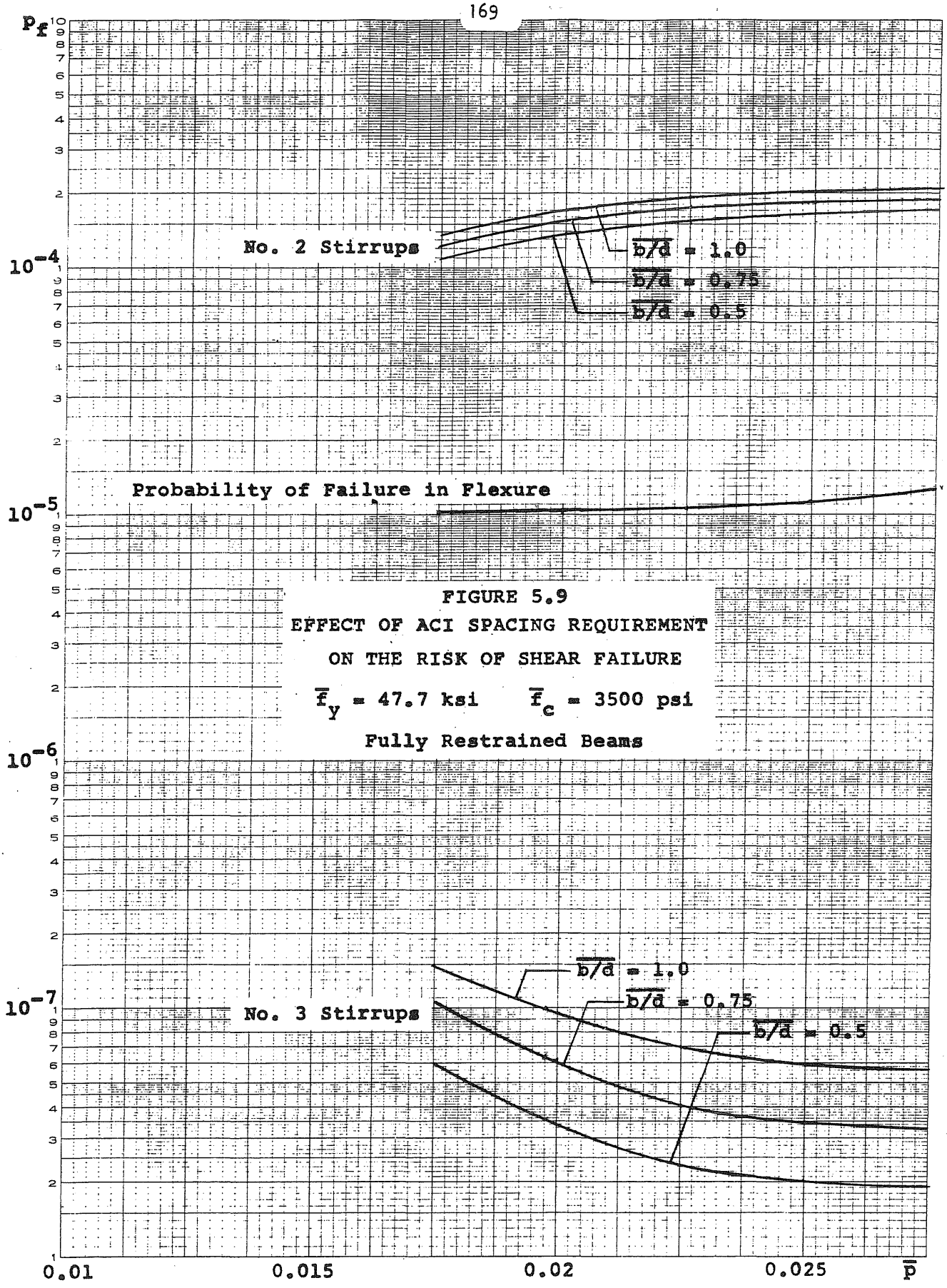

FIGURE 5.9

EFFECT OF ACI SPACING REQUIREMENT ON THE RISK OF SHEAR FAILURE

$\overline{f}_y$ = 47.7 ksi $\overline{f}_c$ = 3500 psi

Fully Restrained Beams

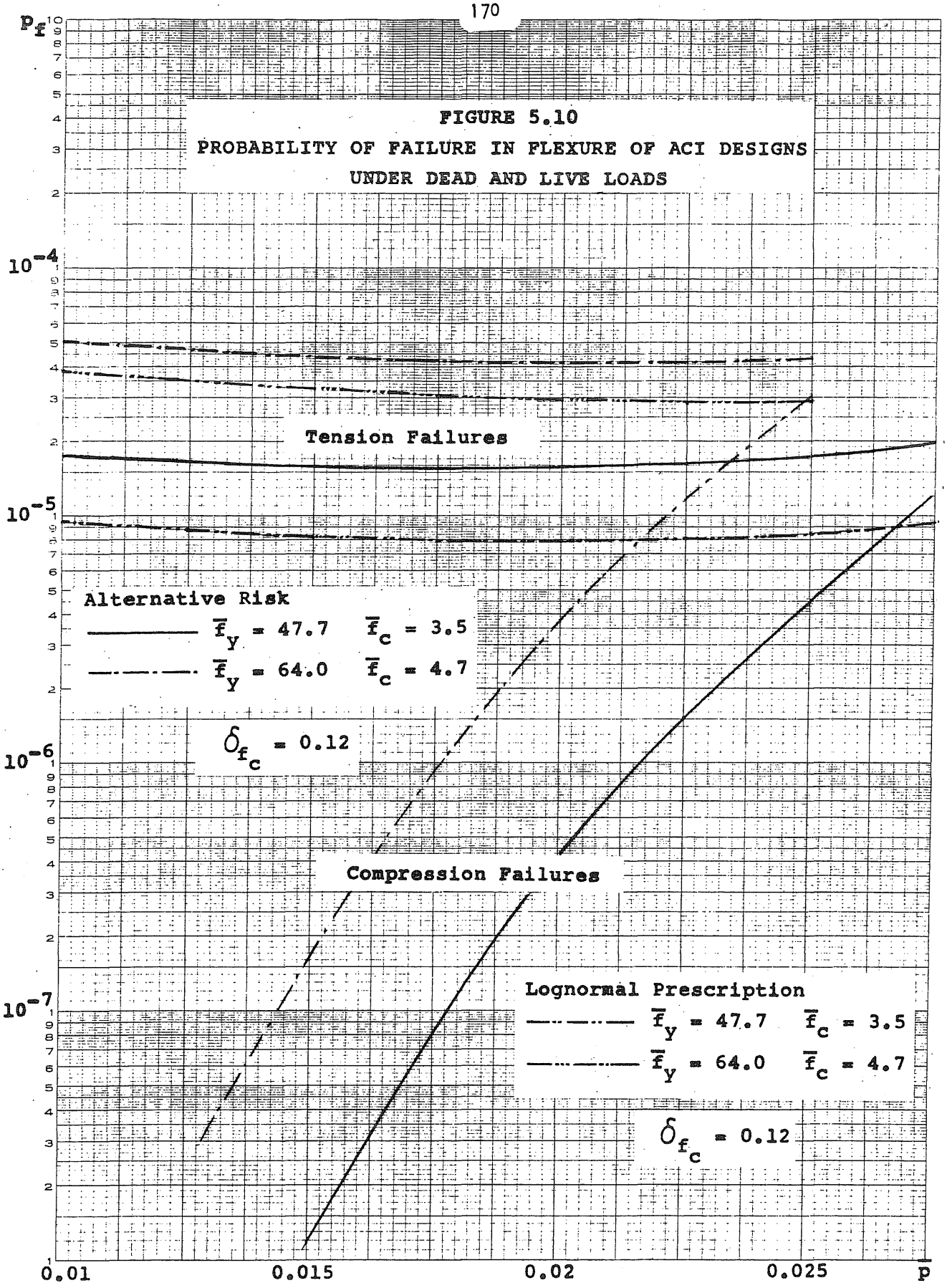

FIGURE 5.10

PROBABILITY OF FAILURE IN FLEXURE OF ACI DESIGNS UNDER DEAD AND LIVE LOADS

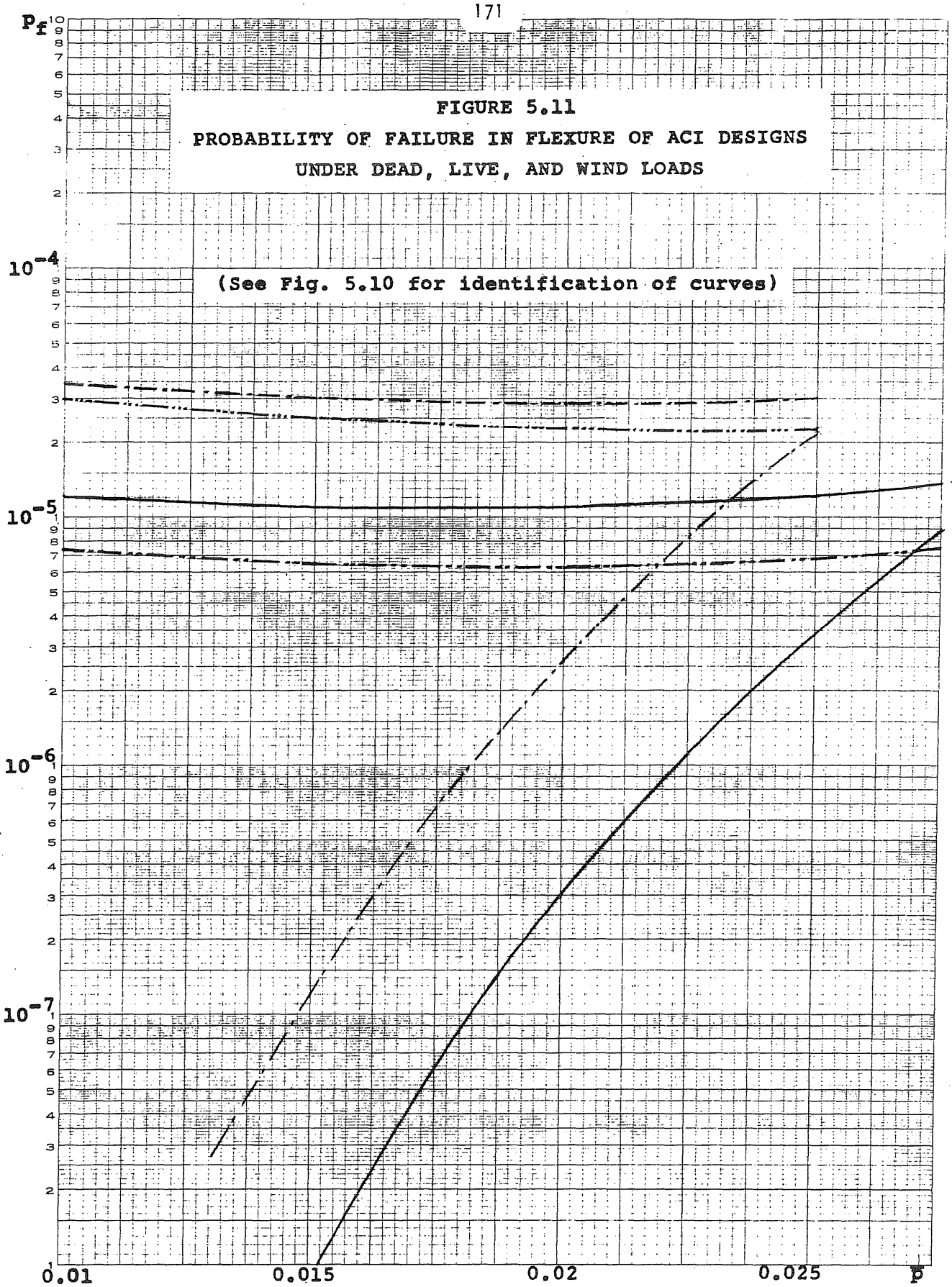

FIGURE 5.11

PROBABILITY OF FAILURE IN FLEXURE OF ACI DESIGNS UNDER DEAD, LIVE, AND WIND LOADS

(See Fig. 5.10 for identification of curves)

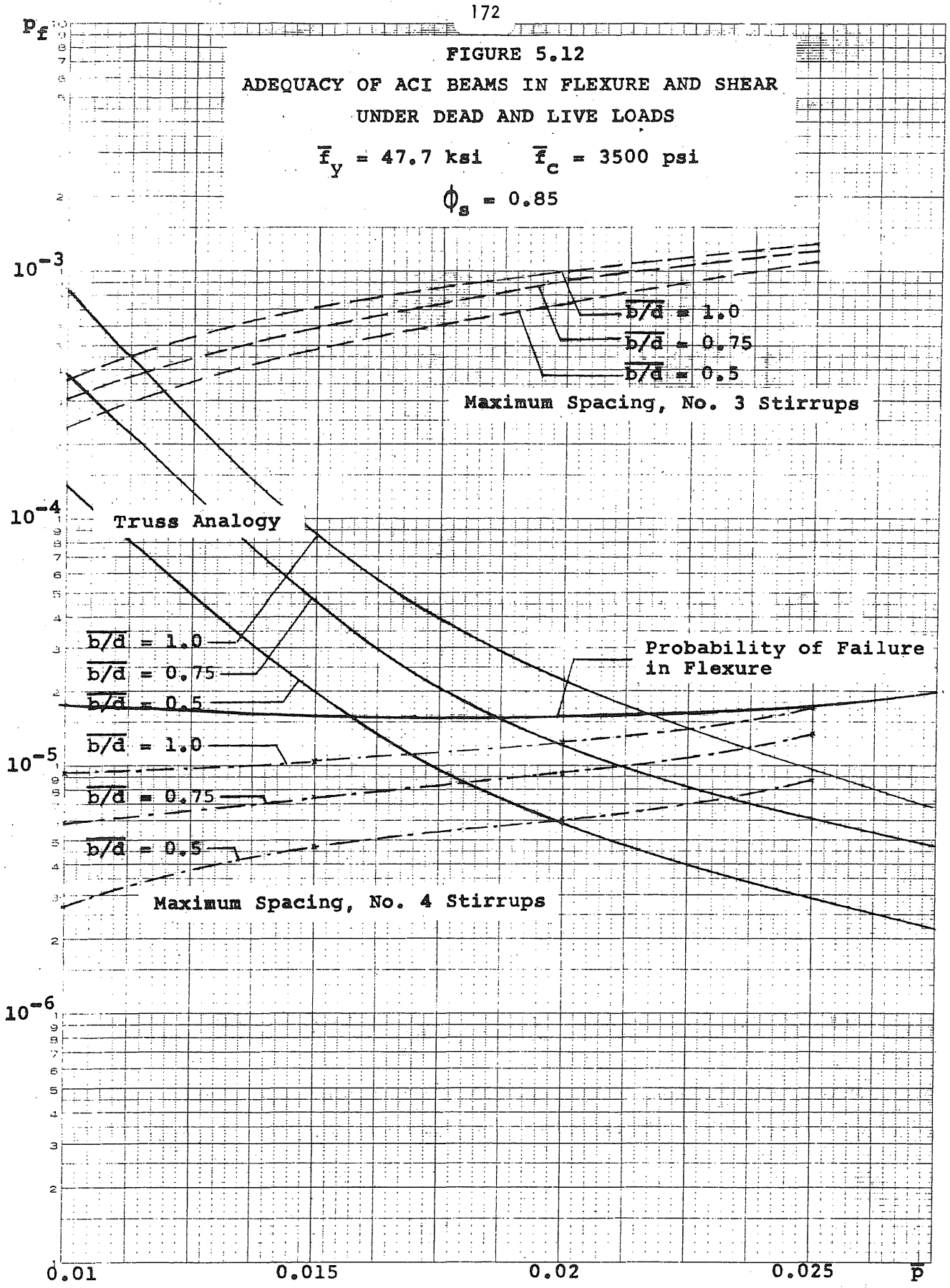

FIGURE 5.12

ADEQUACY OF ACI BEAMS IN FLEXURE AND SHEAR UNDER DEAD AND LIVE LOADS

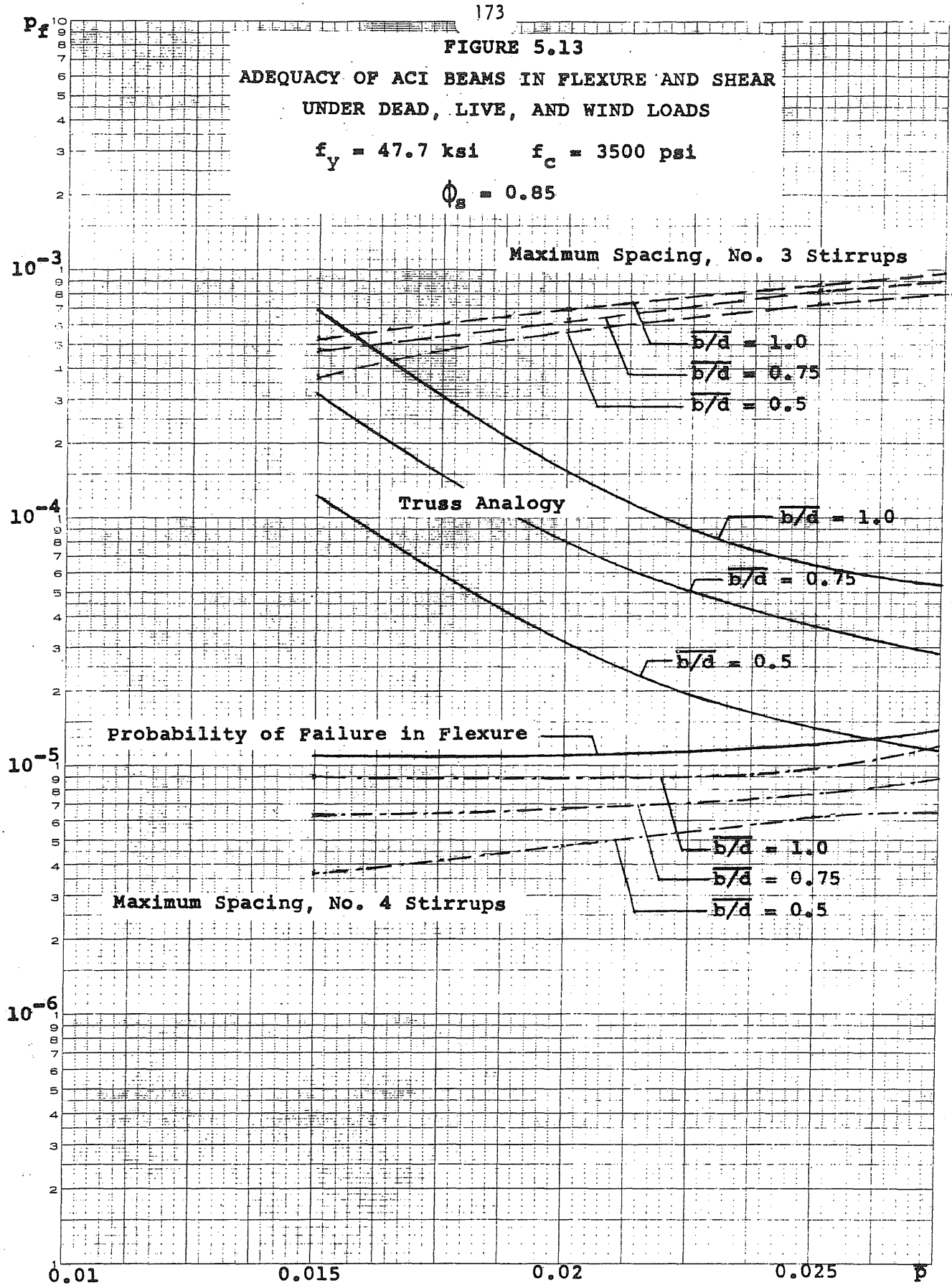
FIGURE 5.13
ADEQUACY OF ACI BEAMS IN FLEXURE AND SHEAR
UNDER DEAD, LIVE, AND WIND LOADS
f_y = 47.7 ksi f_c = 3500 psi
ϕ_s = 0.85
P_f
Maximum Spacing, No. 3 Stirrups
b/d = 1.0
b/d = 0.75
b/d = 0.5
Truss Analogy
b/d = 1.0
b/d = 0.75
b/d = 0.5
Probability of Failure in Flexure
b/d = 1.0
b/d = 0.75
b/d = 0.5
Maximum Spacing, No. 4 Stirrups
10^{-3}
10^{-4}
10^{-5}
10^{-6}
0.01
0.015
0.02
0.025
p

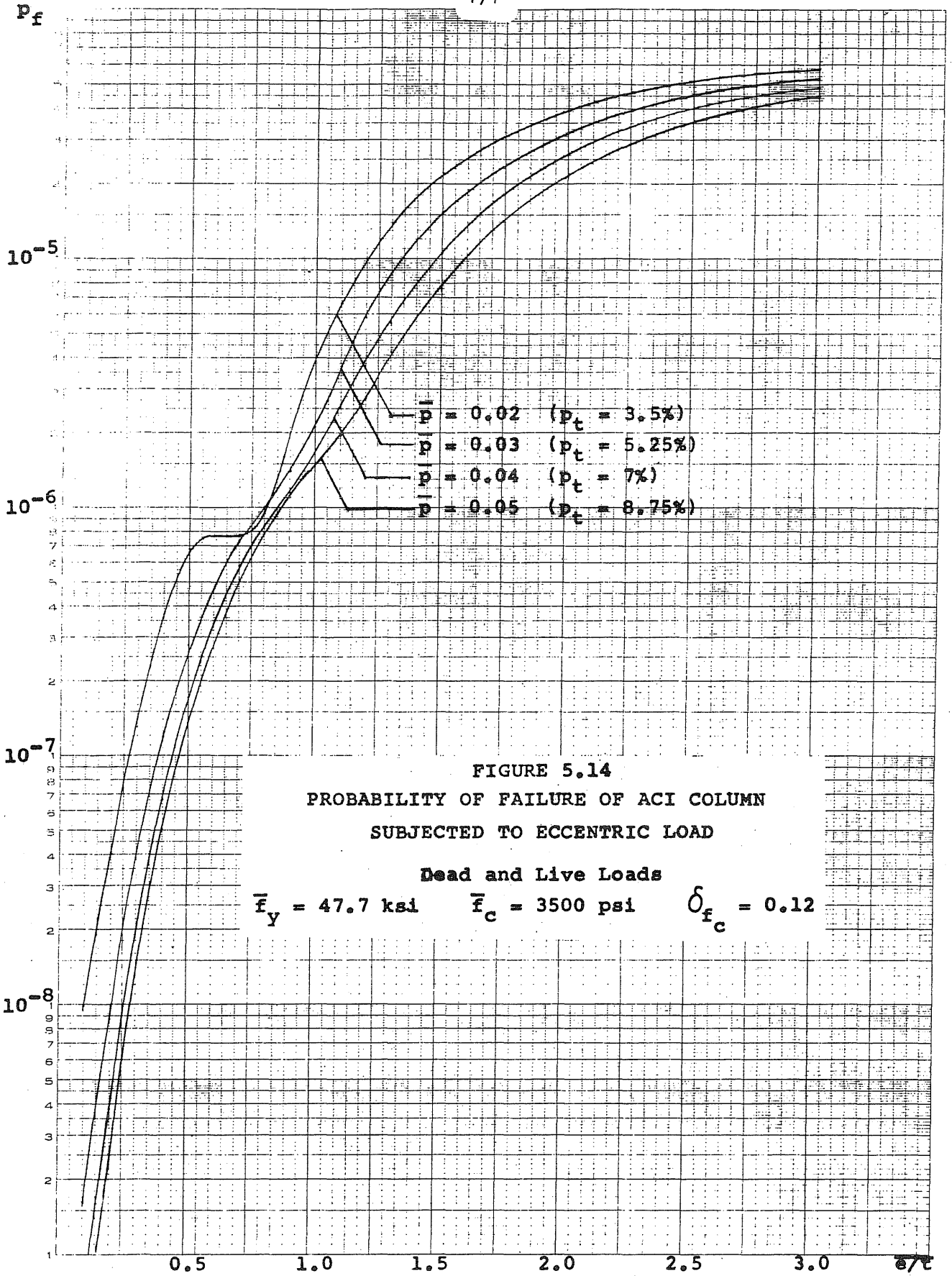

FIGURE 5.14
PROBABILITY OF FAILURE OF ACI COLUMN
SUBJECTED TO ECCENTRIC LOAD

Dead and Live Loads

$\bar{f}_y$ = 47.7 ksi $\bar{f}_c$ = 3500 psi δ_{f_c} = 0.12

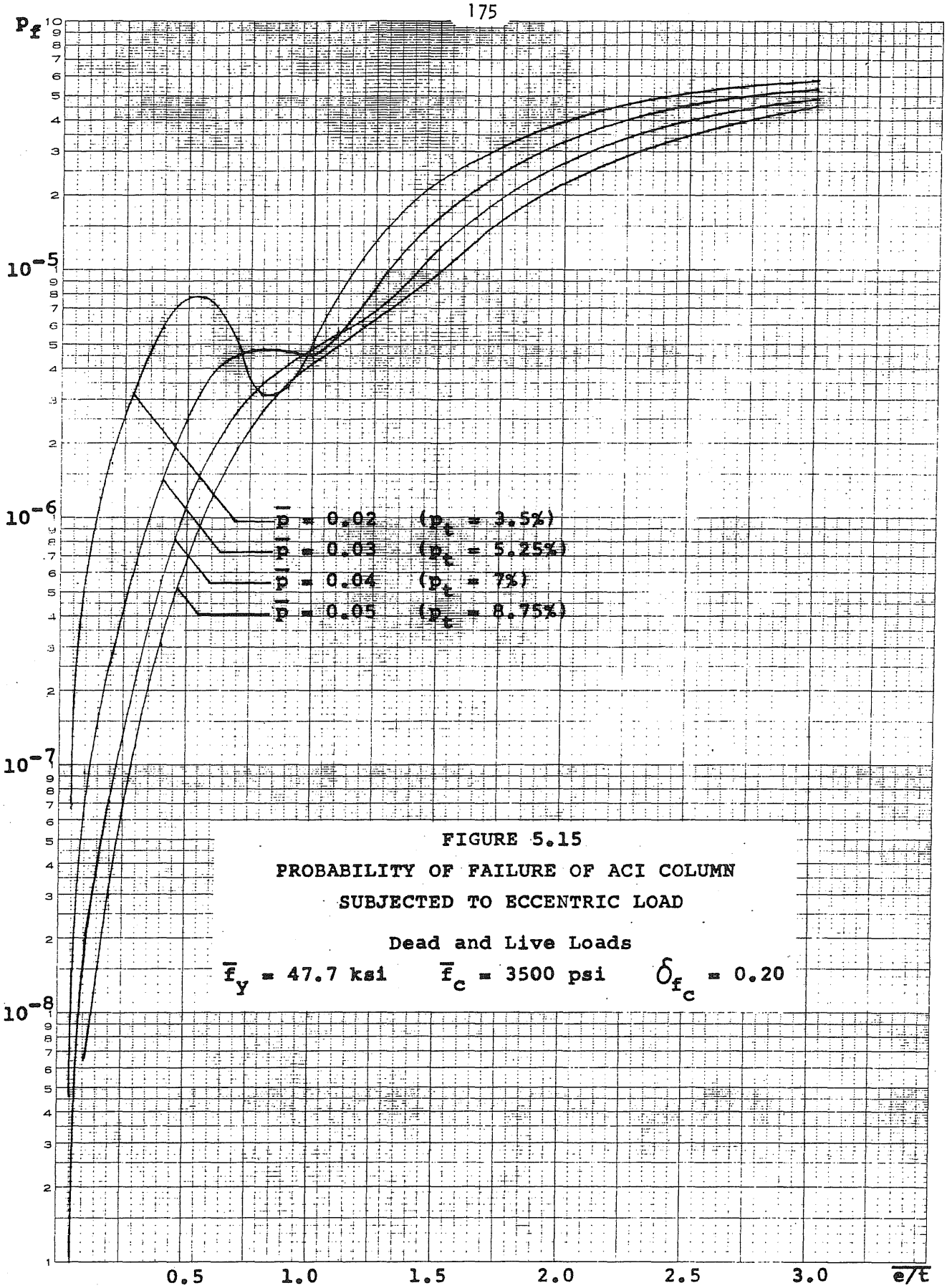

FIGURE 5.15

PROBABILITY OF FAILURE OF ACI COLUMN SUBJECTED TO ECCENTRIC LOAD

Dead and Live Loads

$\bar{f}_y$ = 47.7 ksi $\bar{f}_c$ = 3500 psi δ_{f_c} = 0.20

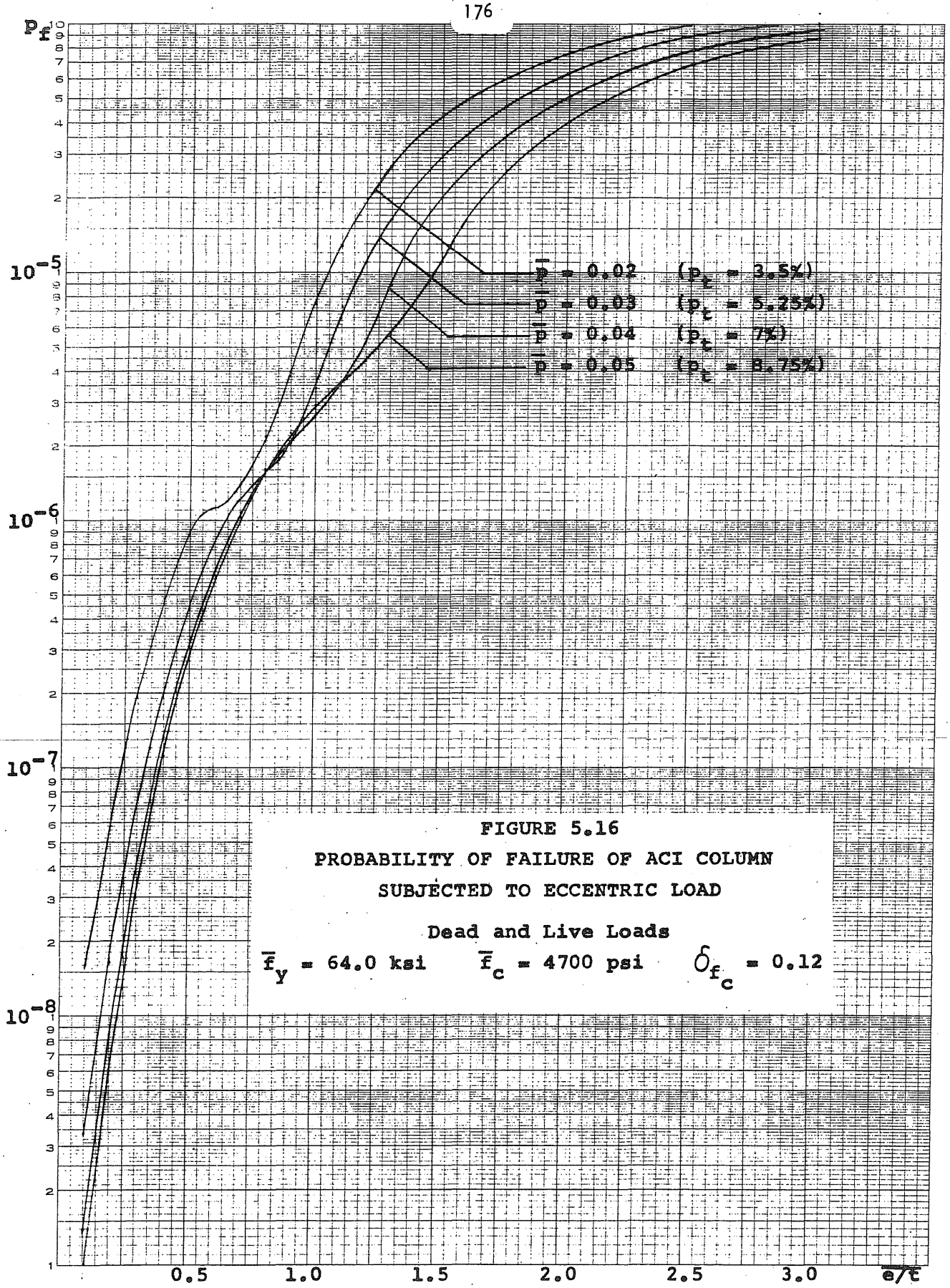

FIGURE 5.16

PROBABILITY OF FAILURE OF ACI COLUMN SUBJECTED TO ECCENTRIC LOAD

Dead and Live Loads

$\bar{f}_y$ = 64.0 ksi $\quad \bar{f}_c$ = 4700 psi $\quad \delta_{f_c}$ = 0.12

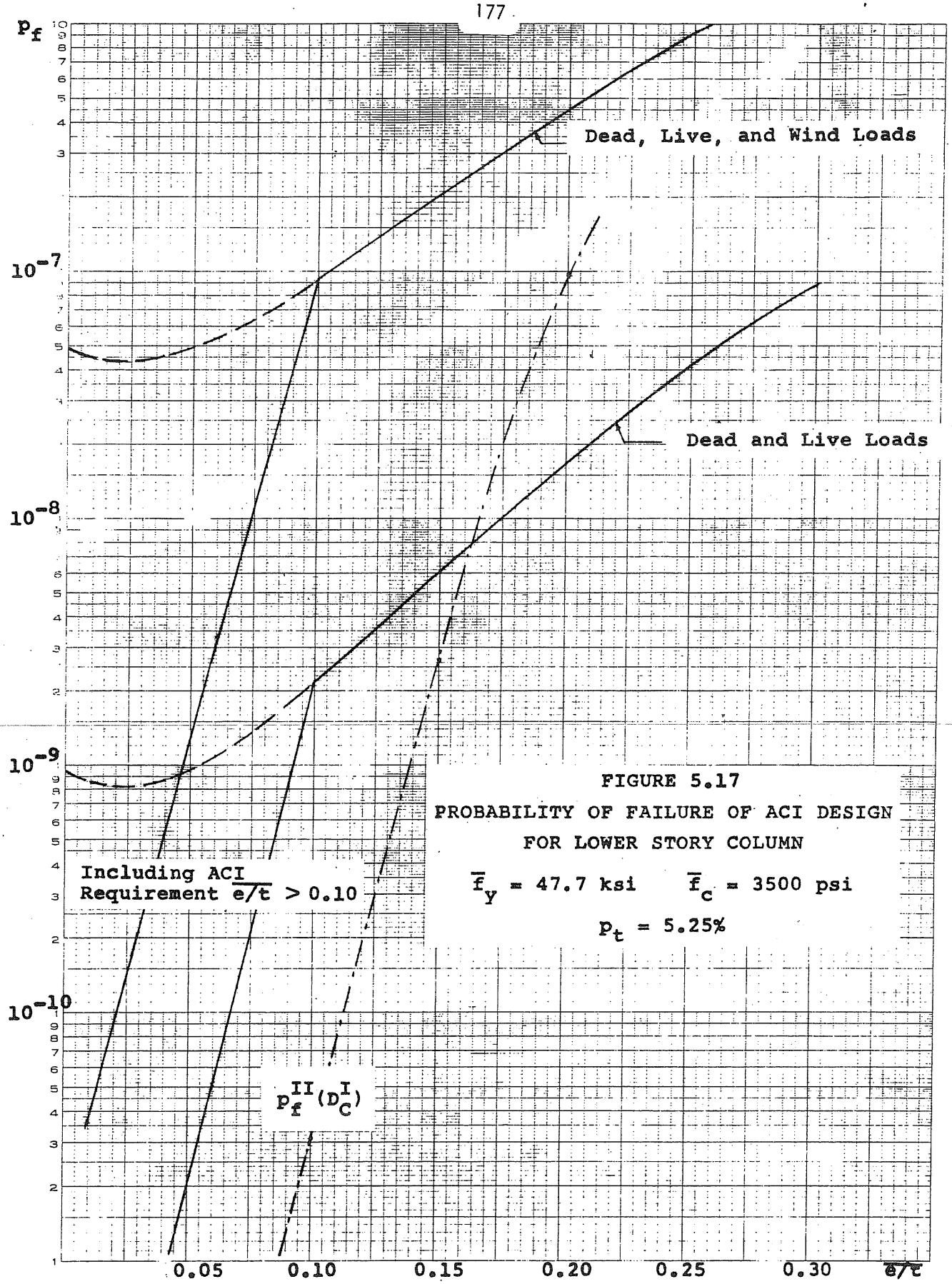

FIGURE 5.17

PROBABILITY OF FAILURE OF ACI DESIGN FOR LOWER STORY COLUMN

$\overline{f}_y$ = 47.7 ksi $\overline{f}_c$ = 3500 psi

p_t = 5.25%

FIGURE 5.18
EFFECT OF ACI MINIMUM ECCENTRICITY RATIO ON RISK OF FAILURE

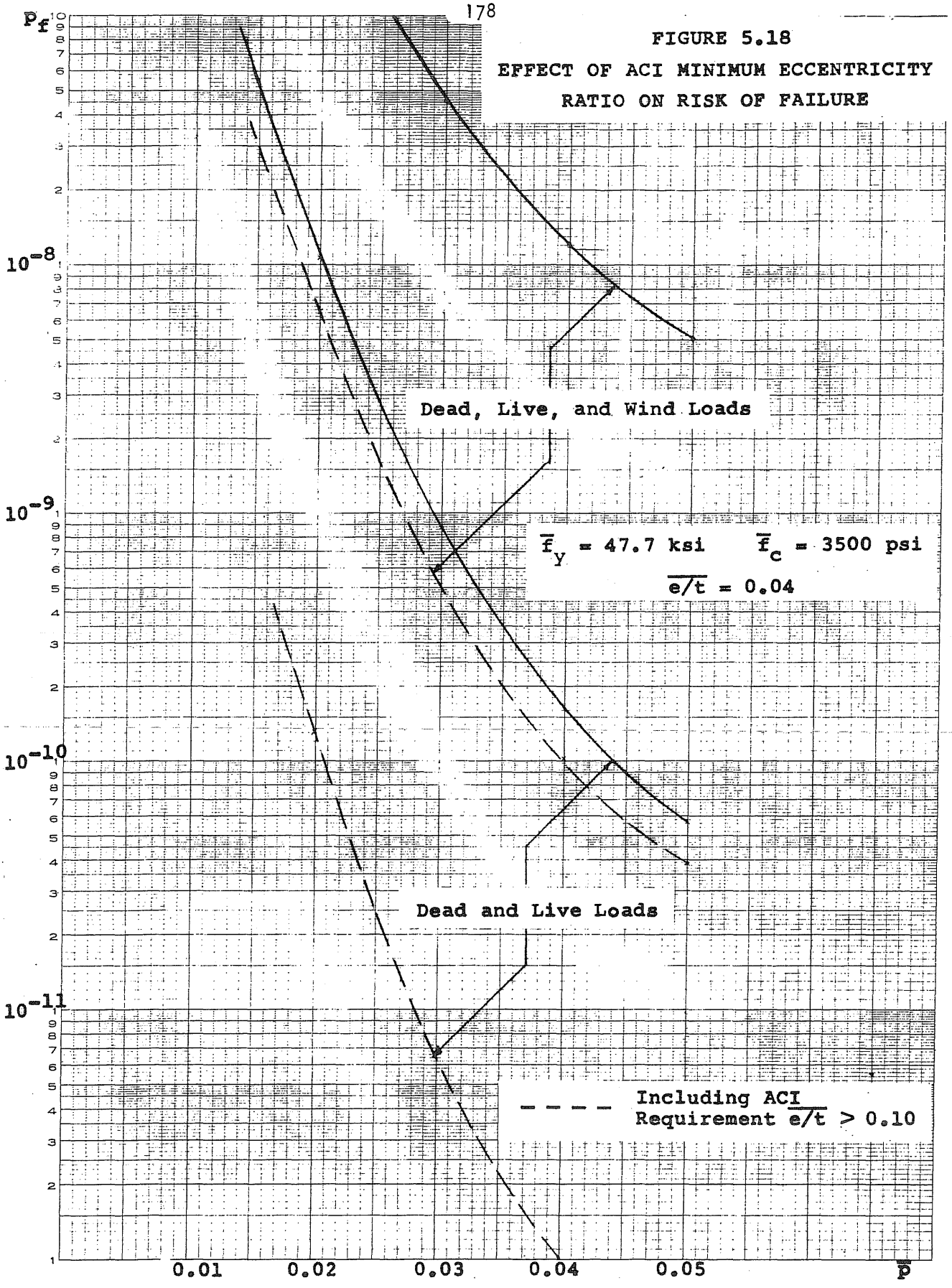

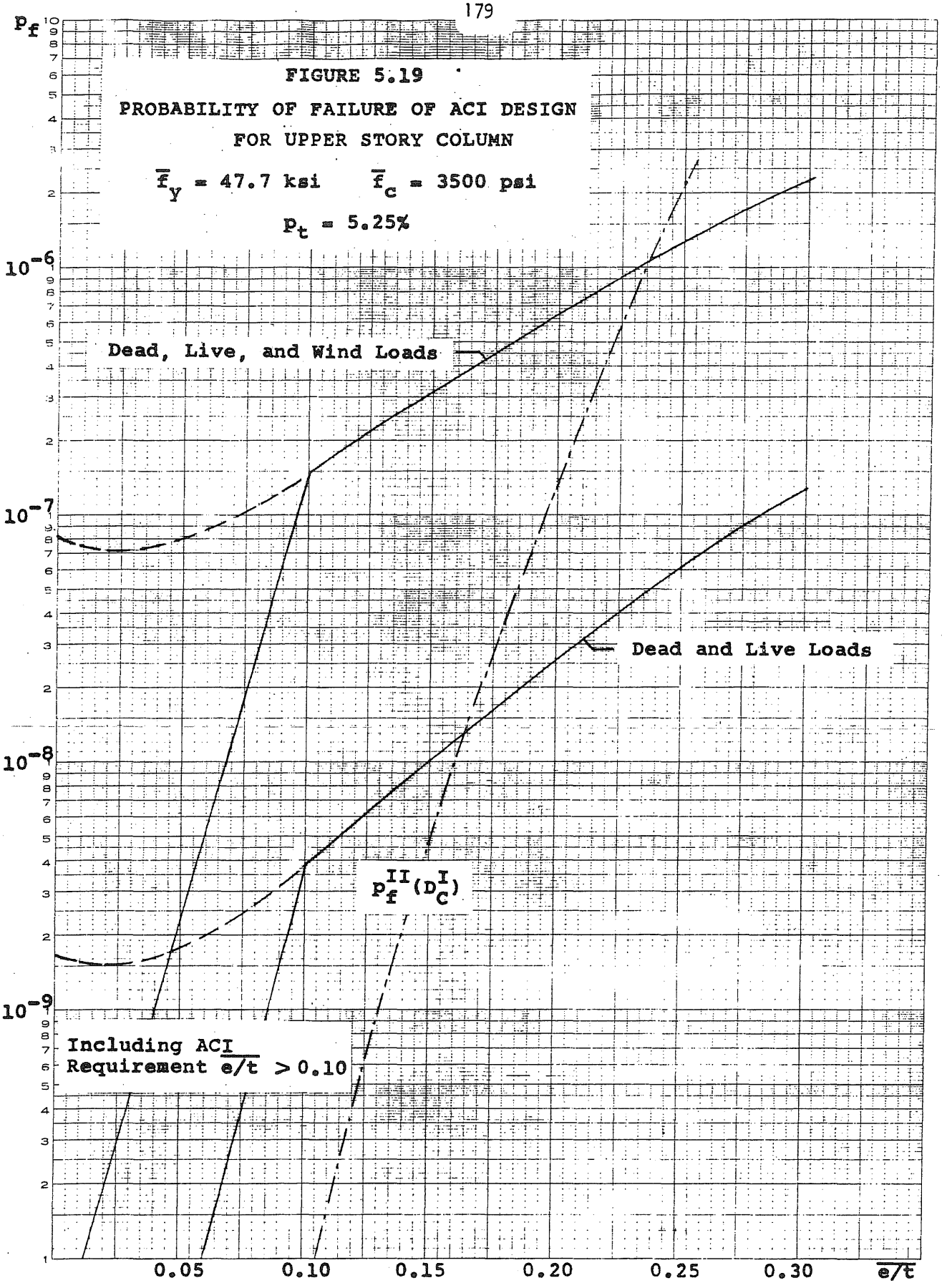

FIGURE 5.19

PROBABILITY OF FAILURE OF ACI DESIGN FOR UPPER STORY COLUMN

$\overline{f}_y$ = 47.7 ksi $\overline{f}_c$ = 3500 psi

p_t = 5.25%

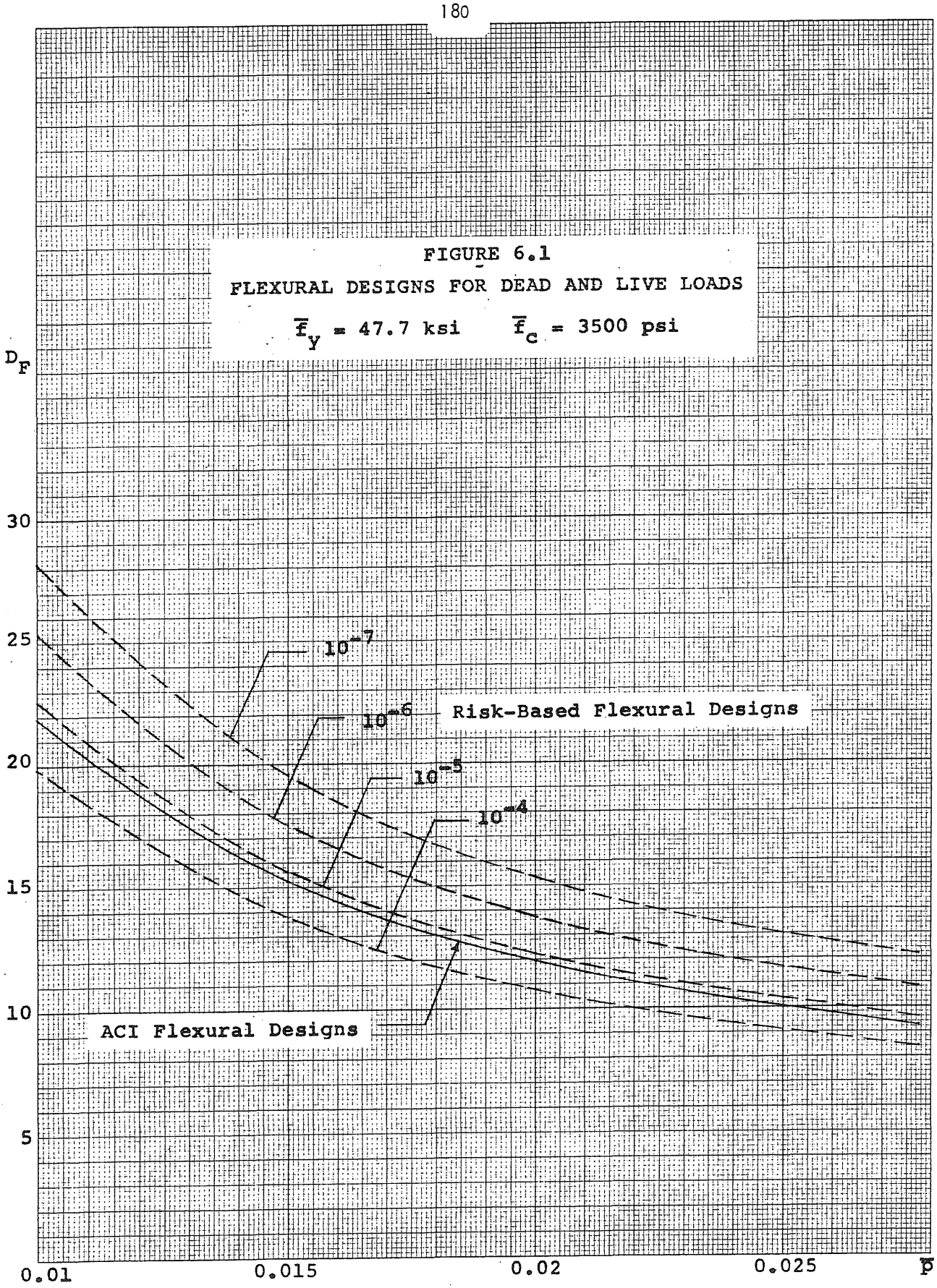

FIGURE 6.1

FLEXURAL DESIGNS FOR DEAD AND LIVE LOADS

$\bar{f}_y$ = 47.7 ksi $\bar{f}_c$ = 3500 psi

APPENDIX A

RISK CALCULATION FOR NONNORMAL VARIATES

In cases where more than two nonnormal variables are involved, $Pr(R < \nu(S_1 + S_2))$ cannot be evaluated in closed form. This probability may be computed to an arbitrary degree of accuracy from

$$p_o = \lim_{N\to\infty} \sum_{k=1}^{N} Pr(R < \nu(S_1 + x_k) \mid S_2 = x_k) \cdot Pr(S_2 = x_k)$$

By assuming all variates are mutually statistically independent,

$$p_o = \lim_{N\to\infty} \sum_{k=1}^{N} Pr(R < \nu(S_1 + x_k)) \cdot Pr(S_2 = x_k) \qquad (A.1)$$

$Pr(S_2 = x_k)$ may be found from discretizing S_2 at N arbitrary points. Then

$$Pr(S_2 = x_k) \simeq F_{S_2}(x_k + \frac{\Delta x}{2}) - F_{S_2}(x_k - \frac{\Delta x}{2}) \simeq \Delta F_{S_2}(x_k) \qquad (A.2)$$

When S_2 is discretized between exceedance values of 10^{-8}, with 40-50 discretization points, the error in Eq. A.1 is very small. For nonnormal R and S_1, $Pr(R < \nu(S_1 + x_k))$ must be computed by numerical integration.

In what follows, $\theta = \overline{S_2/S_1}$, and $w = \gamma_1 + \gamma_2\theta$.

If R, S_1, and S_2 are lognormal, then

$$p_o \simeq \sum_{k=1}^{N} \left\{ \int_{-\infty}^{\infty} \eta(u \mid x_k) e^{-u^2} du \right\} \Delta\Phi \left[\frac{\ln(x_k \sqrt{1 + \delta_{S_2}^2})}{\sqrt{\ln(1 + \delta_{S_2}^2)}} \right] \qquad (A.3)$$

Δ here implies an increment in cumulative probability Φ. x_k is discretized for $\pm$ 7 standard deviations of S_2, and

$$\eta(\mu|x_k) = \frac{1}{\sqrt{\pi}} \Phi \left[\frac{\ln\left[\frac{\nu}{\sqrt{1+\delta_{S_1}^2}} \exp\left(\sqrt{2\ln(1+\delta_{S_1}^2)}\, u\right) + \nu\theta x_k \right]}{\sqrt{\ln(1+\delta_R^2)}} - \frac{\ln\left[\frac{w}{\sqrt{1+\delta_R^2}}\right]}{\sqrt{\ln(1+\delta_R^2)}} \right] \tag{A.4}$$

The integral in brackets is the standard Gauss-Hermite form.

If R is Extremal III (Weibull) and S_1 and S_2 are Extremal I (Gumbel),

$$p_o \simeq \sum_{k=1}^{N} p(x_k)\, p_{S_2}(x_k) \tag{A.5}$$

where

$$p(x_k) = \int_o^\infty \left\{ 1 - \exp\left[- \exp\left\{ - \frac{\pi}{\sqrt{6}\,\delta_{S_1}} \left[\frac{w}{\Gamma(1+\frac{1}{K_R})}\, y^{\frac{1}{K_R}} - \nu\theta x_k - \nu(1 - .45\,\delta_{S_1}) \right] \right\} \right] \right\} e^{-y}\, dy \tag{A.6}$$

the standard Gauss-Laguerre integration form. K_R is a measure of the statistical dispersion in R. The discretized probability measure for S_2 is

$$p_{S_2}(x_k) \simeq \Delta \exp\left[- \exp\left\{ - \frac{\pi}{\sqrt{6}\,\delta_{S_2}} (x_k - 1 + 0.45\,\delta_{S_2}) \right\} \right] \quad (A.7)$$

If R is Extremal III and S_1 and S_2 are Extremal II (Frechet)

$$p_o \simeq \sum_{K=1}^{N} p(x_k)\, p_{S_2}(x_k) \quad (A.5)$$

where

$$p(x_k) = \int_o^\infty \left\{ 1 - \exp\left[- \left\{ \frac{\Gamma(1 + \frac{1}{K_R})}{\Gamma(1 - \frac{1}{K_{S_1}})} \left[\frac{\nu y^{-\frac{1}{K_{S_1}}}}{w} + \frac{\nu\theta x_k \Gamma(1 - \frac{1}{K_{S_1}})}{w} \right] \right\}^{K_R} \right] \right\} e^{-y}\, dy \quad (A.8)$$

and K_{S_1} is a measure of dispersion in S_1, and

$$p_{S_2}(x_k) = \Delta \exp\left[- \left(\frac{1}{\Gamma(1 - \frac{1}{K_{S_2}})\, x_k} \right)^{K_{S_2}} \right] \quad (A.9)$$

APPENDIX B

STATISTICS OF BALANCED ECCENTRICITY RATIO e_b/t

The statistics of the balanced point eccentricity ratio must be known to compute the probability of tension or compression failures for combined bending and axial thrust. The mean is

$$\overline{e_b/t} = \frac{1}{2} - k_2 \frac{E_s \bar{\varepsilon}_{cu}}{E_s \bar{\varepsilon}_{cu} + \bar{f}_y} \left(\frac{\bar{d}}{\bar{t}}\right) + 2\bar{p} \frac{\bar{f}_y}{\overline{k_1 k_3}\ \bar{f}_c} \left(\frac{\bar{d}}{\bar{t}} - \frac{1}{2}\right) \frac{E_s \bar{\varepsilon}_{cu} + \bar{f}_y}{E_s \bar{\varepsilon}_{cu}} \quad (B.1)$$

and the c.o.v. is

$$\delta^2_{\frac{e_b}{t}} = c_1^2\, \delta^2_{f_y} + c_2^2(\delta^2_{f_c} + \delta^2_{A_s} + \delta^2_b + \delta^2_{k_1 k_3}) + c_3^2\, \delta^2_d + c_4^2\, \delta^2_t + c_5^2\, \delta^2_{\varepsilon_{cu}} \quad (B.2)$$

where $|c_j|$ are defined as

$$c_1 = \frac{1}{\overline{e_b/t}} \left\{ k_2 \frac{E_s \bar{\varepsilon}_{cu}\, \bar{f}_y}{(E_s \bar{\varepsilon}_{cu} + \bar{f}_y)^2} \frac{\bar{d}}{\bar{t}} + \frac{2\bar{p}\, \bar{f}_y}{\overline{k_1 k_3}\ \bar{f}_c} \left(\frac{\bar{d}}{\bar{t}} - \frac{1}{2}\right) \frac{E_s \bar{\varepsilon}_{cu} + 2\bar{f}_y}{E_s \bar{\varepsilon}_{cu}} \right\}$$

$$c_2 = \frac{1}{\overline{e_b/t}} \left\{ \frac{E_s \bar{\varepsilon}_{cu} + \bar{f}_y}{E_s \bar{\varepsilon}_{cu}} \left(\frac{\bar{d}}{\bar{t}} - \frac{1}{2}\right) \frac{2\bar{p}\, \bar{f}_y}{\overline{k_1 k_3}\ \bar{f}_c} \right\}$$

$$c_3 = \frac{1}{\overline{e_b/t}} \left\{ \bar{p} \frac{\bar{f}_y}{\overline{k_1 k_3}\ \bar{f}_c} \frac{(E_s \bar{\varepsilon}_{cu} + \bar{f}_y)}{E_s \bar{\varepsilon}_{cu}} - k_2 \frac{E_s \bar{\varepsilon}_{cu}}{(E_s \bar{\varepsilon}_{cu} + \bar{f}_y)} \frac{\bar{d}}{\bar{t}} \right\}$$

$$c_4 = \frac{1}{\overline{e_b/t}} \left\{ k_2 \frac{E_s \overline{\varepsilon}_{cu}}{E_s \overline{\varepsilon}_{cu} + \overline{f}_y} - 2\overline{p} \frac{\overline{f}_y}{\overline{k_1 k_3}\ \overline{f}_c} \frac{E_s \overline{\varepsilon}_{cu} + \overline{f}_y}{E_s \overline{\varepsilon}_{cu}} \right\} \frac{\overline{d}}{\overline{t}}$$

$$c_5 = \frac{1}{\overline{e_b/t}} \left\{ k_2 \frac{\overline{f}_y E_s \overline{\varepsilon}_{cu}}{(\overline{f}_y + E_s \varepsilon_{cu})^2} \frac{\overline{d}}{\overline{t}} + 2\overline{p} \frac{\overline{f}_y}{\overline{k_1 k_3}\ \overline{f}_c} \left(\frac{\overline{d}}{\overline{t}} - \frac{1}{2} \right) \frac{\overline{f}_y}{E_s \overline{\varepsilon}_{cu}} \right\} \qquad \text{(B.3)}$$

APPENDIX C

ANALYSIS OF COMBINED BENDING AND AXIAL THRUST

C.1 Compression Failures

The axial capacity of the member is defined as

$$P_C = \frac{P_o}{1 + \left[\frac{P_o}{P_b} - 1\right]\frac{e}{e_b}} = D\, q_u^C \qquad (C.1)$$

in which $D = k_3 f_c bt$, and where the concentrically loaded capacity P_o for symmetrically reinforced sections is

$$P_o = k_3 f_c (bt - 2A_s) + 2A_s f_y \qquad (C.2)$$

and the balanced point capacity P_b is

$$P_b = k_1 k_3 f_c bd \frac{E_s \varepsilon_{cu}}{E_s \varepsilon_{cu} + f_y} - k_3 f_c A_s \qquad (C.3)$$

If x is some parameter,

$$\frac{\partial P_C}{\partial x} = \frac{\partial P_C}{\partial P_o}\frac{\partial P_o}{\partial x} + \frac{\partial P_C}{\partial P_b}\frac{\partial P_b}{\partial x} + \frac{\partial P_C}{\partial e_b}\frac{\partial e_b}{\partial x}$$

evaluated at the mean values to analyze the second order uncertainties.

With $C = 1/(\overline{e_b/t})$,

$$\frac{\partial P_C}{\partial P_o} = \frac{q_u^C}{q_o} - \frac{q_o}{q_b} C \frac{e}{t}\left[1 + \left(\frac{q_o}{q_b} - 1\right) C \frac{e}{t}\right]^{-2} = a_1$$

$$\frac{\partial P_C}{\partial P_b} = \frac{q_o^2}{q_b^2} C \frac{e}{t}\left[1 + \left(\frac{q_o}{q_b} - 1\right) C \frac{e}{t}\right]^{-2} = a_2$$

$$\frac{\partial P_C}{\partial e_b} = Dq_o C \frac{e}{t} \frac{C}{t}\left(\frac{q_o}{q_b} - 1\right)\left[1 + \left(\frac{q_o}{q_b} - 1\right) C \frac{e}{t}\right]^{-2} = D \frac{a_3}{t}$$

$$\frac{\partial P_C}{\partial e} = - \frac{Da_3}{Ce} \qquad (C.4)$$

The derivatives with respect to P_o are given as

$$\frac{\partial P_o}{\partial f_y} = 2A_s$$

$$\frac{\partial P_o}{\partial f_c} = k_3(bt - 2A_s)$$

$$\frac{\partial P_o}{\partial A_s} = 2f_y - 2k_3 f_c$$

$$\frac{\partial P_o}{\partial b} = k_3 f_c t$$

$$\frac{\partial P_o}{\partial t} = k_3 f_c b \qquad (C.5)$$

The derivatives with respect to P_b are

$$\frac{\partial P_b}{\partial f_y} = - k_1 k_3 f_c b d \frac{E_s \varepsilon_{cu}}{(E_s \varepsilon_{cu} + f_y)^2}$$

$$\frac{\partial P_b}{f_c} = k_1 k_3 b d \frac{E_s \varepsilon_{cu}}{E_s \varepsilon_{cu} + f_y} - k_3 A_s$$

$$\frac{\partial P_b}{\partial A_s} = - k_3 f_c$$

$$\frac{\partial P_b}{\partial b} = k_1 k_3 f_c d \frac{E_s \varepsilon_{cu}}{E_s \varepsilon_{cu} + f_y}$$

$$\frac{\partial P_b}{\partial d} = k_1 k_3 f_c b \frac{E_s \varepsilon_{cu}}{E_s \varepsilon_{cu} + f_y}$$

$$\frac{\partial P_b}{\partial \varepsilon_{cu}} = k_1 k_3 f_c b d \frac{f_y E_s}{(E_s \varepsilon_{cu} + f_y)^2}$$

$$\frac{\partial P_b}{\partial (k_1 k_3)} = f_c b d \frac{E_s \varepsilon_{cu}}{E_s \varepsilon_{cu} + f_y} \qquad (C.6)$$

The derivatives with respect to e_b are

$$\frac{\partial e_b}{\partial f_y} = k_2 \left[\frac{E_s \varepsilon_{cu}}{(E_s \varepsilon_{cu} + f_y)^2} \right] d + 2p \frac{1}{k_1 k_3 f_c} \left(d - \frac{1}{2}\right) \frac{E_s \varepsilon_{cu} + 2 f_y}{E_s \varepsilon_{cu}}$$

$$\frac{\partial e_b}{\partial f_c} = - 2p \frac{f_y}{k_1 k_3 f_c^2} \left(d - \frac{t}{2}\right) \frac{E_s \varepsilon_{cu} + f_y}{E_s \varepsilon_{cu}}$$

$$\frac{\partial e_b}{\partial A_s} = \frac{2p}{A_s} \frac{f_y}{k_1 k_3 f_c} (d - \frac{t}{2}) \frac{E_s \varepsilon_{cu} + f_y}{E_s \varepsilon_{cu}}$$

$$\frac{\partial e_b}{\partial b} = - \frac{2p}{b} \frac{f_y}{k_1 k_3 f_c} (d - \frac{t}{2}) \frac{E_s \varepsilon_{cu} + f_y}{E_s \varepsilon_{cu}}$$

$$\frac{\partial e_b}{\partial d} = - k_2 \frac{E_s \varepsilon_{cu}}{E_s \varepsilon_{cu} + f_y} + p \frac{f_y}{k_1 k_3 f_c} \frac{E_s \varepsilon_{cu} + f_y}{E_s \varepsilon_{cu}} \frac{1}{d/t}$$

$$\frac{\partial e_b}{\partial t} = \frac{1}{2} \left[1 - 2p \frac{f_y}{k_1 k_3 f_c} \frac{E_s \varepsilon_{cu} + f_y}{E_s \varepsilon_{cu}} \right]$$

$$\frac{\partial e_b}{\varepsilon_{cu}} = - k_2 \left[\frac{f_y E_s}{(f_y + E_s \varepsilon_{cu})^2} \right] d - 2p \frac{f_y}{k_1 k_3 f_c} (d - \frac{t}{2}) \frac{f_y E_s}{(E_s \varepsilon_{cu})^2}$$

$$\frac{\partial e_b}{\partial (k_1 k_3)} = - 2p \frac{f_y}{f_c} (d - \frac{t}{2}) \frac{E_s \varepsilon_{cu} + f_y}{E_s \varepsilon_{cu}} \frac{1}{(k_1 k_3)^2} \qquad (C.7)$$

The uncertainty in capacity is found from

$$\begin{Bmatrix} \delta^2_{P_C} \\ \Delta^2_{P_C} \end{Bmatrix} = \sum C_K^2 \begin{Bmatrix} \delta^2_K \\ \Delta^2_K \end{Bmatrix} \qquad (C.8)$$

where

$$C_K = \frac{1}{\overline{P}_C} \left(\frac{\partial P_C}{\partial x_K} \right)_o \overline{x}_K$$

e.g.,

$$c_{f_y} = \frac{1}{\bar{P}_c}\left[a_1 \frac{\partial P_o}{\partial f_y} + a_2 \frac{\partial P_b}{\partial f_y} + D\frac{a_3}{t}\frac{\partial e_b}{\partial f_y}\right]\bar{f}_y$$

$$c_{f_y} = \frac{1}{q_u^c}\left[a_1 p_t m - a_2 k_1 \frac{p_t}{2p}\frac{E_s\varepsilon_{cu}f_y}{(E_s\varepsilon_{cu}+f_y)^2} + a_3\left\{k_2\frac{E_s\varepsilon_{cu}f_y}{(E_s\varepsilon_{cu}+f_y)^2}\frac{p_t}{2p} + 2p\frac{m}{k_1}\left(\frac{p_t}{2p}-\frac{1}{2}\right)\frac{E_s\varepsilon_{cu}+2f_y}{E_s\varepsilon_{cu}}\right\}\right] \qquad (C.9)$$

in which all parameters are evaluated at their mean values in computing c_{f_y}, $p_t = 2A_s/bt$, and $m = f_y/k_3 f_c$.

C.2 Tension Failures

When e is measured from the plastic centroid, and the section is symmetrically reinforced,

$$P_T = k_3 f_c bt\left[\frac{1}{2\eta k_3}\left\{R - \left(\frac{e}{t}-\frac{1}{2}\right)\right\} - \frac{A_s}{bt}\right] = Dq_u^T \qquad (C.10)$$

where $D = k_3 f_c bt$, $\eta = k_2/k_1 k_3$ as in flexure, and

$$R = \sqrt{\left(\frac{e}{t}-\frac{1}{2}\right)^2 + 4\eta\frac{A_s}{btf_c}\left[k_3 f_c\frac{e}{t} + (2f_y - k_3 f_c)\left(\frac{d}{t}-\frac{1}{2}\right)\right]}$$

The derivatives are

$$\frac{\partial P_T}{\partial f_y} = \frac{2A_s}{R}\left(\frac{d}{t}-\frac{1}{2}\right)$$

$$\frac{\partial P_T}{\partial f_c} = -\frac{2A_s f_y}{R f_c}\left(\frac{d}{t}-\frac{1}{2}\right)+\frac{bt}{2\eta}\left[R-\left(\frac{e}{t}-\frac{1}{2}\right)\right]-k_3 A_s$$

$$\frac{\partial P_T}{\partial A_s} = \frac{1}{R}\left[k_3 f_c \frac{e}{t}+(2f_y-k_3 f_c)\left(\frac{d}{t}-\frac{1}{2}\right)\right]-k_3 f_c$$

$$\frac{\partial P_T}{\partial b} = -\frac{1}{R}\frac{A_s}{b}\left[k_3 f_c \frac{e}{t}+(2f_y-k_3 f_c)\left(\frac{d}{t}-\frac{1}{2}\right)\right]$$

$$+\frac{f_c t}{2\eta}\left[R-\left(\frac{e}{t}-\frac{1}{2}\right)\right]$$

$$\frac{\partial P_T}{\partial d} = \frac{A_s}{R}(2f_y-k_3 f_c)\left(\frac{1}{t}\right)$$

$$\frac{\partial P_T}{\partial t} = \frac{f_c b}{2\eta}\left[-\frac{1}{R}\left\{\left(\frac{e}{t}-\frac{1}{2}\right)\frac{e}{t}+\frac{4\eta A_s}{btf_c}\left[k_3 f_c \frac{e}{t}\right.\right.\right.$$

$$\left.\left.\left.+(2f_y-k_3 f_c)\left(\frac{d}{t}-\frac{1}{4}\right)\right]\right\}+\frac{e}{t}\right]+\frac{f_c b}{2\eta}\left[R-\left(\frac{e}{t}-\frac{1}{2}\right)\right]$$

$$\frac{\partial P_T}{\partial e} = \frac{f_c bt}{2\eta}\left[\frac{1}{R}\left\{\left(\frac{e}{t}-\frac{1}{2}\right)\frac{1}{t}+2\eta k_3 \frac{A_s}{bt^2}\right\}-\frac{1}{t}\right]$$

$$\frac{\partial P_T}{\partial \eta} = \frac{A_s}{R\eta}\left[k_3 f_c \frac{e}{t}+(2f_y-k_3 f_c)\left(\frac{d}{t}-\frac{1}{2}\right)\right]$$

$$-\frac{f_c bt}{2\eta^2}\left[R-\left(\frac{e}{t}-\frac{1}{2}\right)\right] \qquad \text{(C.11)}$$

The overall uncertainty in capacity is found similarly to the compression case. The c_k are given by

$$c_k = \frac{1}{\overline{P}_T} \left(\frac{\partial P_T}{\partial k} \right)_o \overline{k} \qquad (C.12)$$

e.g.,

$$c_{f_y} = p_t \frac{\overline{f}_y}{\overline{k}_3 \overline{f}_c} \frac{1}{\overline{R}} \left(\frac{\overline{d}}{\overline{t}} - \frac{1}{2} \right) \frac{1}{q_u} T$$

in which $p_t = 2 \overline{A}_s / \overline{b}\ \overline{t}$.

APPENDIX D

EVALUATION OF STATISTICS OF THE GUST FACTOR

The gust factor to be used in design is defined by Eq. 4.29, repeated here.

$$G_D = 1 + \sqrt{2 \ln(f_o t_d)}\, \sigma_y \tag{D.1}$$

in which f_o is the fundamental frequency, t_d is the averaging period, and

$$\sigma_y^2 = \frac{16}{3} k \left(\frac{30}{h}\right)^{2\alpha} \left[\frac{\pi}{\beta} g_1 g_2 g_3 + g_4\right] \tag{D.2}$$

and where g_1, g_2, g_3, and g_4 have been defined in Eq. 4.27. Its mean is found by substituting the mean values of the individual parameters into Eqs. D.1 and D.2.

$$\overline{G}_D = G_D(\overline{k}, \overline{\alpha}, \overline{\beta}, \overline{f}_o, \overline{U}_o, \overline{c}_y, \overline{c}_z) \tag{D.3}$$

and its second order statistics are found as

$$\begin{Bmatrix} \delta^2_{G_D} \\ \Delta^2_{G_D} \end{Bmatrix} = \sum a_m^2 \begin{Bmatrix} \delta_m^2 \\ \Delta_m^2 \end{Bmatrix} \tag{D.4}$$

in which

$$a_m = \frac{1}{\overline{G}_D} \left(\frac{\partial G_D}{\partial m}\right)_o \overline{m}$$

and m is one of the variables in Eq. D.3. When $m = f_o$,

$$\frac{\partial G_D}{\partial f_o} = \sqrt{2 \ln(f_o t_d)} \quad \frac{\partial \sigma_y}{\partial f_o} + \frac{1}{f_o \sqrt{2 \ln(f_o t_d)}} \quad \sigma_y \qquad (D.5)$$

otherwise

$$\frac{\partial G_D}{\partial m} = \sqrt{2 \ln(f_o t_d)} \quad \frac{\partial \sigma_y}{\partial m} \qquad (D.6)$$

Defining constants

$$c = \sqrt{2 \ln(f_o t_d)}$$

$$t_1 = \frac{c_y}{2} \left(\frac{30}{h}\right)^{\alpha} \quad \frac{f_o b}{U_o}$$

$$t_2 = \frac{c_z}{3} \left(\frac{30}{h}\right)^{\alpha} \quad \frac{f_o h}{U_o}$$

$$t_3 = 4000 \quad \frac{f_o}{U_o} \quad \left(\frac{30}{h}\right)^{\alpha}$$

$$g = \frac{\pi}{\beta} \; g_1 \; g_2 \; g_3 + g_4 \qquad (D.7)$$

the derivatives are then

$$\frac{\partial G_D}{\partial k} = c\sigma_y \left(\frac{1}{2k}\right)$$

$$\frac{\partial G_D}{\partial \alpha} = c\sigma_y \left\{ 1 + \frac{\pi}{2g\beta} g_1 g_2 g_3 \left[\frac{2(3 - t_3^2)}{3(1 + t_3^2)} - g_1 t_1 - g_2 t_2 \right] \right\} \ln \left(\frac{30}{h}\right)$$

$$\frac{\partial G_D}{\partial \beta} = - c\sigma_y \frac{\pi}{2g\beta} g_1 g_2 g_3 \left(\frac{1}{\beta}\right)$$

$$\frac{\partial G_D}{\partial U_o} = c\sigma_y \frac{\pi}{2g\beta} g_1 g_2 g_3 \left\{ g_1 t_1 + g_2 t_2 - \frac{2(3 - t_3^2)}{3(1 + t_3^2)} \right\} \frac{1}{U_o}$$

$$\frac{\partial G_D}{\partial c_y} = - c\sigma_y \frac{\pi}{2g\beta} g_1 g_2 g_3 (g_1 t_1) \frac{1}{c_y}$$

$$\frac{\partial G}{\partial c_z} = - c\sigma_y \frac{\pi}{2g\beta} g_1 g_2 g_3 (g_2 t_2) \frac{1}{c_z}$$

$$\frac{\partial G}{\partial f_o} = c\sigma_y \left\{ \frac{\pi}{2g\beta} g_1 g_2 g_3 \left[\frac{2(3 - t_3^2)}{3(1 + t_3^2)} - g_1 t_1 - g_2 t_2 \right] + \frac{1}{c^2} \right\} \frac{1}{f_o} \qquad (D.8)$$

where all parameters in Eqs. D.7 and D.8 are taken at their mean values in the evaluation of a_m.